Addressing the Challenges Posed by Human Machine Interfaces Based on Force Sensitive Resistors for Powered Prostheses

by

Chakaveh Ahmadizadeh

B.A.Sc., Simon Fraser University, 2014

Thesis Submitted in Partial Fulfillment of the
Requirements for the Degree of
Doctor of Philosophy

in the
School of Engineering Science
Faculty of Applied Sciences

SIMON FRASER UNIVERSITY
Fall 2020

Declaration of Committee

Name: **Chakaveh Ahmadizadeh**

Degree: **Doctor of Philosophy**

Thesis title: **Addressing the Challenges Posed by Human Machine Interfaces Based on Force Sensitive Resistors for Powered Prostheses**

Committee:

Chair: Michael Sjoerdsma
Senior Lecturer
School of Engineering Science

Carlo Menon
Supervisor
Professor
School of Engineering Science
School of Mechatronic Systems Engineering

Faranak Farzan
Committee Member
Assistant Professor
School of Mechatronic Systems Engineering

Jie Liang
Committee Member
Professor
School of Engineering Science

Mirza Faisal Beg
Examiner
Professor
School of Engineering Science

Shane Xie
External Examiner
Professor
School of Electronic and Electrical Engineering
University of Leeds

Ethics Statement

The author, whose name appears on the title page of this work, has obtained, for the research described in this work, either:

a. human research ethics approval from the Simon Fraser University Office of Research Ethics

or

b. advance approval of the animal care protocol from the University Animal Care Committee of Simon Fraser University

or has conducted the research

c. as a co-investigator, collaborator, or research assistant in a research project approved in advance.

A copy of the approval letter has been filed with the Theses Office of the University Library at the time of submission of this thesis or project.

The original application for approval and letter of approval are filed with the relevant offices. Inquiries may be directed to those authorities.

Simon Fraser University Library
Burnaby, British Columbia, Canada

Update Spring 2016

Abstract

Despite the advancements in the mechatronics aspect of prosthetic devices, prostheses control still lacks an interface that satisfies the needs of the majority of users. The research community has put great effort into the advancements of prostheses control techniques to address users' needs. However, most of these efforts are focused on the development and assessment of technologies in the controlled environments of laboratories. Such findings do not fully transfer to the daily application of prosthetic systems. The objectives of this thesis focus on factors that affect the use of Force Myography (FMG) controlled prostheses in practical scenarios. The first objective of this thesis assessed the use of FMG as an alternative or synergist Human Machine Interface (HMI) to the more traditional HMI, i.e. surface Electromyography (sEMG). The assessment for this study was conducted in conditions that are relatively close to the real use case of prosthetic applications. The HMI was embedded in the custom prosthetic prototype that was developed for the pilot participant of the study using an off-the-shelf prosthetic end effector. Moreover, prostheses control was assessed as the user moved their limb in a dynamic protocol.

The results of the aforementioned study motivated the second objective of this thesis: to investigate the possibility of reducing the complexity of high density FMG systems without sacrificing classification accuracies. This was achieved through a design method that uses a high density FMG apparatus and feature selection to determine the number and location of sensors that can be eliminated without significantly sacrificing the system's performance.

The third objective of this thesis investigated two of the factors that contribute to increased errors in force sensitive resistor (FSR) signals used in FMG controlled prostheses: bending of force sensors and variations in the volume of the residual limb. Two studies were conducted that proposed solutions to mitigate the negative impact of these factors. The incorporation of these solutions into prosthetic devices is discussed in these studies.

It was demonstrated that FMG is a promising HMI for prostheses control. The facilitation of pattern recognition with FMG showed potential for intuitive prosthetic control. Moreover, a method for the design of a system that can determine the required number of sensors and their locations on each individual to achieve a simpler system with comparable performance to high density FMG systems was proposed and tested. The effects of the two factors considered in the third objective were determined. It was also demonstrated that the proposed solutions in the studies conducted for this objective can be used to increase the accuracy of signals that are commonly used in FMG controlled prostheses.

Keywords: Force myography; Gesture classification; Assistive technology; Pattern recognition; Electromyography; Human machine interface; Feature selection; Prostheses control; Robotic hand; Max relevancy, min redundancy; Sequential forward selection; Genetic algorithm; Random forest; volume fluctuation; FSR bending; Regression

Dedication

I would like to dedicate this thesis to individuals struggling with loss of a limb. Towards the day they can live a normal life.

Acknowledgements

First and foremost, I would like to express my gratitude for the invaluable support and guidance of my senior supervisor, Dr. Carlo Menon. He has helped me stay focused on my original intentions for pursuing this field of research. He has repeatedly inspired me through his professionalism and patience. I would also like to thank my supervisors Dr. Faranak Farzan and Dr. Jie Linag for their support and valuable feedback on my research.

I would like to thank all member of the MENRVA lab for their support and assistance in reviewing articles used in this document. I would like to thank Brittany Pousett and Dave Moe and all other members of Barber Prothetics Clinic for making this research possible and being patient through many stages of experimentation required for this thesis.

Last but not least, I would like to extend my special thanks to my lovely family and dear friends for their support and companionship. I would like to thank Sajjad Gholami for his support and also reviewing this document.

Table of Contents

Declaration of Committee ii

Ethics Statement iii

Abstract iv

Dedication vi

Acknowledgements vii

Table of Contents viii

List of Tables xii

List of Figures xiii

1 Introduction 1

1.1 Chapter Overview 1

1.2 Motivation 2

1.3 Objectives 9

1.4 Thesis Structure 10

1.5 Contributions 11

2 Background 13

2.1 Chapter Overview 13

2.2 Human Machine Interfaces for Prosthesis Control 13

2.2.1 Electromyography (EMG) 14

2.2.2 Force Myography (FMG) . . . 16
2.2.3 Electroneurography (ENG) . . . 17
2.2.4 Mechanomyography (MMG) . . . 18
2.2.5 BMI . . . 19
2.2.6 Hybrid HMIs . . . 21
2.3 Channel Selection . . . 23
2.3.1 Filter Methods . . . 24
2.3.2 Wrapper Methods . . . 24
2.3.3 Embedded Methods . . . 24

3 Possibility of Using FMG for Control of Powered Prosthesis 26
3.1 Chapter Overview . . . 26
3.2 Introduction . . . 27
3.3 Material and Methods . . . 28
3.3.1 Participant . . . 28
3.3.2 Hardware . . . 28
3.3.3 Software . . . 30
3.3.4 Experimental Setup and Protocol . . . 31
3.3.5 Data Analysis . . . 34
3.4 Results . . . 36
3.4.1 Classification Algorithm . . . 36
3.4.2 FSR Placement . . . 38
3.4.3 Addition of EMG Features . . . 38
3.5 Discussion . . . 39
3.5.1 FSR Placement . . . 39
3.5.2 Addition of EMG . . . 40
3.5.3 Cybathlon . . . 41

4 Possibility of Reduction of System Complexity in High Density FMG Systems 43

4.1 Chapter Overview . . . 43
4.2 Introduction . . . 44
4.3 Materials and Methods . . . 47
4.3.1 Participant . . . 48
4.3.2 Data collection . . . 48
4.3.3 Data analysis . . . 50
4.4 Results . . . 56
4.4.1 Classification Accuracy . . . 56
4.4.2 Stability . . . 60
4.4.3 Running Time . . . 60
4.5 Discussion . . . 61
4.5.1 Classification Accuracy . . . 62
4.5.2 Running Time . . . 68
4.5.3 Stability . . . 69

5 The Effect of Bending of Force Sensitive Resistors on Signals Used in FMG Controlled Prostheses 70

5.1 Chapter Overview . . . 70
5.2 Introduction . . . 71
5.3 Materials and Methods . . . 77
5.3.1 Sensor Matrices . . . 77
5.3.2 Data Acquisition . . . 78
5.3.3 Test Setup . . . 80
5.3.4 Data Collection . . . 83
5.3.5 Regression Methods . . . 83
5.4 Results . . . 86
5.4.1 Algorithm Selection . . . 87
5.4.2 Method Selection . . . 87
5.5 Discussion . . . 89

6 The Effect of Variations in the Volume of the Residual Limb on Signals Used in FMG Controlled Prostheses **97**

6.1 Chapter Overview . . . 97

6.2 Introduction . . . 98

6.3 Materials and Methods . . . 101

6.3.1 Participants . . . 101

6.3.2 Hardware . . . 101

6.3.3 Protocol . . . 103

6.3.4 Data Analysis . . . 105

6.4 Results . . . 107

6.4.1 Phase 1 . . . 107

6.4.2 Phase 2 . . . 110

6.5 Discussion . . . 111

7 Conclusions and Future Works **116**

7.1 Chapter Overview . . . 116

7.2 Challenges in the Field . . . 117

7.3 Conclusions and Future Works . . . 118

Bibliography **123**

Appendix A Raw Signal Visualization **138**

Appendix B Feature Selection for Extended Grips **141**

Appendix C Feature Selection Using an Alternate Method **145**

List of Tables

Table 3.1 The classes of motion groups 36

Table 3.2 The classification accuracies obtained in this study 39

Table 4.1 Number of features selected in LOOCV using different feature selection methods 58

Table 4.2 The grip with highest classification error for each dataset, using each FS method 59

Table 4.3 Percentage decrease in input features using different feature selection methods 60

Table 4.4 Running time for each FS method for each dataset (s) 61

Table 4.5 Classification accuracies obtained using half of the data 64

Table 4.6 Number of selected features with limited feature number 66

Table 5.1 Regression-based error compensation methods 85

Table 5.2 Comparison of when sensors were laid flat vs. when all 6 conditions were considered 88

Table 5.3 Results of method selection 89

Table 6.1 Summary of weight range, amputation side, and prosthesis type of participants of this study 102

Table 6.2 Mean peaks of FSR signals obtained in the first phase of this study. . 108

Table 6.3 Mean peaks of FSR signals obtained in the second phase of this study. 111

List of Figures

Figure 1.1 Different types of prostheses 3

Figure 1.2 Some of the powered prostheses available in the market 5

Figure 3.1 Main components of the prosthetic system 30

Figure 3.2 The software architecture for experimental data collection and offline processing 31

Figure 3.3 The software architecture for online use of the device 32

Figure 3.4 The dynamic protocol 33

Figure 3.5 The classes of motion used in the dynamic protocol 33

Figure 3.6 The two FSR placements 35

Figure 3.7 The classification accuracies obtained by SVM and LDA algorithms 37

Figure 3.8 The classification accuracies obtained for sensor placement investigation 38

Figure 3.9 The classification accuracies obtained for addition of EMG 39

Figure 3.10 The confusion matrix for the three-class problem used for the 2016 Cybathlon 42

Figure 4.1 Custom made prosthetic socket and the Bebionic 3 robotic hand . . 48

Figure 4.2 FSR strips placed inside the inner socket 49

Figure 4.3 The six grips used in this study 50

Figure 4.4 The dynamic protocol 50

Figure 4.5 Feature selection process used in this study 55

Figure 4.6 Results for dataset1 57

Figure 4.7 Results for dataset2 57

Figure 4.8 Results for dataset3 58
Figure 4.9 Percentage variation in feature subsets as amount of training data is decreased 61
Figure 4.10 Classification accuracy for dataset1 with limited number of features 66
Figure 4.11 Classification accuracy for dataset2 with limited number of features 67
Figure 4.12 Classification accuracy for dataset3 with limited number of features 67

Figure 5.1 Illustration of the variations in the response of FSRs when they are curved 71
Figure 5.2 FSR matrix and the data acquisition PCB used in this study 78
Figure 5.3 FSR matrix representation 79
Figure 5.4 Cross talk compensation circuit 80
Figure 5.5 Curved structured used to bend the sensor matrix 82
Figure 5.6 Experimental setup using a pressure chamber 82
Figure 5.7 Comparison of the response of one of the FSRs when sensor was laid flat vs. when it was bent 86
Figure 5.8 Comparison of performance of three regression algorithms 87
Figure 5.9 Outcome measures for the four proposed methods 88
Figure 5.10 Comparison of the response of one of the FSRs when sensors were laid flat vs. when they were bent in low pressure values 90
Figure 5.11 Comparison of predicting pressure from output of one of the sensors without and with considering sensor's curvature information 91
Figure 5.12 Comparison of the response of one of FSRs when sensors are positioned on structures with varying curvatures 93

Figure 6.1 Main components of the system and the prosthetic socket 103
Figure 6.2 Data analysis process used in this study 106
Figure 6.3 Results of phase 1 109
Figure 6.4 Results of phase 2 110
Figure 6.5 Adjusted normalized means of peaks of force 111

Chapter 1

Introduction

The material presented in this chapter is excerpted, reproduced, and modified with permission from the following papers:

 C. Ahmadizadeh, L.-K. Merhi, B. Pousett, S. Sangha, and C. Menon, "Toward Intuitive Prosthetic Control: Solving Common Issues Using Force Myography, Surface Electromyography, and Pattern Recognition in a Pilot Case Study," IEEE Robot. Autom. Mag., no. December, pp. 102-111, 2017.

C. Ahmadizadeh, B. Pousett, and, C. Menon, "Investigation of Channel Selection for Gesture Classification for Prosthesis Control Using Force Myography: a Case Study," Frontiers in Bioengineering and Biotechnology, vol. 7, no. December, pp. 1-15, 2019.

C. Ahmadizadeh, B. Pousett, and C. Menon, "Towards Management of Residual Limb Volume: Monitoring the Prosthetic Interface Pressure to Detect Volume Fluctuations - a Feasibility Study," Applied Sciences, vol. 10, no. 19, p. 6841, 2020.

C.Ahmadizadeh, M. Khoshnam, and C. Menon, "Human Machine Interfaces in Prosthesis Control: a Survey"," IEEE SPM Special Issue on Signal Processing for Neurorehabilitation and Assistive Technologies, **Submitted**.

Sections of this chapter are reprinted or adapted from the above articles for clarification and to fit the formatting and scope of this document.

1.1 Chapter Overview

This chapter outlines the motivation behind the research questions addressed in this thesis. Objectives of this work are defined, and finally structure of this document is explained.

1.2 Motivation

In 2005, in the United States alone, 1.6 million individuals were living with the loss of a limb, 42% of which had undergone a major amputation of the upper or the lower limb [1]. This number is expected to more than double by the year 2050 [1].

Personal autonomy is one of the key factors affecting quality of daily life of individuals, and it is drastically affected by an amputation. Limitations introduced by the lack of functionality of the amputated limb narrow the scope of tasks that affected population is capable of performing without assistance. This affects various aspects of their life, from activities of daily living such as maintaining their personal hygiene, cooking, walking on different terrains, and dressing themselves to tasks required for their occupations [2]. Although majority of individuals with amputations maintain gainful employment after the loss of their limb - approximately 70% as reported in literature [3], [4], [5], studies have shown that in most cases a change in occupation is needed [3], [6], [7], [8]. In a study by Datta et al. that focused on individuals with upper limb amputations, it was reported that only 6.6% of their observed population returned to the same job after amputation [3]. In another study of factors impacting the outcome of job reintegration of individuals with lower limb amputations, Schoppen et al. reported that approximately 53% of their observed population with successful job reintegration changed their type of employment after amputation [8]. In some extreme cases, lifestyle changes due to an amputation can lead to depression in affected individuals. Studies have reported varying statistics (up to 35%) for depression due to an amputation [3], [9].

Prosthetic devices can be used to mitigate some of the limitations caused by a minor or a major amputation. It has been reported that using a prosthesis contributes to individuals' chances of maintaining employment after their amputation and is essential to their personal and occupational activities [3], [7], [10], [5]. Prostheses provide an artificial replacement for the lost limb through a coupling attached to the residual limb, i.e. the prosthetic socket. In the case of prostheses for major limb loss, a prosthetic hand/gripper or foot is attached to the distal end of the prosthetic socket for cosmesis, to provide some of the functions of the lost hand/foot, or for both.

Various types of prostheses are available for both the upper and the lower limbs. There are two ways to categorize them. First, based on the level of amputation. This method categorizes upper limb prostheses from the most major to the most minor levels of amputation to: shoulder disarticulation prostheses, transhumeral prostheses (for above elbow amputations), elbow disarticulation prostheses, transradial prostheses (for below elbow amputations), and hand/finger prostheses [11]. Similarly, lower limb prostheses can be categorized to prostheses for the following amputations: hip disarticulation, transfemoral (above the knee amputations), knee disarticulation, transtibial (below the knee amputations), ankle disarticulation, and foot/toe amputations[12].

The second method for prostheses categorization is to classify them based on their function. This splits them to cosmetic prostheses, body powered prostheses, and externally powered prostheses [11]. Some examples are shown in Figure 1.1.

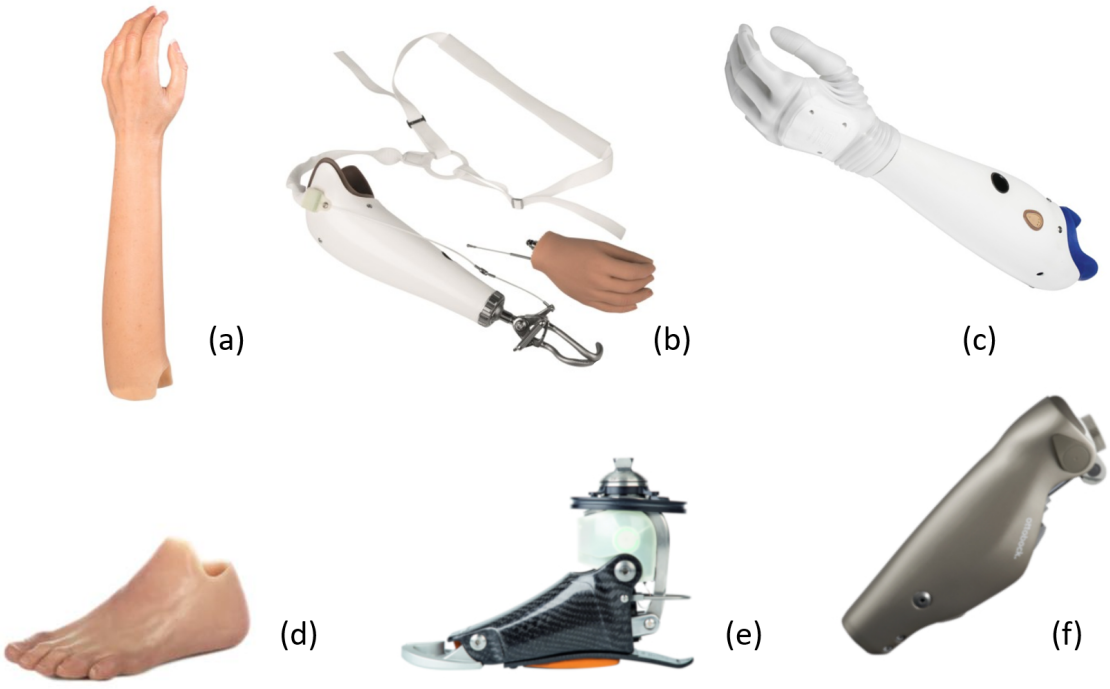

Figure 1.1: Different types of prostheses: (a) a cosmetic arm prosthesis [13], (b) a body powered upper extremity prosthesis [14], (c) an externally powered hand [15], (d) a cosmetic foot [16], (e) a robotic foot [17], (f) an externally powered knee [18].

Cosmetic prosthetic devices are mainly used for their appearance. Although they provide limited functionality such as holding objects and minor manipulation of them, the main

use of them is their cosmesis. On the other hand, the focus of the other two types of prostheses is their functionality. The main difference between body powered prostheses and externally powered ones is their method of control. Body powered prostheses are powered and controlled by the user's body either actively or passively. For example, user's shoulder can be used to actively control the function of a gripper attached to a transradial prosthesis [11] while cantilevered feet are passively controlled body-powered prostheses for the lower extremity [19]. Externally powered prostheses operate using external power sources which, in most cases, are batteries. These devices hold the unique potential to be able to mimic functions and motions of the lost limb [11]. Two aspects of these devices play significant roles towards achieving such potentials: first, the design and performance of the mechatronics devices that are used in the prostheses , such as the robotic hand/foot that is assembled at the distal end of the prosthesis to manipulate objects and imitate motions of the natural limb; and the second aspect is control of these systems.

The first aspect has improved immensely in the past decade [20]. The robotics community has put great focus on mechatronics devices that could bring back more natural human body function. Today, multiple sophisticated powered prosthetic hands, robotic knees and ankles, etc, are available in the market, such as Otto Bock's Bebionic and Michelangelo hands, the i-limb hand by Touch Bionics, Ottobock's Empower foot and Kenevo above the knee prosthesis [21]. These devices are shown in Figure 1.2.

Figure 1.2: Some of the powered prostheses available in the market: (a) Bebionic hand [22], (b) Michelangelo hand [23], (c) I-limb hand [24], (d) Empower foot [25], and (e) Kenevo above knee prosthesis [26].

The second aspect is the control of externally powered prostheses which requires a human machine interface (HMI) to allow the user to control the system. Different HMIs have been proposed and examined for control of externally powered prostheses. Some of the options for these HMIs incorporate external sensors, switches, cameras, etc., with the system for control of the prosthesis. The more advanced methods however use biosignals - by themselves or as synergists to other sensory systems - to interpret users' intentions for control of their prostheses. Some of these methods are electromyography(EMG) [27], [28], [29], [30], electroneurography (ENG) [31], mechanomyography (MMG) [32], [33], force

myography (FMG) [34], [35], electroencephalography(EEG) [36], and electrocorticography (ECoG) [37].

Despite advancements in both aforementioned aspects in the past decade, rejection rates of both the upper and the lower limb prostheses are relatively high [20], [38], [19], [39]. Davidson et al. conducted a study in which they reported that only 44% of the population under study wore their prosthetic limbs half of the time or more [10]. It is probable that these numbers underestimate the rejection rates of prostheses since most of the studies reporting such rates recruit their participants through rehabilitation centers that do not include population of non-users. Also, individuals with positive experience using prostheses are more prone to participate in studies with the goal of enhancing the technology they use [40].

Various reasons have been reported as the cause of rejection of prostheses by their users. Some of these reasons are based on environmental and personal conditions of the individual, such as availability of help from caregivers [7]. Some of the other factors affecting acceptance rate of prostheses is the level of amputation, dominance of the lost limb, age of the user, time since amputation, affordability for the individual, education, other disabilities, and employment situation [3], [7], [41].

The other causes of prostheses rejection are related to the available system not fulfilling expectations of the users. Some of these include limited functionality, discomfort, heaviness of the prostheses, device's energy consumption, unintuitive control, insufficient feedback, frequency of unplanned movements, and reliability [42], [10], [19], [43].

Studies that investigated expectations of users for future advancements in prostheses suggest that they value function and comfort the most [42]. Their priorities include mostly functional factors such as stability and reliability of control [42], [44], sensory feedback, durability, lifelike control, and increased number of controllable states [38].

A group of expected improvements relate to control strategies used in these devices. In spite of availability of sophisticated externally powered prostheses, reliable and natural control of such devices is still an issue. The traditional methods used for control cannot keep up with complexity of sophisticated robotic prostheses that attempt to emulate the human

body's function [21], [38]. For instance, to use multiple hand gestures and wrist movements using this strategy, concentrations and Morse code like signalling is required which makes the control very unintuitive [21].

Recently, natural prosthetic control using pattern recognition technology has drawn lots of attention in academic research [10],[11], [45]. Pattern Recognition based control has the potential to allow for natural control of externally powered prostheses. In the past few years, commercial devices using pattern recognition for more intuitive control have also become available such as CoApt Engineering Complete Control, Chicago, Illinois (https://coaptengineering.com/) and Ottobock's Myo Plus pattern recognition system [46]. However, there are still issues with pattern recognition based control when it comes to clinical practice [47]. The sensory systems for control of robotic prostheses that is currently available in the market have specific downfalls. Some of these HMIs function based on signals that are affected by interference from ambient noise, electrode shifts, sweat and humidity, and signal cross-talk between adjacent electrodes [21], [48], [49]. Such problems make these HMIs less suitable for prolonged use [21].

Force Myography (FMG) has demonstrated to be a promising alternative to conventional sensing techniques [50]. FMG is based on pressure sensing and has the potential to provide high accuracy in prediction, stability over time, wearability, simplicity in socket embedding, and affordability of cost [50]. Gesture recognition in individuals with upper extremity amputations using FMG has been demonstrated to be feasible in various studies [21], [51]. FMG has also shown promise for control of lower limb prostheses in the research community [52], [35], [53]. Performances of FMG and EMG based systems have been compared in multiple studies [50], [54], [55]. It has been shown that force myography can outperform EMG-based approaches for various prosthesis control tasks [54], [55].

FMG is a relatively new technology that has been tested using healthy participants in some studies (*e.g.* [54], [56], [57]). Although the application of this HMI for prosthesis control has been investigated, healthy participants have been employed for most of the assessments performed in such studies. Even in the limited research that has employed participants with amputations, tests were not performed using prosthetic sockets [21], [58].

The use of FMG with healthy participants and/or without prosthetic sockets generally involves the use of flexible bands embedded with FSR sensors. Contrarily, to use this HMI in prosthetic applications, sensors need to be embedded inside rigid prosthetic sockets and do not have the freedom to flex in various directions like they do when used in flexible bands. As a result, it is important to take the constrained environment of the rigid prosthetic socket into account when FMG is considered for prosthetic applications. Moreover, FMG signals produced for various movements by the muscles of healthy participants are more distinguishable compared to individuals with amputations. As a result, tests with healthy individuals or with flexible FSR bands are not suitable representations of the performance of FMG inside prosthetic sockets, and it is important that this HMI is assessed with individuals with amputations wearing rigid prosthetic sockets.

One of the other limitations of the studies conducted with a focus on FMG controlled prosthesis is the use of protocols [21], [51] that limit the types of movements during experiments, which cannot ensure usability of the systems in dynamic movements used in daily life [47].

Despite efforts of the research community towards enhancement of control technologies used for powered prostheses control, traditional methods are still the widely selected choice in clinics. One of the factors limiting the adoption of state-of-the-art technologies developed in laboratories by clinics and users is the controlled environments in which these technologies are developed and tested. For assessment of the functionality of the proposed techniques in real life applications, it is essential for them to be tested in less controlled situations. Some of the conditions in real case applications of powered prostheses that can greatly affect performance of these devices are: the weight of the prosthetic socket and the electronic components of the prostheses; and also the types of movements of the limb as the user tries to control the prosthesis.

In this thesis, a case study is reported that attempts at determining quality of performance of FMG under aforementioned conditions. Due to a wider range of motion of the upper limb, and larger variability in the weight the device would be used to carry, the two conditions have more significant effects in the case of the upper limb. As a result, this case

study was based on a participant with a transradial amputation. For this purpose, a standard socket was custom made for the pilot, and an off-the-shelf robotic hand was used to simulate a real-life scenario. In order to simulate Activities of Daily Living (ADL) we used a proven dynamic protocol as a reasonable simulation for ADLs [54].

Findings of this case study, led to the motivation for an investigation to assess the possibility of advancement of FMG controlled prostheses by using a design method that reduces complexity of the system required to achieve performance of high density FMG systems.

Results obtained in the first two studies led to the motivation for two additional studies to investigate two factors that could contribute to errors in the signals used in the FMG HMI during its practical use: bending of the force sensors and fluctuations in the volume of the residual limb. Although volume changes occur in both upper and lower residual limbs, this effect is more considerable in the lower extremity residual limbs due to their weight bearing nature. As a result, the study conducted and explained in this thesis to asses the effect of variations in the residual limb on signals used in FMG controlled prosthesis focused on the lower limb.

1.3 Objectives

This thesis is structured based on three objectives. The first objective assesses the use of FMG controlled prosthesis in conditions that are relatively close to the practical application of the device. Findings of objective 1 provided motivation for objectives 2 and 3. The second objective is to investigate the possibility of a design method that allows for development of customized FMG powered prostheses that are comparable to high density FMG systems in performance, but are less complex. The last objective is to investigate some of the factors that potentially contribute to increased errors in signals used in FMG controlled prostheses. Two factors are considered in the third objective: bending of sensors used to acquire FMG signals, and fluctuations in the volume of the residual limb. The objectives of this thesis are listed below:

- Objective 1: To assess the use of FMG for control of powered prostheses in the following conditions:
  - HMI is embedded in the externally powered prosthesis of an individual with an amputation
  - Prosthesis is controlled in a dynamic protocol
- Objective 2: To investigate a design method that reduces complexity of prosthetic devices that are controlled using high density FMG
- Objective 3: To investigate possible factors contributing to errors in signals used in FMG controlled prostheses:
  - Objective 3.a: The effect of bending of force sensitive resistors on signals used in FMG controlled prostheses
  - Objective 3.b: The effect of variations in the volume of the residual limb on signals used in FMG controlled prostheses

1.4 Thesis Structure

Subsequent content of this thesis are structured in six chapters as follows:

- Chapter 2 provides an overview of the background of the technology explored in this thesis. Various HMIs used for powered prosthesis control are outlined and related works are mentioned. Also, an overview of features selection methods used in this thesis are explained.
- Chapter 3 explains methods used toward fulfilling **Objective 1**. This includes hardware and software design used for development of the prototype used for data collection, the pilot volunteer who participated in the case study, and data analysis methods used. Results of the study are reported and discussed at the end of this chapter.
- In Chapter 4, the study conducted to answer the research question of **Objective 2** is explained. Materials and methods in terms of hardware, algorithms and data analysis

methods used, etc. are explained. Subsequently, observations and results are reported and discussed.

- Chapter 5 outlines the study conducted towards fulfilment of **Objective 3.a**. Materials and methods used in this study are explained in this chapter. Results of the study are reported and discussed towards the end of the chapter.

- Chapter 6 provides the details of the study conducted to answer the research question of **Objective 3.b**. The sensory system used in this study is explained in addition to the data analysis method used to obtain results that are reported in this chapter. Results are discussed at the end of the chapter.

- Chapter 7 outlines conclusions drawn based on results of the four studies explained in Chapters 3, 4, 5, and 6. It explains how the objectives are fulfilled and lists future works that can to be done to build on findings of this thesis.

1.5 Contributions

To achieve the objectives of this thesis, four studies were conducted. An FMG controlled prosthesis was assessed with a participant with an amputation, using a standard prosthetic socket and an off-the-shelf robotic hand in a protocol involving dynamic movements of the limb. The findings of this thesis showed that FMG is a valuable solution to assist individuals with amputations to control robotic prostheses. Moreover, in this thesis, factors were investigated that, if addressed, can potentially further improve the performance of FMG controlled prosthesis. Scientific contributions resulted from studies that were conducted for fulfillment of the objectives of this thesis are as follows:

- C. Ahmadizadeh, L.-K. Merhi, B. Pousett, S. Sangha, and C. Menon, "Toward Intuitive Prosthetic Control: Solving Common Issues Using Force Myography, Surface Electromyography, and Pattern Recognition in a Pilot Case Study," IEEE Robot. Autom. Mag., no. December, pp. 102-111, 2017.

- C. Ahmadizadeh, B. Pousett, and C. Menon, "Investigation of Channel Selection for Gesture Classification for Prosthesis Control Using Force Myography: a Case Study," Frontiers in Bioengineering and Biotechnology, vol. 7, no. December, pp. 1-15, 2019.

- C. Ahmadizadeh and C. Menon, "Investigation of Regression Methods for Reduction of Errors Caused by Bending of FSR-Based Pressure Sensing Systems Used for Prosthetic Applications," Sensors, vol. 19, no. 24, p. 5519, 2019.

- C. Ahmadizadeh, B. Pousett, and C. Menon, "Towards Management of Residual Limb Volume: Monitoring the Prosthetic Interface Pressure to Detect Volume Fluctuations - a Feasibility Study," Applied Sciences, vol. 10, no. 19, p. 6841, 2020.

Chapter 2

Background

The material presented in this chapter is excerpted, reproduced, and modified with permission from the following paper:

C. Ahmadizadeh, B. Pousett, and, C. Menon, “Investigation of Channel Selection for Gesture Classification for Prosthesis Control Using Force Myography: a Case Study,” Frontiers in Bioengineering and Biotechnology, vol. 7, no. December, pp. 1-15, 2019.

C.Ahmadizadeh, M. Khoshnam, and C. Menon, “Human Machine Interfaces in Prosthesis Control: a Survey",” IEEE SPM Special Issue on Signal Processing for Neurorehabilitation and Assistive Technologies, **Submitted**.

Sections of this chapter are reprinted or adapted from the above article for clarification and to fit the formatting and scope of this document.

2.1 Chapter Overview

This chapter provides background information about some of the technologies used in this thesis. First, some of the biosignals used for control of powered prosthesis that have attracted some attention in the research community are introduced. Then, a background on feature selection algorithms used for the second objective of this thesis is provided.

2.2 Human Machine Interfaces for Prosthesis Control

Various methods are used for control of powered prostheses depending on the type of the prosthesis being controlled. For body powered prosthesis, movement of healthy parts of user’s body or reaction forces of the environment are often used for control of the end effector

of the prosthesis. For externally powered prosthesis, more advanced control schemes have been introduced and explored since the introduction of these devices. Various invasive and non-invasive HMIs have been explored for control of powered prostheses, some of the these HMIs facilitate external switches and sensors. Some focus on the use of technologies such as computer vision and motion tracking, and others use biosignals to predict user's intentions. Hybrid methods have also been explored that combine various inputs from multiple HMIs to make prosthesis control more intuitive.

Some of the biosignal-based HMIs for upper limb prosthesis control that have gained interest in the research community are: gaze tracking [59], electromyography (EMG) [27], [28], Force myography (FMG) [34], electroneurography (ENG) [31], mechanomyography (MMG) [32], Electroencephalograhy (EEG) [37], and Electrocorticography (ECoG) [60].

In the lower limb powered prostheses, control is commonly based on state machines that are based on pre-defined locomotion modes such as flat surface walking, and stair ascent/descent. Traditionally, sensory systems used for control in this type of prostheses commonly consist of inertial sensors, force sensors at the bottom of the foot, joint encoders, etc. Recently, biosignal-based HMIs, such as EMG and FMG have also gain interest in the research community for control of such devices [19], [61], [35].

2.2.1 Electromyography (EMG)

EMG is the most widely used control technique for upper limb powered prosthesis; it has also shown promising results for lower limb prostheses [19], [33]. EMG monitors the electrical stimulation of the muscles that determine muscle activation [36]. From this information, muscle contraction can be inferred. Contrary to some of the alternative HMIs such as FMG, EMG can be used by individuals with higher levels of amputations as it monitors the electrical stimulation of the muscles rather than the state of the muscles' contractions directly. As a result, EMG is a suitable HMI for individuals having undergone the targeted muscle reinnervation (TMR) procedure in addition to individuals with higher levels of amputations. EMG signals are acquired through two methods which categorize the technique to two groups of surface EMG (sEMG) and internal EMG.

Internal EMG requires electrodes to be placed invasively in the muscles. Despite higher clarity of the signals acquired using this method in terms of cross-talk compared to sEMG, its invasiveness makes this technique less favorable [36]. Contrarily, sEMG can be acquired by placing electrodes on user's skin [36].

SEMG is the most commonly used technique in clinics and commercially available externally powered upper limb prostheses. SEMG is often used in these setups by placing two electrodes on the extensor and the flexor muscle bellies of the user. These electrodes are embedded in the prosthetic socket by prosthetists. In the lower limb prosthesis, sEMG signals obtained from muscles in the residual limb can be used to control a particular joints such as an active prosthetic knee [33].

Yang et al. conducted a study using sEMG with 10 participants with transradial amputations controlling a 5 degrees of freedom (DOF) prosthetic hand [62]. In this study, up to 8 sEMG electrodes were placed in the socket circumferentially so that they would be placed on users' muscle bellies. Reported accuracies range from 44.3% for 7 patterns to 95.5% for 5 motions.

Riillo et al. examined the use of sEMG for prosthesis control by having 12 healthy participants and one participant with transradial amputation perform 5 hand gestures while they collected sEMG signals from their limbs [63]. 6 sEMG electrodes were used in this study. They reported classification accuracy of 92.04% for the participant with an amputation and accuracies ranging from about 69% to 98% for healthy participants.

Geng et al. investigated the use of accelerometry information combined with sEMG signals for classification of hand gestures in a dynamic movement of the arm [64]. They had collected sEMG and tri-axial accelerometer mechanomyography (ACC-MMG) signals from five participants with amputations as they performed six arm and hand movements in five different arm positions. They reported classification error of 9% when signals were acquired from the residual limb.

Other studies considering sEMG for prosthesis control that have participants with amputations have reported classification accuracies of 81% to 90% for 4 to 11 classes of motion [38].

Hang et al. conducted a study that investigated detection of locomotion modes for control of lower limb powered prostheses using sEMG. Two individuals with transfemoral amputations participated in this study. Results of this research reported an average accuracy of approximately 86% for intent recognition using this HMI for recognition of six locomotion modes [65].

2.2.2 Force Myography (FMG)

FMG is an HMI used for intent recognition for various applications such as prosthesis control [66], [67], [56], [68]. For this purpose, FMG monitors volumetric changes in the residual limb which can be indicative of contraction or relaxation of muscles [69]. This information is then used to determine a movement of the limb or a movement intention. FMG has attracted attention in the research community due to its performance that is comparable to the more traditionally accepted HMIs such as sEMG, and also its potential to mitigate some shortcomings of these HMIs such as sEMG's sensitivity to environmental variables, cost of commercial electrodes, etc [21].

Volumetric changes of muscles that are tracked in this technique are often acquired through the pressure profile of the interface of the muscles and a rigid surface around it. This makes FMG especially practical in prosthesis control applications. For this purpose, a common method for FMG acquisition is to use force sensitive resistors (FSRs) at the interface of the residual limb and the prosthetic socket [20], [70]. FSRs are polymer thick film sensors made of multiple layers of conductive and semi-conductive materials. These sensors' resistances change as a function of the pressure applied on them.

Cho et al. investigated the use of FMG on four participants with transradial amputations. In this study, participants performed 11 grips in a static arm position [21]. They reported classification accuracies of 62.61% and 41.73% for 6 and 11 gestures, respectively, when signals were acquired from the residual limb and 78.67% and 66.34% when signals were acquired from participants' sound limb. In this study, sensors are embedded in a wrist band placed on participants' forearm without the use of a prosthetic socket.

Englehart et al., conducted a study in which they used a high density FMG (HD-FMG) apparatus consisting of 16 x 24 FSRs on 14 healthy participants and a participant

with transradial amputation [51]. They reported classification accuracy of 83.4% for the participant with an amputation for classification of 7 wrist and hand movements.

Radmand et al. also used a high density array of FSRs to classify 8 wrist and hand movements in a static and a dynamic protocol [54]. They collected data from 10 healthy participants and reported classification error of 0.33% for the static protocol. They showed that training their classifier in multiple positions of the dynamic protocol increased the accuracy they obtained for the dynamic protocol. The value of this error varies depending on the method they used for training and the number of positions at which they train their classifier.

Godiyal et al. conducted a study to investigate the use of FMG for gait event detection with applications such as prosthesis control in mind. In this study, FMG was used to detect the heel strike and toe-off events for five healthy individuals in both overground and ramp walking. They reported average detection errors of about 11 ms for heel strike and 47.63 ms for toe-off. Their proposed method obtained results comparable with those obtained using pressure measurement insoles, sEMG, accelerometers, and gyroscopes [35].

Younger et al. compared performance of FMG vs sEMG for gait phase analysis and determined a high correlation between the two signals. They reported that FMG pattern was more consistent from stride to stride compared to sEMG. This study suggests that these signals can be used for prosthesis control [61].

2.2.3 Electroneurography (ENG)

ENG is a technique that acquires signals from the peripheral nervous system (PNS). It requires electrodes to be implanted to directly interface with the PNS [36], [31]. Although the invasiveness of this technique makes it less favorable for the end users, it has the advantage of potentially being able to restore sensory function of the lost limb in addition to being able to extract information about movement intentions and providing sensory feedback [36], [31]. Another positive aspect of this kind of control is the intuitiveness of the control. This means that contrary to the more traditional EMG, there's no need for the user to go through a training phase where they learn unintuitive control sequences that allow for control of multiple actions with EMG [31].

Multiple studies have investigated the use of ENG for prosthesis control [71], [72]. Rossini et al. reported success rates of up to 85% for control of three movements in real-time using ENG with multiple electrodes interfacing with various nerves [36], [73]. Studies have also shown the possibility of finger movement control using ENG [36], [74]. It is suggested that using ENG, users can improve their ability to control their prosthesis over time [36].

Although the use of this HMI has been mostly investigated for control of upper limb prostheses [33], its use for control of lower limb prostheses has also been suggested. Tracing of the angle of ankle joint using this HMI has been explored and shown possible by Lin et al. The information about ankle joint angle can be used to control lower limb prosthesis [75]. It has also been suggested that providing sensory feedback using this method can potentially enhance the function of such prophetesses [76].

2.2.4 Mechanomyography (MMG)

In addition to EMG that monitors muscle activation, MMG (vibromyography) can be used for prosthesis control using information about muscle activation. MMG tracks vibrations emitted from the muscle on the event of contraction [77], [36]. Similar to sEMG, MMG data can be acquired non-invasively from the surface of user's skin. However, MMG is not as suitable as EMG for individuals with higher levels of amputations, especially those having undergone TMR. Vibrations monitored in MMG can be acquired using microphones, accelerometers, and piezoelectric contact sensors [77], [36]. Studies have shown that using MMG, an external prosthetic hand can be controlled [78].

Alves et al. showed that about 7 hand movements can be identified using MMG signals recorded from the forearm of 9 non-disabled participants with an accuracy of 90% [77]. They also reported classification accuracy of 98% for detection of five contraction patterns in a participant with an amputation.

Another study showed that four hand motions can be detected using MMG with classification accuracy of 79.66% [36]. Some studies suggest that MMG is more suitable for force estimation compared to gesture classification since the signal is more affected by the increasing force [36].

The use of mechanomyography for control of lower limb prostheses has also been explored. It has been suggested that this HMI has the advantage of being less sensitive to fatigue compared to the more traditional EMG which can especially enhance control of lower limb prostheses. MMG can be used for estimation of the force exerted by the muscle. This parameter can also be measured using force sensors, e.g. with the FMG HMI. Measured force can then be used for inverse dynamics calculations [33]. Wu et al. used MMG signals from thigh muscles of 8 healthy participants to classify 6 knee motions with powered prosthesis control application in mind. They reported classification accuracy of 88% [79].

2.2.5 BMI

Brain-machine interface can be used to control prosthetic devices. Many signals that can be acquired from the brain can be used for prediction of user's movement intentions [60]. These signals include neuron spike rates in the cortex, electroencephalography (EEG), electrocorticography (ECoG) signals, and functional near-infrared spectroscopy (FNIRS) signals [33].

Electrodes that record spiking rates of neurons need to be placed inside the cortex. This makes this method very invasive. On the other hand, EEG signals can be acquired non-invasively from the scalp. ECoG is an invasive technique but it does not require electrodes to penetrate the cortex [60]. ECoG provides signals with higher signal-to-noise ratio and higher spatial resolution compared to EEG [60], [80].

Electroencephalograhy (EEG)

EEG provides one of the most intuitive control schemes for robotic prostheses [37]. Compared to some of the other prosthetic control methods such as EMG and FMG, EEG is often acquired from a higher density of sensors and requires more post processing for feature extraction and feature selection to reduce complexity of the system and also to eliminate noisy signals to increase accuracy of intention prediction [36]. The use of EEG signals for prostheses control has been explored for both the upper and the lower extremity prostheses [33], [36].

Gugar et al. conducted a study that showed success rates in the range of 82% to 90% for control of a prosthetic hand by a healthy participant [37]. Studies have reported accuracies of up to about 70% for 5 movements using EEG signals [36].

A study conducted by Murphy et al. examined the feasibility of using this HMI to control a prosthetic knee and reported success rates of from 50% to 100% for the different test regimens in their protocol [81]. Brantley et al. determined correlation between difficulty of a locomotion task and EEG signals. Information about difficulty of a locomotion task can be used to identify transitions between different types of terrains during locomotion [82]. In another study, classification of left vs right leg movement in 12 healthy participants using EEG signals was examined by Rakshit et al. in which they reported the average classification accuracy of approximately 78% [83].

Electrocorticography (ECoG)

ECoG is an HMI based on the measure of cortical potential that can be used for prosthetic control in addition to other applications [36], [84]. This is an invasive method that requires electrodes to be placed on the surface of the cortex [37]. However, compared to some other invasive methods such as spike recordings, ECoG has the advantage of being less invasive. On the other hand, compared to the non-invasive EEG, it produces higher quality signals in terms of noise and spatial specificity [80].

ECoG is one of the more feasible clinical options for prosthesis control using cortical signals [36] since it occupies a middle ground in terms of pros and cons of neural signal extraction technologies [60]. Studies with patients with epilepsy show promise for detection of movements or intentions of movements using ECoG with accuracies that allow control of devices such as a computer cursor in up to two dimensions [36], [60]. Studies have shown the possibility of control of individual finger movements and gesture control using this signal [60]. Pioneers in utilizing this signal for prosthesis control have reported accuracies in the range of 68% to 81% for classification of five isometric gestures in three participants with epilepsy [37].

While the use of this HMI for prosthetic applications has mainly been explored for control of upper limb prostheses, detection of movements of the lower limb has also been

investigated in multiple studies [85], [86]. McCrimmon et al. conducted a study in which they were able to characterize the lower limb during walking of human participants using this HMI [87]. Such information can potentially be used for control of lower limb prostheses.

2.2.6 Hybrid HMIs

In prosthesis control, one of the factors affecting user satisfaction is the intuitiveness of the control scheme used. As the function of human body adapts to user's needs and abilities, an intuitive prosthetic system would be able to do the same [88]. Castellini et al. explains this with the example of grasping a pen for handwriting [88]. In this scenario, the grasp needs to be precise yet strong enough to be able to hold on to the pen as it moves against the paper. In today's prosthetic technology, the grip used to hold a pen is similar to that used to hold objects of similar shapes without any adjustments for the specific function of the grip.

A solution to this problem is to use hybrid systems that incorporate multiple indicators from the user to make prosthetic control more intuitive. It has been suggested that using hybrid HMIs can allow for a more intuitive and more stable control scheme [36]. It has also been suggested that using such control schemes can lower cognitive workload required for control of the system [33]. Although the use of multiple sensing modalities in theses HMIs increases cost and complexity, their potential to provide more intuitive control schemes makes them worthwhile for prosthetic applications. Some of the HMIs used in such multi-sensory systems used in these studies are inertial transducers, eye trackers, EMG, FMG, MMG, and EEG.

Cui et al. conducted a study to investigate the use of fusion of three HMIs, i.e. EEG, EMG, and MMG for detection of movement intentions of the lower limb. This study was based on data collected from 12 healthy participants as they performed 9 lower limb multi-joint tasks. They reported classification accuracies of up to 98.61% for classification of the 9 motions. This study reported that the fusion of these three HMIs outperformed the cases where only one of the HMIs or the fusion of two of them were used [89].

Brantley et al. suggest that one of the limitations of the widely used HMI for lower limb prostheses control, namely EMG, is its inability to detect transitions between different

modes of locomotion, e.g. stair ascent/descent vs. level ground walking. They proposed a solution based on a hybrid HMI consisting of both EMG and EEG to mitigate this problem. They showed the feasibility of detecting various modes of locomotion from EEG data collected from healthy participants[82].

Gaze Tracking

In a study, Castellini et al. proposed a hybrid system that facilitates gaze tracking, sensory data from pressure and tactile sensors and machine learning algorithms to advance prosthetic control. In this study, as a prototyping experiment, they use a teleportation setup to simulate control of a hand prosthesis. Their setup can successfully predict users intentions after a period of training and grasp a variety of objects [88].

The HMI used in this study is a hybrid of a sensory glove that provides information about the position of user's fingers and wrist, a magnetic tracker, and an eye tracker to determine location of user's gaze. User's gaze contain useful information in this scenario since its movement is voluntary and can be used to predict user's intention. By monitoring movements of user's eyes over a predefined time window, steadiness of their gaze, its fixation on an object can be determined. In this study, Castellini et al. use gaze tracking in combination with hand location since it is assumed that when the user's gaze is fixated on an object and they move their hand toward it, they intend to grasp the object [88].

In another study, McMullen et al. developed a Hybrid Augmented Reality Multimodal Operation Neural Integration Environment (HARMONIE) that uses computer vision and eye tracking in combination with EEG for control of modular prosthetic limb (MPL). The MLP is an advanced prosthetic limb with 17 controllable DOFs. McMullen et al. found that hybrid HMIs prevent almost all unintended initiations of the system which according to them is one of the main areas of improvement needed by users. In this study, computer vision was used to identify spherical objects in the work space, the result of which was provided to the user as a video on a monitor. Eye tracking was then used for object selection by the user through control of a mouse cursor on the monitor. EEG was then used to predict initiation of the reach signal to pick and place the selected object in a container. Results showed that

the participants were able to perform the task using HARMONIE in about 70% of trials after some training [90].

The use of gaze tracking has also been explored for control of lower limb prostheses. Duvinage et al. investigated the use of gaze tracking for control of active lower limb prostheses. They detected movements of the eye using electrooculography (EOG) which is a methods that places electrodes around the eye to record electrical activity of the eye ball [91]. In this study, eye movements are decoded and translated to control commands such as accelerate, decelerate, and stop. They suggest that their proposed method can be used for smooth transitions between walking speeds [92].

Hybrid HMIs show potential to mitigate some of the problems of prosthesis control that reduce user satisfaction. However, more work focused on a practical system design is required toward integration of these systems into a prosthesis that is portable and can be used on a daily basis.

2.3 Channel Selection

Channel selection or feature selection (FS) is a technique that reduces dimension of input data by removing irrelevant input variables while maintaining the ones with vital information in the selected feature subset that leads to no or little reduction of performance of the system [93], [94].

Feature selection is widely used in various fields due to its advantages such as decreasing the dimension of input features that leads to lower computational costs and removing the effect of noisy input which leads to increased classification accuracy. [95], [93].

Feature selection methods mostly involve iterations of two steps until their stopping criterion is met [96]. The two iterative steps are feature subset selection and evaluation of performance of the chosen subset [96]. FS algorithms utilize various search techniques for selection of feature subsets [96] based on which they fall under three main categories: filter methods, wrapper methods, and embedded methods [97], [98], [99].

2.3.1 Filter Methods

Filter methods generally rank features based on a scoring criterion with no dependence on the classifier [99]. "N" highest ranked features are then selected as the final feature subset. "N" depends on the predefined stopping criteria that can be either a percentage of total number of features [96], a threshold for the score assigned to the features [100], or a performance-based criterion which depends on how performance of the system is measured. Various scoring mechanisms are used in filter methods such as mutual information (MI), correlation coefficient, principle component analysis (PCA), and Chi-squared [96], [100], [99], [101].

2.3.2 Wrapper Methods

Wrapper methods select feature subsets base on their classification performance. These methods directly utilize the corresponding classifier as a wrapper for their search mechanism [102], [97], [95]. In wrapper methods, a feature subset is chosen using a search technique and then evaluated by assessing resulting classification accuracy when only chosen features are fed to the classifier [96]. These steps are repeated until stopping criteria is met [96].

Based on the search strategy used for feature subset selection, wrapper methods are divided to two main categories: sequential selection algorithms and heuristic search algorithms [100]. Sequential selection methods start with an empty (or full) set and features are added (or eliminated) in each iteration until stopping criteria is met [100], [96]. Some of the sequential selection methods are backward feature selection, forward feature selection, and sequential floating forward selection [100], [96]. In Heuristic search algorithms, feature subsets are created by solving an optimization problem or searching in a search space [100]. Some of the heuristic search algorithms mentioned in literature are genetic algorithm and hill-climbing [100], [99].

2.3.3 Embedded Methods

Embedded methods incorporate feature selection into classification's training process to reduce cost of re-classification in wrapper methods [100], [96]. Some of the embedded methods mentioned in literature are decision trees, random forest, and support vector machine

recursive feature elimination (SVM-RFE) [100], [99], [98]. [103].

Comparing the three categories of channel/feature selection methods, filter methods are expected to be faster as they do not need to perform classification tasks in their iterations. Wrapper methods, although slower in most cases, select feature subsets for the specific application in consideration as they assess the performance of the selected feature subset based on its classification performance in each iteration. The embedded method, compared to wrapper methods, reduces the cost of re-classification.

Chapter 3

Possibility of Using FMG for Control of Powered Prosthesis

The material presented in this chapter is excerpted, reproduced, and modified with permission from the following paper:

 C. Ahmadizadeh, L.-K. Merhi, B. Pousett, S. Sangha, and C. Menon, "Toward Intuitive Prosthetic Control: Solving Common Issues Using Force Myography, Surface Electromyography, and Pattern Recognition in a Pilot Case Study," IEEE Robot. Autom. Mag., no. December, pp. 102-111, 2017.

Sections of this chapter are reprinted or adapted from the above article to fit the formatting and scope of this document.

3.1 Chapter Overview

This chapter explains the case study conducted towards fulfillment of the **first objective** of this thesis which is to assess the possibility of using FMG for control of powered upper limb prosthesis in conditions that are relatively close to the real use case of the proposed system.

The factors being investigated in this objective - that limit generalizability of research conducted in constrained environments of the labs - are the use of a real prostheses and the dynamic movements of the limb. As explained in chapter 1, these factors have more significant effects in control of powered upper limb prostheses. As a result, the study conducted towards fulfilment of the first objective of this thesis focused on control of a robotic hand.

For this study, a custom prosthetic socket using either one or both FMG and EMG HMIs for gesture control was fabricated for the pilot participant with transradial amputation. The possibility of controlling up to 10 classes of motion in a dynamic movement of the arm was assessed. Moreover two configurations for placement of FSR sensors used for FMG were examined. An investigation was also carried out to determine whether a synergy of FMG and EMG performs better than one of those methods alone.

3.2 Introduction

During the past decade, several sophisticated robotic prostheses have become available in the market, yet the rejection rate for electric prostheses remains high [40] due to user dissatisfaction regarding issues such as cosmetics, comfort, function, ease of control, reliability, and cost [40]. Dissatisfaction in the control aspect is one of the main reasons that limit the rate of adoption of powered prosthesis. Problems such as limited reliability and lack of intuitiveness of control negatively impact user experience which my lead to prostheses abandonment. For advancements in prosthesis control, a reliable human machine interface is needed to be used for user intention recognition.

Various HMIs have been explored for control of powered prostheses, amongst which FMG has demonstrated to be a promising option that can potentially mitigate some of the traditional sEMG's shortcomings. Studies using FMG with pattern recognition have shown promising results that demonstrate potential for the use of this technology towards intuitive control of sophisticated externally powered prostheses [21]. Despite FMG's demonstrated promise to be a reliable HMI for prostheses control, this technology is not yet widely accepted for practical use. One of the main reasons that prevent adoption of such systems for real-life applications is that these systems are developed and tested in constrained environments of the labs. Most studies conducted to assess functionality of FMG for prosthesis control have carried out their assessments using non-disabled participants and with static protocols. This limits generalizability of results obtained in these studies since factors such as the weight of the prosthetic device and the dynamic movements of the limb can have considerable effect on performance of these systems.

In the study presented in this chapter, the use of an FMG controlled prosthesis is assessed in conditions that are relatively close to the real use case of the device. The findings of this study showed that FMG is a suitable solution for individuals with amputations to control their robotic prosthesis.

3.3 Material and Methods

3.3.1 Participant

This pilot case study was conducted on a 59-year-old right-handed male participant with acquired transradial amputation of the left arm due to a work accident in 1980. His current prosthetic device is a body-powered mechanical hook. The participant used a myoelectric prosthesis for two years but abandoned the device due to multiple factors, such as a lack of reliability in control, slow response, and unsuitability of an electric prosthesis to his career and lifestyle.

3.3.2 Hardware

The main objective of this study was to investigate the possibility of an FMG-based HMI in a near-to-real-case scenario where the HMI was embedded in the prosthesis of an individual with an amputation using an off-the-shelf robotic hand and performing a protocol with dynamic movements of the limb. To achieve this goal, all system components were designed to maximize portability, compatibility with the current standards of prosthetics, and repeatability of use. All standalone system components were embedded in a custom prosthetic socket so that the system was comparable to a standard myoelectric prosthetic device in portability.

The robotic hand used in this experiment was a large size Bebionic 3 prosthetic hand loaned from Steeper Group - producer of Bebionic at the time. The Bebionic hand was attached to a custom fitted prosthetic socket. The total mass of the system was 1.523 kg. This includes the Bebionic hand: 598 g and the rest of the system including electronics and battery: 925 g. The sensory unit of the arm consisted of two 13E200 Ottobock MyoBock Electromyography electrodes and 5 FMG based sensor strips each consisting of 16 force sensitive resistors (FSRs). Sensory data was acquired through a custom designed cape for

the Beaglebone Black (BBB) development board which was the main processing unit of the system. In this study, BBB was chosen as our processing unit since it could facilitate the rapid realization of a functional prototype. An easy to use user interface was provided on the outer prosthetic socket that contained buttons and LEDs for user input and feedback which is shown in Figure 3.1.

Electronics were placed in a box between the inner and outer sockets and powered by the BeBionic hand's Lithium-ion polymer battery (1300 mAh, 7.4 V). The box was part of the custom prosthetic socket structure and had slits for FSR strip tails to be inserted inside the box and connected to the board.

FMG Sensor Strips

Each of the five custom printed FMG strips used in this research contained 16 0.5 inch sensors (Force Sensitive Resistors(FSRs)) in a row. The individual sensors had similar electrical properties to the Interlink Electronics' FSR 402 sensors. Dimensions of the FSR strips were: 0.75 inches wide, 11.02 inches long with a tail of 2.37 inches. These sensor strips were fixed inside the prosthetic inner socket using adhesive glue and were in contact with the participant's residual limb.

Although each sensor strip contained 16 individual sensors, not all the sensors could reside inside the inner socket due to space constraints. The sensors that were inside the inner socket and were in contact with participant's residual limb are referred to as active sensors in this chapter. The number of active sensors depended on specific placement of the sensor strips inside the inner socket and varied for the two FSR placement configurations described later.

Electronic Cape

The electronic cape was designed to acquire data from sensors and provide these data to our custom-written pattern recognition software running on the processing unit, BBB, through universal asynchronous receiver/transmitter communications. The board was designed to stack on the BBB board headers for communication. The cape consisted of zero insertion force connectors providing a link to the sensor strips, a voltage regulator, con-

nectors for the EMG sensors, connectors for transferring control signals to the hand and the user interface, voltage dividers for FMG signals, and two programmable system-on-chip (PSoC) Cypress (San Jose, California) chips (CY8C4247AXI-M485), each containing 48 general-purpose input/outputs for sensor data acquisition. The cape is shown in Figure 3.1.

The board could acquire data from up to 78 FSR sensors. This function was executed by providing individual sensors on the strips with 3.3 V serially and reading voltage values through a voltage divider with resistance value of 10 kΩ by the analog-to-digital converters on the Cypress chips.

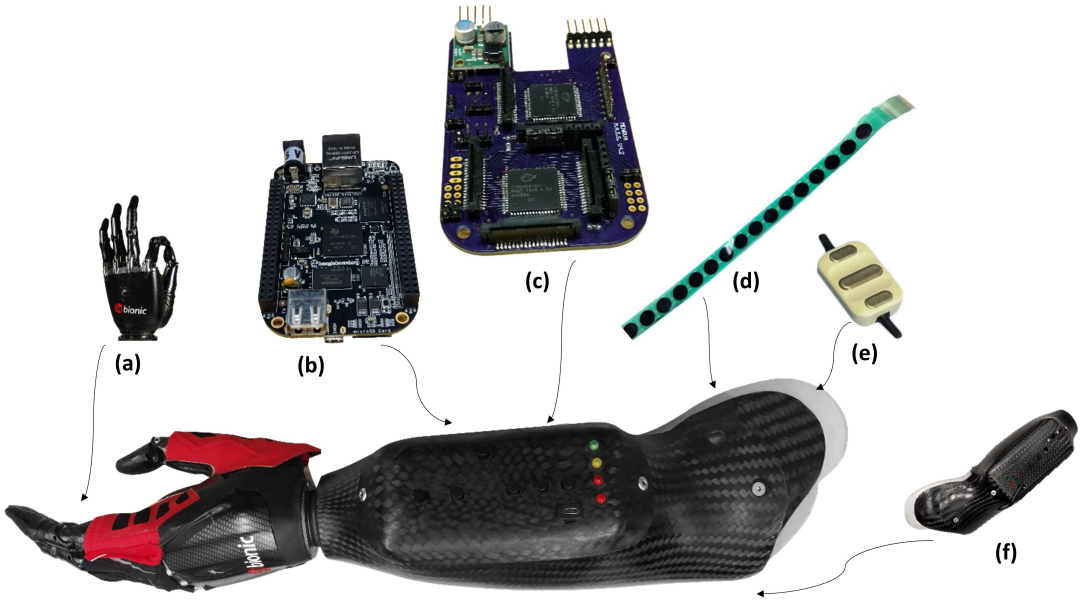

Figure 3.1: Main components of the system: (a) a bebionic 3 robotic hand (b) the BBB development platform (c) the Custom-made cape (d) an FSR strip (e) an EMG electrode from LTI (http://www.liberatingtech.com), and (f) a prosthetic socket. Reproduced from [20] © [2017] IEEE with permission.

3.3.3 Software

The software was composed of two main components: firmware for the Cypress chips and firmware running on the BBB. Communication between these two components was of the master/slave type, where the BBB initiated commands and sent them to the Cypress chips. The chips executed the commands and sent the results back to the BBB development board. Sensor data were sampled at 10 Hz because the dynamic of human hands has a

frequency lower than 4.5 Hz [104]. Thus, the Nyquist limit provides that a sampling rate of 10 Hz is great enough to capture hand motion. System structures for offline and online data acquisitions and analysis are shown in Figures 3.2 and 3.3, respectively.

Training Procedure for Real-Time System Use

To use the system online, the participant was required to record at least one repetition of the multiple different grips he wanted to accomplish for training purposes. Then, with the provided interface, the user could build the predictive model and start using the bebionic 3 hand. The minimum number of grips was three, and the maximum was set to 14 (the total number of configurable grips provided by the bebionic 3). The labeling of the grips was hard-coded into the program, and these labels were then used to send proper control signals to the robotic hand. The first three grips were relax, open, and closed fist (force), which simulated the conventional on-off control.

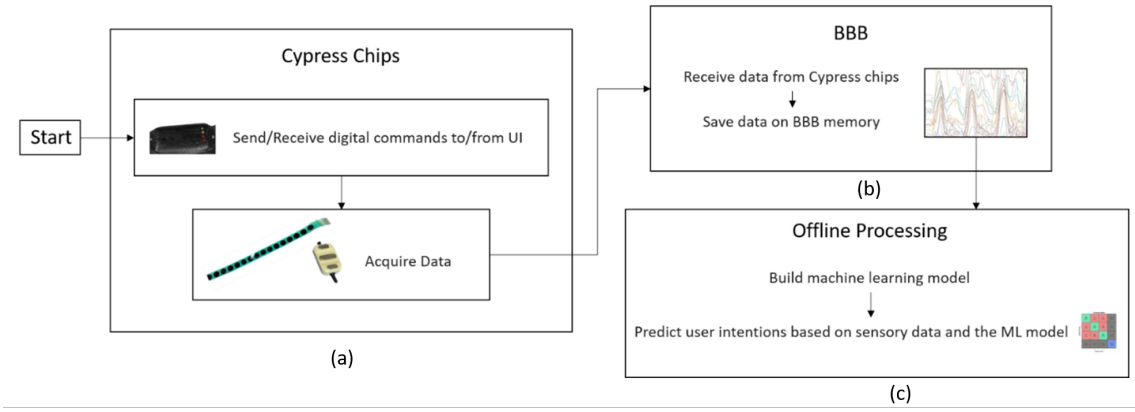

Figure 3.2: The software architecture for experimental data collection and offline processing. (a) The sensory data collection is started by the user interface (UI) and performed by Cypress chips. (b) The BBB receives and saves sensory data. (c) Offline processing uses recorded data to obtain results. Reproduced from [20] © [2017] IEEE with permission.

3.3.4 Experimental Setup and Protocol

All of the experiments carried out for this study were approved by the Simon Fraser University Office of Research Ethics in Burnaby, British Columbia, Canada. Although several studies have been done to investigate various HMIs for static control of prosthetic hands,

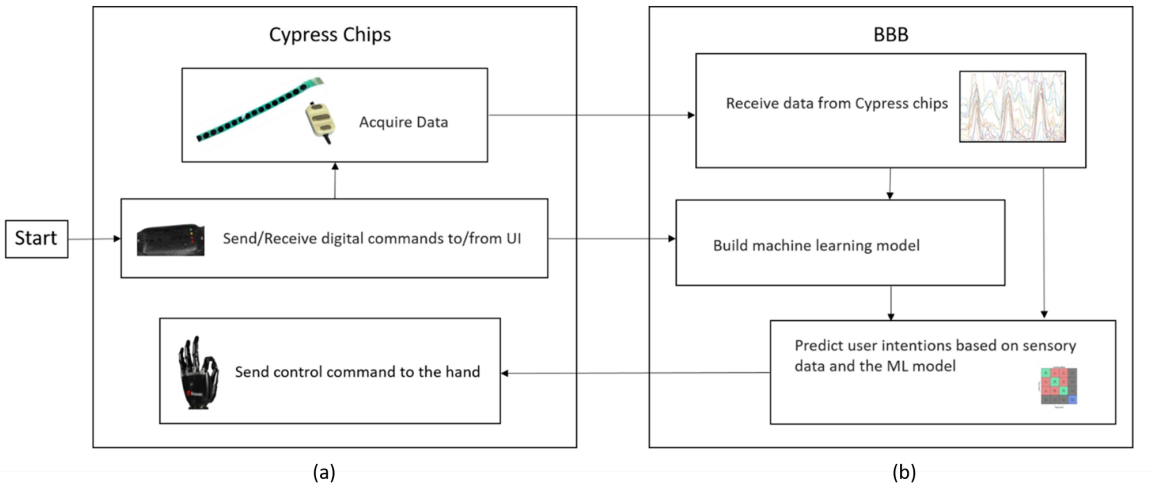

Figure 3.3: The software architecture for online use of the device. (a) Cypress chips interact with the UI, acquire sensory data, and send control signals to the bebionic 3 hand when commanded. (b) The BBB receives data, builds a machine-learning model, and executes real-time prediction. Reproduced from [20] © [2017] IEEE with permission.

dynamic motions are better representatives of a real-case scenario of prosthesis usage. Because this study's objective was to investigate a practical system, all experimental data were recorded using the dynamic protocol [54] shown in Figure 3.4. The dynamic protocol required the participant to move his arm in a circular motion through the humeral plane to cover the area used for most ADL. This dynamic protocol is consistent with other studies [105].

The dynamic protocol examined ten classes of upper-extremity motion comprising six grip patterns (relax, open, force, tripod, finger point, and key) and four gross-arm movements (wrist extension, wrist flexion, supination, and pronation), as shown in Figure 3.5. These specific classes of motion were chosen to include two separate groups: 1) six primary grips for ADL [106](relax, open, force, tripod, finger point, and key), and 2) eight classes of motion consistent with other research groups [54](relax, open,force, tripod, wrist extension, wrist flexion, supination, and pronation). Compared to the cited study [54], the pinch grip was replaced by a tripod grip because it is one of the primary grips of bebionic 3 and its corresponding muscle activation is similar to a pinch. When performing the dynamic protocol, each motion was held for 15 s and executed five times.

The effects of two factors on the performance of the device were studied: 1) the impact of different FSR configurations inside the socket and 2) the impact of EMG features on classification accuracy.

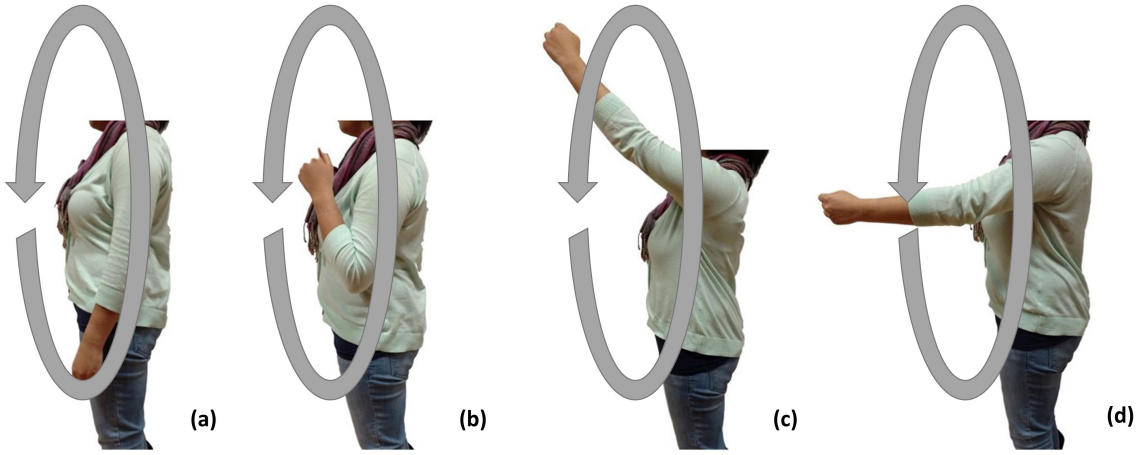

Figure 3.4: The dynamic protocol: in one iteration, the user traverses positions (a), (b), (c), (d), and (a) in the stated order. Reproduced from [20] © [2017] IEEE with permission.

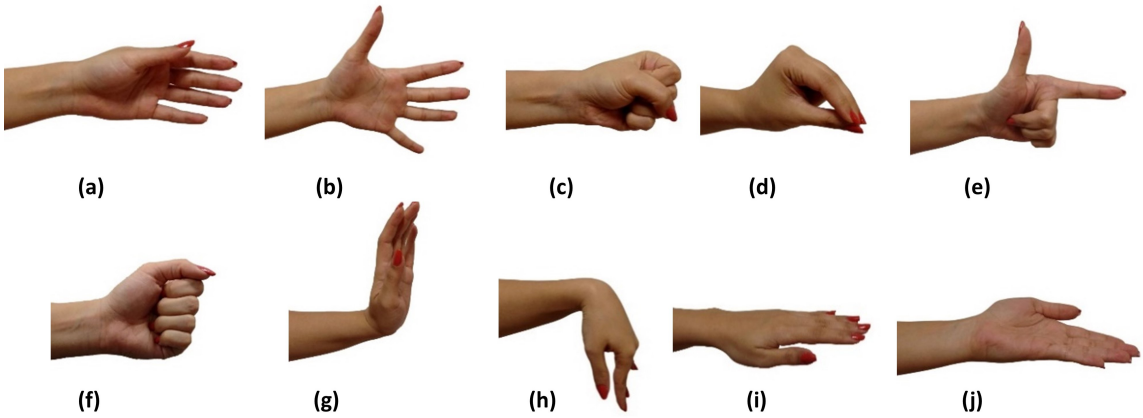

Figure 3.5: The classes of motion: (a) relax, (b) open, (c) force, (d) tripod, (e) finger point, (f) key, (g) wrist extension, (h) wrist flexion, (i) pronation, and (j) supination. Reproduced from [20] © [2017] IEEE with permission.

FSR Placement

One factor affecting system performance was the position of FSR sensors inside the inner socket. Two different configurations, A and B, were investigated and compared [as shown in Figure 3.6(a) and (b)]. In configuration A, FSR strips 1 and 3 were placed on the ex-

tensor muscles, and sensor strips 2 and 4 were placed over the flexor muscles. These four sensor strips were placed so that they would cover the muscle bellies while not covering the EMG sensor cutouts. FSR strip 5 was placed circumferentially over the muscle bellies. In configuration B, FSR strips 1 and 2 were positioned just distal to EMG sensors to capture the maximum amount of contraction of the extensor and the flexor muscles. In this configuration, sensor strip 3 was placed where sensor strip 1 was located in configuration A, and sensor strip 4 remained in the same location in both configurations. FSR strip 5 was placed on the anterior side of the forearm.

The number of active FSR sensors in the two configurations differed. In configuration A, 58 active sensors were embedded in the inner socket; however, to avoid the cutouts provided for EMG sensors, these strips could not be placed directly over the muscle bellies, with the most palpable deformation during contractions controlling gross hand movement. In configuration B, two of the FSR strips were placed directly on the muscle bellies under the EMG sensors; however, this resulted in a lower number of active sensors (37). The other difference in these two configurations was the fifth sensor strip. In the configuration A, it covered the muscle bellies circumferentially, while, in configuration B, the fifth FSR strip was placed so that it could catch the effect of the weight of the socket during vertical dynamic movement.

3.3.5 Data Analysis

Data analysis was performed on the four classes of motion groups represented in Table 3.1. The analysis was performed offline. To examine the performance of the system in different experiments, machine learning accuracies were compared. Numerous machine learning algorithms have been used in similar studies to classify hand gestures. In this study, we examined three algorithms that are among the most popular reported in literature: k-nearest neighbors (kNN), support vector machine (SVM), and linear discriminant analysis (LDA) [107]. Classification accuracies were obtained through a five-fold leave-one-out cross validation (LOOCV) method, withholding one repetition at a time for testing. This method has been widely selected in similar studies as it takes into account that factors such as muscle fatigue and swelling affect the signals used in the FMG HMI over time. As a result, there

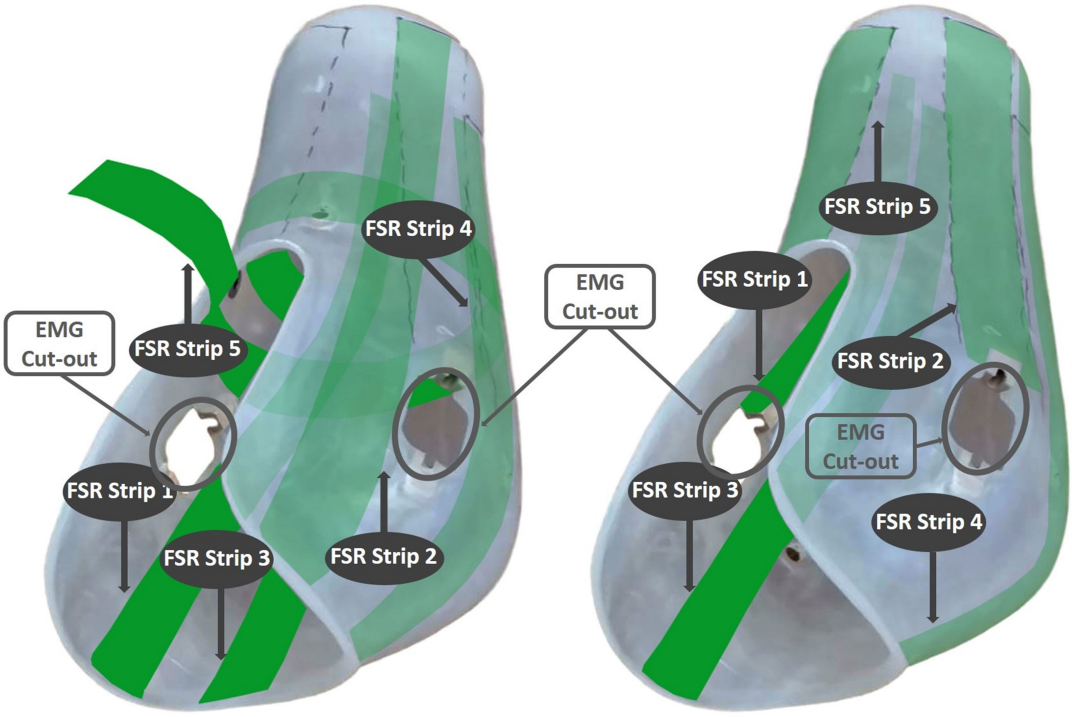

Figure 3.6: The FSR placement: configuration A on the left and configuration B on the right. Reproduced from [20] © [2017] IEEE with permission.

is more variability in signals as times goes on, *e.g.* between the first and the last repetitions compared with between the first and the second repetitions. Withholding one repetition at a time for testing in the k-fold leave-one-out cross validation, when k equals the number of repetitions, without shuffling of data, takes into account such variability in signals over time and thus is more representative of the practical application of the HMI for prosthesis control compared with its alternatives.

The reported results are the mean and standard deviation of the accuracies obtained by leaving out each of the five repetitions.

Addition of EMG Features

One of the factors examined in this study is the effect of including EMG signals as additional features. For this investigation, the classification accuracies obtained using FSR signals alone were compared to classification accuracies that resulted from the combination of FSR and EMG signals. EMG signals were extracted from two EMG sensors placed inside

Group Number	Number of Classes of Motion	Classes of Motion	Reason
1	3	relax, open, force	Represent the on-off performance of conventional myoelectric
2	6	relax, open, force, tripod, finger point,key	These are identified as primary grips for ADL
3	8	relax, open, force, tripod, wrist extension/flexion, supination, and pronation	consistent with previous studies
4	10	relax, open, force, tripod, finger-point, key, wrist extension/flexion, supination, and pronation	all the classes of motions performed in this study

Table 3.1: The classes of motion groups investigated in this study. Adapted from [20] with permission.

the inner socket and positioned on the flexor and extensor muscle bellies. The EMG electrodes' outputs were digital signals. The presented results are obtained by concatenating raw EMG signals to FSR signals as input features to the classifier.

3.4 Results

3.4.1 Classification Algorithm

Three classification algorithms were examined: kNN, SVM, and LDA. To investigate the performance of these algorithms on this study's data, classification accuracies for all presented cases were calculated and compared. This study was composed of two parts: FSR placement and the addition of EMG, which included a total of three different sensor configurations (FSR and EMG). Four groups of motion classes were studied in each configuration.

The kNN was not promising for the data obtained in this study. Maximum accuracy was reached with a number of neighbors (k) equal to one in most cases, which was in the range of 65% to 70% for ten classes of motion, while validation accuracy for the same model was within the range of 94% to 97%. This indicates that the model overfits training data. Increasing the value of k decreased the difference between the test and validation accuracies while also decreasing validation accuracy. At approximately k = 30, this difference was decreased by roughly 40%, which indicated that the model created with k = 30 was more generalized as compared to the one created with k = 1, according to the bias-variance

tradeoff [106]. At this value of k, test accuracies were within the range of 68% to 72% for ten classes of motion.

Multiple kernels were tested for SVM to find the most suitable one for this experiment's data, and the Gaussian kernel produced the best results. Gaussian SVM's hyperparameters were optimized for each case using cross validation, with 20% of the training data used for validation and 80% for training the model. As previously mentioned, LDA and SVM accuracies were obtained using the LOOCV method by leaving out each repetition (20% of all data in each experiment) and averaging the results for five repetitions. These accuracies are shown in Figure 3.7. The difference between these algorithms' results is inconsiderable relative to obtained standard deviations. To compare our results with a study [54] focused on dynamic protocols, classes of motion, and HMI that are similar to the ones used in this study, the rest of the offline data analysis described in this study used the LDA classification algorithm.

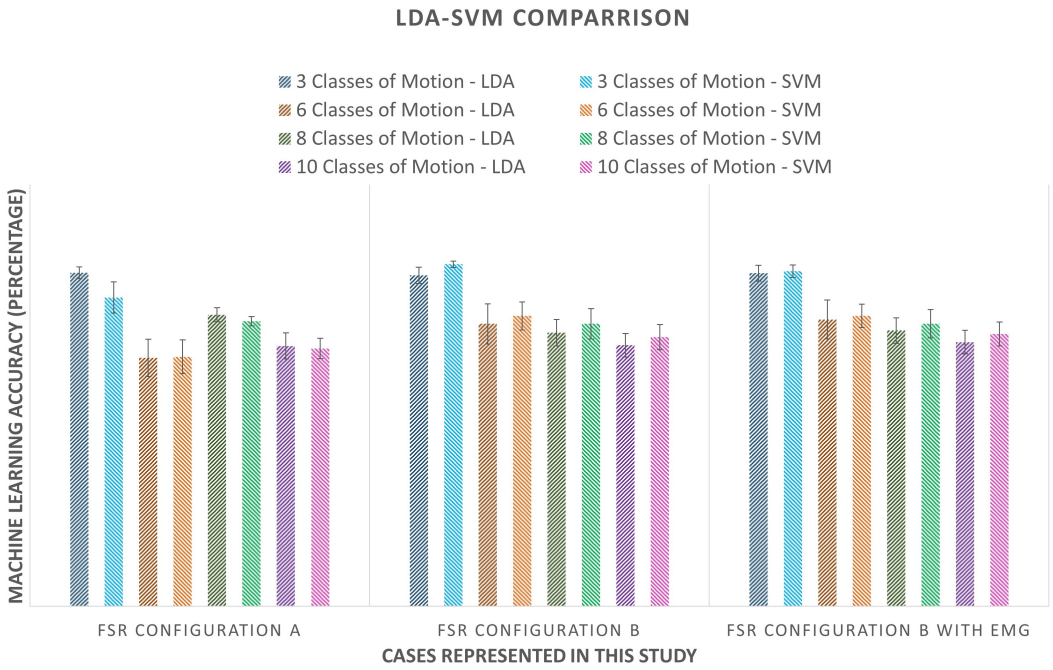

Figure 3.7: The classification accuracies obtained by SVM and LDA algorithms. Reproduced from [20] © [2017] IEEE with permission.

3.4.2 FSR Placement

Neither of the configurations performed better for all groups of motion classes. The configurations performed similarly for the groups containing three grips and ten classes of motion. Configuration B resulted in a better performance (9.7% increase in mean classification accuracy) in six motion classes compared to configuration A, while configuration A performed better (5.1% increase in mean classification accuracy) in eight motion classes. The results obtained by the two configurations are shown in Figure 3.8.

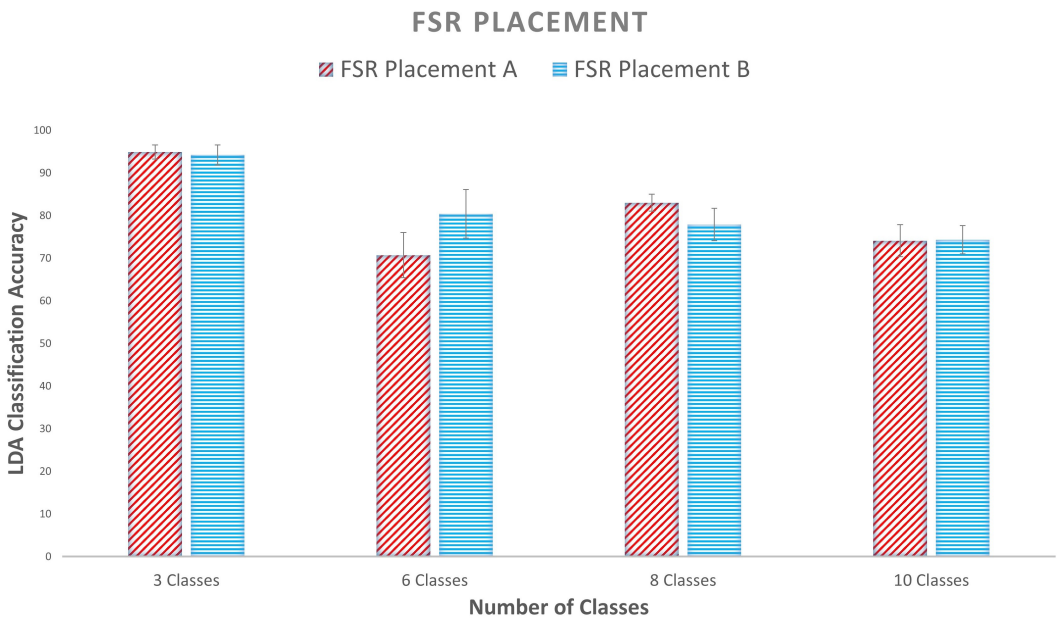

Figure 3.8: The classification accuracies obtained for sensor placement investigation of three grips, six grips, eight classes of motion, and ten classes of motion. Reproduced from [20] © [2017] IEEE with permission.

3.4.3 Addition of EMG Features

The accuracies after adding EMG sensor data for the four groups of motion classes did not increase considerably, as shown in Figure 3.9. The average increase for the four groups was roughly 0.83 $\pm$ 0.29%. Although an increase can be observed in classification accuracies after the addition of EMG, this increase in small relative to standard deviations.

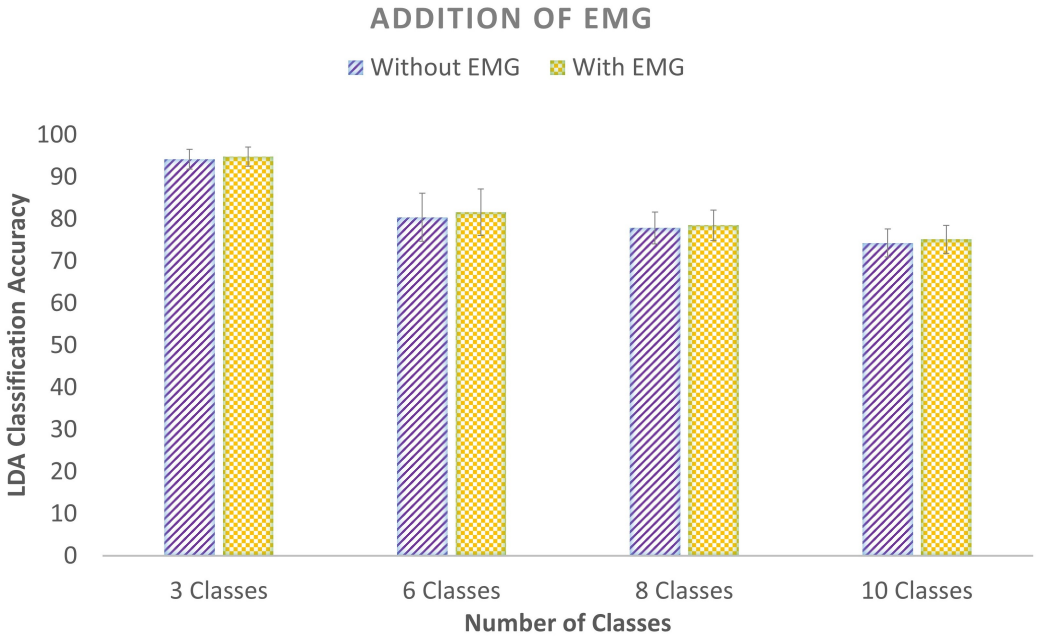

Figure 3.9: The classification accuracies obtained for addition of EMG for three grips, six grips, eight classes of motion, and ten classes of motion. Reproduced from [20] © [2017] IEEE with permission.

Groups of Classes of Motion	FSR Placement A, without EMG	FSR Placement B, without EMG	FSR Placement B, with EMG
3 Classes	94.9%± 1.7%	94.2%± 2.3%	94.8%± 2.3%
6 Classes	70.7%± 5.3%	80.4%± 5.7%	81.6%± 5.5%
8 Classes	83.0%± 2.0%	77.9%± 3.8%	78.5%± 3.6%
10 Classes	74.1%± 3.7%	74.3%± 3.3%	75.2%± 3.3%

Table 3.2: The classification accuracies obtained in this study for three grips, six grips, eight classes of motion, and ten classes of motion. Adapted from [20] with permission.

3.5 Discussion

3.5.1 FSR Placement

As presented in the "Results" section, configuration B provided a better performance (9.7% increase in mean classification accuracy) in six classes of motion as compared to configuration A. However, classification accuracies obtained from the two configurations were not considerably different for three classes. This shows that configuration B was able to capture the muscle movements responsible for three additional grips, tripod, key, and finger

point, better than configuration A. This is likely because the change in the placement of the bands resulted in more sensors being located over the bellies of the muscles that were activated in finger movements rather than in gross hand movements. However, configuration A performed better (a 5.1% increase in mean classification accuracy) in eight motion classes. This is because the last four motion classes in this group could be significantly distinguished through more gross hand movements.

For ten motion classes, the performance was almost similar for the two configurations. This is because the ten classes included both motion classes that involved gross hand movements and fine finger movements. The slightly better performance of configuration B for three and ten motion classes is believed to be due to the placement of sensor strip 5, which can make different motion classes more differentiable during vertical dynamic movement. (See Table 3.2 for a summary of these classification accuracies.)

In a study [54], Radmand et. al. reported a classification accuracy of 89% using high-density FMG and a dynamic protocol similar to the one used in this study, with motion classes similar to the motions in group number 3 in Table 3.1. The aforementioned study used ten healthy participants. In this study, we obtained a maximum classification accuracy of $83\% \pm 2\%$ for the 8 classes of motion (FSR configuration A: 58 FSRs) and similar dynamic protocol using one participant with transradial amputation. The decrease in classification accuracy is believed to be due to the weight of the prosthetic socket and the prosthetic hand and also to a degeneration of the forearm muscles in the participant with amputation, which resulted in the production of less distinguishable signals.

3.5.2 Addition of EMG

With the addition of EMG signals as extra features to FMG signals, there was a consistently slight increase in classification accuracies for all groups of motion classes. The increase in mean accuracy for the different categories ranged from 0.6% to 1.2%. The amount of increase in classification accuracies was small compared to their standard deviations. This result shows that FMG can capture most of the information EMG can and thus shows high potential as an alternative to EMG.

3.5.3 Cybathlon

The device described in this study was used to participate in the upper-extremity category of the 2016 Cybathlon. This category consisted of six main tasks representing ADL. Based on the information provided by Cybathlon organizers, these tasks were recreated to be used for training before the competition. Then, a task-specific dynamic training protocol was employed. The training consisted of six sets of data, each including three grips: relax, open, and close. Each of the grips was held for 15 s as the participant was mirroring the performance of one of the competition tasks while using our recreated setup. All six data sets were then used to train the model used on the day of the competition. The confusion matrix in Figure 3.10 shows the classification accuracy obtained for the three grips that applied the training data used for the competition. The analysis appropriated the same LOOCV technique used in all of the offline analysis reported in this study.

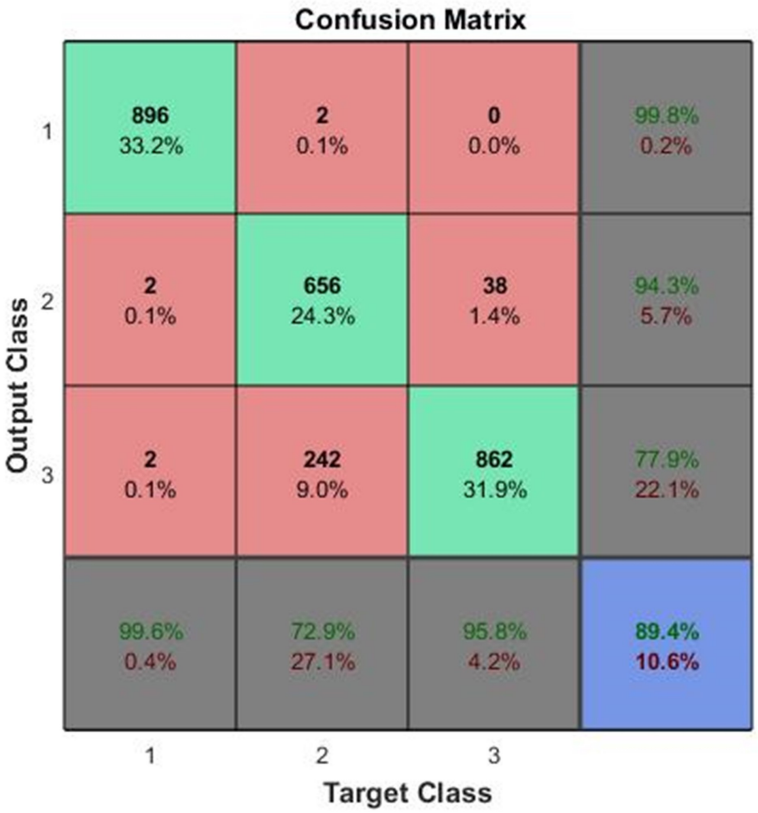

Figure 3.10: The confusion matrix for the three-class problem used for the 2016 Cybathlon. Classes 1, 2, 3 are relax, open, and force respectively. Reproduced from [20] © [2017] IEEE with permission.

Chapter 4

Possibility of Reduction of System Complexity in High Density FMG Systems

The material presented in this chapter is excerpted, reproduced, and modified with permission from the following paper:

C. Ahmadizadeh, B. Pousett, and C. Menon, "Investigation of Channel Selection for Gesture Classification for Prosthesis Control Using Force Myography: a Case Study," Frontiers in Bioengineering and Biotechnology, vol. 7, no. December, pp. 1-15, 2019.

Sections of this chapter are reprinted or adapted from the above article for clarification and to fit the formatting and scope of this document.

4.1 Chapter Overview

This chapter explains the case study conducted towards fulfillment of the **second objective** of this thesis. In this study, possibility of using a design method is examined that uses a high density FMG device to customize a simpler, less costly FMG controlled prosthesis that can achieve performance comparable to that of high density FMG.

The study outlined in this chapter was motivated by the results of the study conducted towards fulfilment of the first objective of this thesis. Since the focus of most high density FMG research is on upper limb prostheses [51], [54], and to build on the work of the first study, this study continues to focus on upper limb prostheses. The methods used in this study can also be used for lower limb prosthesis.

4.2 Introduction

The quality of life of an individual with an amputation could be drastically affected by their decreased autonomy as a result of the loss of their limb [59]. Powered prostheses can provide users with means to gain back some of the lost functionality of their limb and subsequently increase their self-sufficiency. Reliability and intuitiveness of prostheses control play important roles in user experience and are amongst factors lack of which can lead to prostheses abandonment [42], [20]. Issues concerning these factors are commonly addressed through advancements in robustness of human machine interfaces (HMIs) used for prostheses control and through the use of pattern recognition for more intuitive control.

Various invasive and non-invasive HMIs have been introduced for the control of powered prostheses. Recent studies have demonstrated FMG to be a promising HMI for powered prosthesis control [56], [20], [21], [54], [108]. FMG monitors changes in volumetric pattern of user's forearm and detects intentions of the user based on these changes [109]. Various methods are used to monitor these volumetric variations, one the most common of which is the use of force sensitive resistors (FSRs) [56], [66].

A study by Jiang et al. showed that FMG has the potential to outperform the more traditionally accepted HMI, i.e. sEMG, for hand gesture classification [56]. In this study, Jiang et al. reported classification accuracies of as high as 83.5% for 48 static hand gestures using 8 FSRs with 12 healthy participants. Cho et al. reported 62.61% and 41.73% classification accuracies for 6 and 11 static hand gestures, respectively, by placing eight FSRs on the residual limbs of 4 participants with transradial amputations [21].

High density FMG (HD-FMG) is a potentially enhanced alternative for low density FMG. Belyea et al. conducted a study to demonstrate possibility of using high density force myography - by using a grid of 16 by 24 pressure sensors - for proportional control of upper limb prostheses [51]. Radmand et al. also investigated high-density force myography for upper limb powered prosthesis control [54]. Despite the potentially increased performance of high density sensory systems, their higher cost in terms of computation, signal acquisition hardware, and problem complexity can lead to their incompatibility for many applications. A system with reduced complexity is less expensive, less prone to failure, lighter, easier to

calibrate, easier to fabricate and maintain, and thus, has a higher chance of being adopted in practice. The wide use of EMG controlled prostheses with only two electrodes in clinical and commercial devices provides evidence that reduction of complexity is important for practical applications of prosthetic devices. Reduction of complexity of HD-FMG systems could be possible through the use of channel selection.

Channel Selection (CS) is a technique that reduces the dimension of input data by removing irrelevant input variables while maintaining the ones with vital information in the selected feature subset. The final channel subset leads to no or little reduction of performance of the system [94],[93]. In cases without feature extraction such as this study, input channels - sensor data in this study - and input features are the same [110], and channel selection is the same as feature selection. Moving forward, in this chapter, the term 'feature selection (FS)' is used due to its more common use in this field and others.

The use of feature selection in gesture classification has been explored in multiple studies. Wang et al. conducted a study to investigate the feasibility of using FS for channel optimization of sEMG for gesture recognition. In this study, they used Genetic Algorithm to select channels based on data recorded from 6 able-bodied participants performing 13 gestures. They reported classification accuracy of 72.3% (97% of maximum accuracy that is obtained using all channels) after 0.125% reduction in the number of channels [111]. Li et al. also conducted a study in which they performed channel selection for both sEMG and EEG that were used in fusion for control of upper limb prostheses. This study investigated data from four individuals with amputations performing five motion classes. In this study, Sequential Forward Selection was used for channel selection from 32 sEMG and 64 EEG channels. They reported classification accuracies of 84.2% and 87.0% for two optimized channel numbers (10 sEMG and 10 EEG channels, 10 sEMG and 20 EEG channels). The maximum classification accuracy (91.7%) was obtained when all channels were used [112].

Dimension reduction for the FMG HMI systems has been attempted by Jiang et al. [56] and Radmand et al. [54]. Jiang et al. utilized a sequential forward feature selection algorithm for selection of 8 sensors out of a total of 16 sensors [56]. They reported a statistically significant decrease in accuracy of the system due to this reduction in the number

of sensors [56]. Radmand et al. conducted a study that used channel reduction to reduce input dimension. In this study, reduction of groups of channels was investigated. Channels were grouped based on location of their corresponding sensor in the matrix. They reported that they were able to maintain classification accuracy with a lower density of sensors with some of the channel reduction options they explored [54]. To the best of our knowledge, no study has attempted feature selection for high density FMG without grouping sensors based on their location.

In addition to the robustness of the HMI used for prostheses control, intuitiveness of control also affects prostheses user satisfaction. Pattern recognition plays an important role in enhancement of this aspect of user experience in prostheses applications. Various classification methods have been assessed for FMG controlled prostheses, some of the commonly used ones of which are linear discriminant analysis (LDA), support vector machine (SVM), and k-nearest neighbors (KNN) [107],[20]. Amongst these, LDA is one of the most widely used classifiers due to its capability in separating different classes of gestures and also its computational efficiency [113], [54], [21], [113]. A study by Ahmadizadeh et al. compared performance of the three aforementioned classifiers for gesture classification using FMG data and determined LDA to be the classifier of choice for their study [20].

Although FMG has been processed with various classification methods in different studies, in most cases, the difference between them was not statistically significant[20], [54],[21],[113], [68]. Whereas, the influence of feature selection, which is the focus of this study, is critical in this experiment. As a result, for all classification purposes LDA was used in this study due to its good performance for baseline accuracy (which is the leave-one-out cross validation accuracy (LOOCV) using all features), and its simplicity.

This study explores the use of feature selection for dimension reduction in a high density FMG system without grouping sensors. This is done towards the goal of achieving a design method that uses feature selection for FMG HMI to achieve performance of high density FMG in systems with lower cost and complexity. This could be attained by collecting data from the user with a high density system, determining location of features with the most contribution to gesture recognition, and finally designing a custom device for the individual

that embeds sensors in selected locations. To examine the possibility of this method, feature selection methods were assessed for reduction of input dimension in this case study.

Three datasets were used in this study. All three datasets were collected from the same individual with a transradial amputation using the same custom-made socket with FMG sensors embedded inside to control an off-the-shelf prosthetic hand. All datasets were collected using protocols including the same six gestures essential to activities of daily living. One of the datasets was collected using a static protocol and the other two with a dynamic protocol. Different sensor configurations were used in these datasets. The three datasets were used to include data from various sensor configurations, sample sizes and with both static and dynamic protocols. The analysis performed on all datasets was the same. This is a case study based on one specific individual and a specific prosthetic device used. For this experiment, a custom-made prosthetic socket was used to be compatible with the off-the-shelf prosthetic hand. For this reason and also due to the difficulty of recruiting participants with amputation, all datasets were collected from one individual.

This study explored the use of four feature selection algorithms for the three collected datasets. These algorithms contain one commonly used method from each category of FS algorithms: sequential forward selection (SFS), minimum redundancy, maximum relevance (mRMR), Genetic algorithm (GA), and Boruta (an embedded method that uses Random Forest (RF)). These are explained in more detail in the 'Materials and Methods' section.

Findings of this study indicated that mRMR, GA, and Boruta were able to decrease the number of input features considerably without significantly decreasing classification accuracy. This shows the possibility of the proposed method to use HD-FMG in the design phase to reduce complexity of custom FMG controlled prostheses without compromising the performance of the system.

4.3 Materials and Methods

This section explains the materials and methods that were used to conduct data collection and data analysis for this study. A high density FMG controlled powered upper limb prosthesis was custom designed for the pilot participant using an off-the-shelf robotic hand as

shown in Figure 4.1 to collect data in protocols consisting of hand gestures essential to activities of daily living. Collected data were then analyzed to determine which sensors had the most impact on the accuracy of classification of intended gestures.

Experiments of this study were approved by the Office of Research Ethics at Simon Fraser University and the participant provided informed consent.

Figure 4.1: Custom made prosthetic socket and the Bebionic 3 robotic hand. Reproduced from [114] with permission.

4.3.1 Participant

In this study, data were collected from a right handed, 59 year old male with a transradial amputation of the left arm acquired in a work-related accident in 1980. He had experience using an EMG controlled powered prosthesis for two years, but used a body powered mechanical hook prosthesis on a daily basis. The participant was recruited by Barber Prosthetics Clinic (BPC).

4.3.2 Data collection

Hardware

Data were collected from the pilot participant wearing a custom-made prosthetic socket and a robotic hand (medium Bebionic 3, Ottobock, Duderstadt, Germany). The inner surface of the inner socket was covered with custom printed FSR strips each containing 16 0.5-in sensors similar to the FSR 402 from Interlink Electronics (Camarilo, California) [20]. Three datasets were collected with different sensor placements and with both dynamic and static protocols to reduce bias of analysis based on a specific sensor placement or protocol. The number of strips and their configuration were different for the three different datasets. In

dataset1, nine FSR strips were located in the socket so that it was covered by sensors as much as the physical shape of the socket allowed as shown in Figure 6.1. Not all sensors on the strips were located inside the socket. In the configuration used for dataset1, 63 sensors were located inside the socket to cover the inner surface of the socket as much as its physical shape allowed as shown in Figure 6.1. For dataset2, 4 strips were located on the extensor and flexor muscles to cover the muscle bellies. Another strip was located around the forearm over the muscle bellies in a circumferential manner. The total number of sensors used in this configuration was 58. For dataset3, five strips were located over extensor and flexor muscle bellies and on the anterior side of the forearm. The total number of sensors used in this configuration was 37. More detail on dynamic datasets can be found in [20].

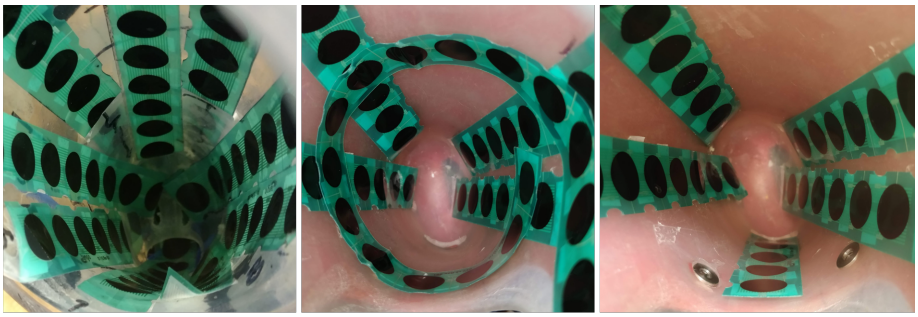

Figure 4.2: FSR strips placed inside the inner socket representing: (a) the sensor configuration for dataset1, (b) the sensor configuration used for dataset2, and (c) the sensor configuration used for dataset3. Reproduced from [114] with permission.

Protocol

The protocol used in this study consisted of 6 grips: relax, open, force, tripod, finger point, and key as shown in Figure 4.3. This set of grips was chosen to include neutral hand gestures and also functional movements important in activities of daily living (ADL) [21], [70], [20].

To collect data, the participant was asked to wear the custom designed prosthesis. No preparation was needed prior to donning the prosthesis. He would then perform the 6 grips of the protocol and hold them for 15 to 25 seconds. This process was done for 5 repetitions with rest in between as needed. For dataset1, gestures were performed as the participant held their arm in a stationary position with their elbow flexed at 90 degrees. For dataset2

and dataset3, participant held the grips as he was moving his arm in the circular dynamic motion shown in Figure 4.4. FSR data were collected at sampling rate of 10 Hz [70], [56].

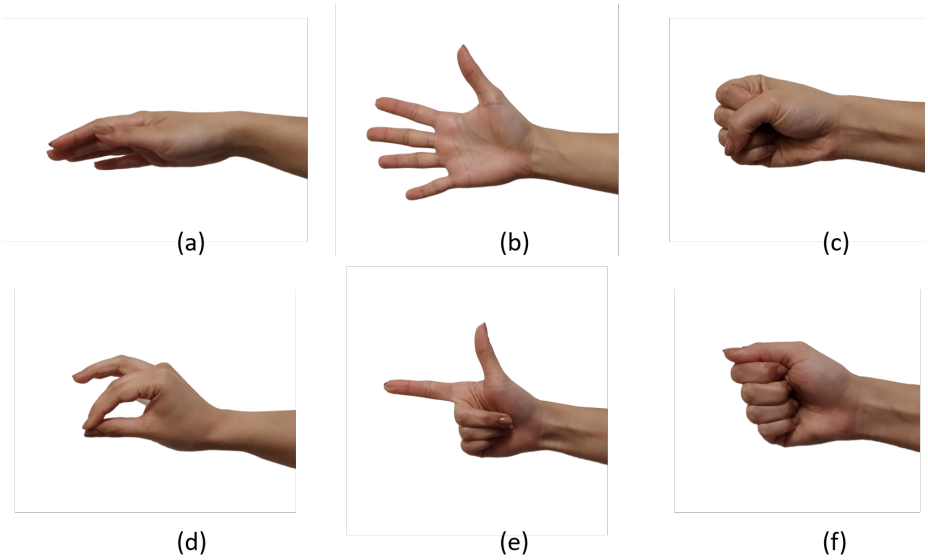

Figure 4.3: The six grips used in this protocol: (a) relax, (b) open, (c) force, (d) tripod, (e) finger point, (f) key. Reproduced from [114] with permission.

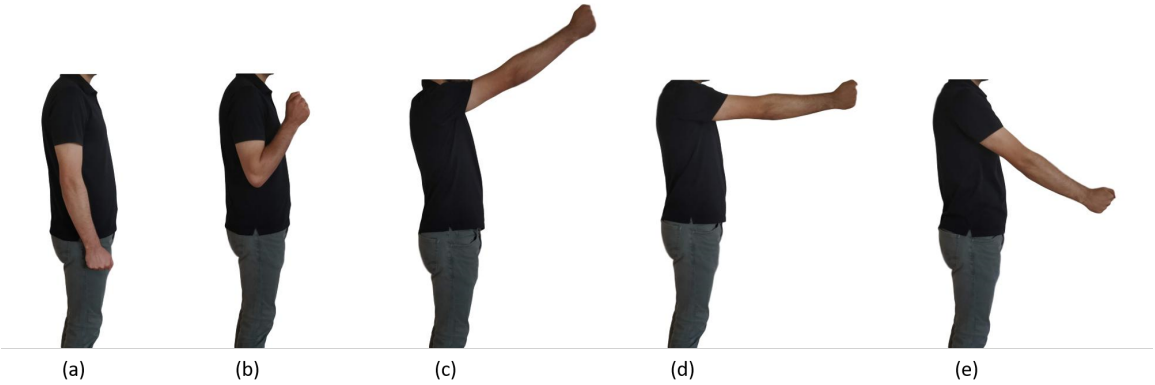

Figure 4.4: The dynamic protocol used for dataset2 and dataset3. Participant moved his arm through positions (a) to (e) in a circular motion. Reproduced from [114] with permission.

4.3.3 Data analysis

In this section, feature selection (FS) algorithms used in this study are explained. It is also explained how the data were analyzed and what outcome measures were used to compare selected FS algorithms.

In this study, no feature extraction was performed and each feature (channel) corresponded to one of the sensors. As a result, feature selection (channel selection) selects sensors whose values had the most contribution to the gesture classification accuracy. At each sample point (10 samples per second), input to the classifier was the combination of sensor values at that point in time from all selected sensors (features). There were 10 classification outputs per second each corresponding to one of the sample points as the sampling frequency is 10 Hz.

Feature selection algorithms

As explained in the 'Background' chapter, feature selection algorithms can be categorized to three major classes: filter methods, wrapper methods, and embedded methods [97], [98], [99]. Wrapper methods are then split to two main categories depending on their method of selecting features in each of their iterations: sequential selection algorithms and Heuristic algorithms [100].

Here, one commonly used algorithm from each of the aforementioned categories was chosen and its performance was assessed when applied to data collected from the pilot participant. Selected algorithms for this study were : minimum redundancy, maximum relevance (mRMR) which is a filter method [115], [100], Sequential forward selection (SFS) [100] as the sequential selection wrapper method, Genetic algorithm which is a heuristic wrapper method [100], [116], [101], and Random forest as the embedded method [102], [98].

MRMR is an FS algorithm that improves on mutual information and attempts to choose a feature subset that minimizes redundancy defined as having highly correlated features in the chosen subset. It also tries to maximize relevancy so that chosen features are highly informative about their corresponding class labels [95].

The implementation of mRMR used in this study maximized relevancy of selected features with the targeted class, which is represented by the mutual information of the feature and the targeted class. It also tries to minimize redundancy of the selected features with each other which is quantified using the mutual information of each feature with all other features in the feature subset. The quantity that is maximized in this algorithm is the following [95]:

$$\frac{I(a,l)}{\frac{1}{|F|}\sum_{b\in F} I(a,b)} \tag{4.1}$$

Where l is the targeted class, a is the feature being investigated, I is the mutual information of two variables, F is the subset of features, and $|F|$ is the number of features in the subset.

A third-party implementation of mRMR for MATLAB was used to apply the Mutual Information Quotient criterion (MIQ) version of the algorithm on collected data. MIQ was chosen since it has been recommended for discrete features in a study by Ding et al. For more details on the implementation of the algorithm, refer to [95].

The selected sequential wrapper algorithm for this study, SFS, selects features by starting with an empty set and adding one feature in each iteration. The feature added in each step is chosen so that the objective function, which is defined as the LOOCV classification, is minimized. This can be represented by the following steps [112]:

$$\begin{aligned}
&SF_0 = \emptyset \\
&RF_0 = allfeatures \\
&For\ i\ =\ 1\ to\ n \\
&\quad accuracy(SF_i) = \underset{b\in RF_{i-1}}{Max}\ (accuracy(SF_{i-1}\ + b)) \\
&\quad RF_i = RF_{i-1} - a \\
&\quad SF_i = SF_{i-1} + a \\
&end
\end{aligned} \tag{4.2}$$

Where SF_i is the selected feature subset in iteration i, RF_i is the remaining feature subset (not yet selected) in iteration i, and n is the number of all features

MATLAB's implementation of the algorithm was used with Linear Discriminant Analysis (LDA) as its classifier [100]. Information about settings used for the two stopping criteria used for this algorithm is provided in the next section.

Genetic algorithm is an evolutionary optimization algorithm [100] that is used in this study as the Heuristic FS method. In this application,GA tries to optimize (minimize in our case) the objective function which was defined as the LOOCV classification error using LDA classifier in this experiment. The algorithm's MATLAB implementation was used for this purpose. Due to inherent randomness of GA, the process was performed 10 times for each dataset and for each outcome measure, and average values were reported. GA was implemented using uniform mutation, tournament selection, arithmetic crossover, elite cont of 2, and random initial population. Information about stopping criteria used for GA is provided in the next section.

For the embedded feature selection method, Boruta package for R was used. Boruta starts with creating shadow variables by copying original variables and shuffling their values. It then trains a classifier (random forest (RF)) using the original and shadow variables. The importance score of original variables are determined based on comparison of their z-score with the z-score of shadow variables. This is performed in iterations until the final decision is made and feature scores are returned [102]. In the implementation of Boruta, number of trees for RF was set to 500 and the maximum number of importance source runs was set to 100.

Stopping Criterion

In order to decide what the optimum feature subset is, performance-based criterion was used. Performance base stopping criterion defines a condition based on system performance that determines when the algorithm stops and returns the resulting feature subset. Convergence conditions vary depending on the selection algorithm used.

One possible stopping criterion is the relative iterative improvement (RII) in classification accuracy. This method is suitable for SFS since the algorithm tries to improve classification accuracy in each iteration. In the implementation of SFS used in this study, the algorithm stopped when improvement in current iteration was less than a relative threshold defined by the following formula where $eps = 2.2204e-16$ and $TolFun$, which determines the tolerance for termination based on improvement of the objective function (classification error in this case) value is set to $1e-6$:

$$critTh = oldCrit - (abs(oldCrit) + sqrt(eps)) * TolFun \tag{4.3}$$

In this formula, $critTh$ is the threshold against which improvement of the objective function in each iteration is compared, and $oldCrit$ is the value of the objective function in the previous iteration.

Another stopping criterion used in this study was the global maximum. It is used for algorithms that output ranking of features or order features in term of their importance. Accuracy of feature sets with 1 to all features is calculated as features are added according to their rank and the feature subset resulting in the maximum accuracy is selected. In this study, global maximum was used for mRMR and Boruta. SFS was also examined using this criterion as well as RII.

The last stopping criterion used in this study was Function Tolerance over Stall Generations, which is used for GA. This is also a performance criterion that concludes the process when average performance enhancement over a predefined number of generations is less than a threshold. In the analysis done for this study, function tolerance was set to 1e-6 and maximum stall generations was set to 50.

To summarize, five feature selection methods were examined in this study: SFS with RII stopping criterion, SFS with global maximum stopping criterion, mRMR with global maximum stopping criterion, GA with function tolerance over stall generations stopping criterion, and Boruta with global maximum stopping criterion.

Algorithm assessment

Chosen feature selection algorithms were assessed based on three outcome measures: their running time, the algorithms' performance in terms of classification accuracy, and their stability.

Reported running time for each of the methods for each dataset is the amount of time it took for the implementation of the method used in this study to run. Running time is an indication of the algorithm's computational complexity and can be important in cases where computational power is limited or the sample sizes are large.

Classification accuracy The goal of using FS in this study was to reduce input dimension with no significant loss of vital information regarding gesture classification. As a result, classification accuracy is the first outcome method used for assessment of the five FS methods.

To obtain classification accuracy yielded by each feature selection algorithm in this study, five-fold leave-one-out cross validation (LOOCV) was used to separate one repetition of collected data as test data and the remaining four repetitions as training data. Feature subset was chosen using LOOCV on the four repetitions of training data. This process was repeated for the five permutations of test data. Then only the features that were mutually selected in all five iterations were chosen for the final feature subset. This process is illustrated in Figure 4.5. Reported classification accuracies were the result of performing LOOCV on all five repetitions of data using only the selected features. These accuracies were compared with the baseline accuracy.

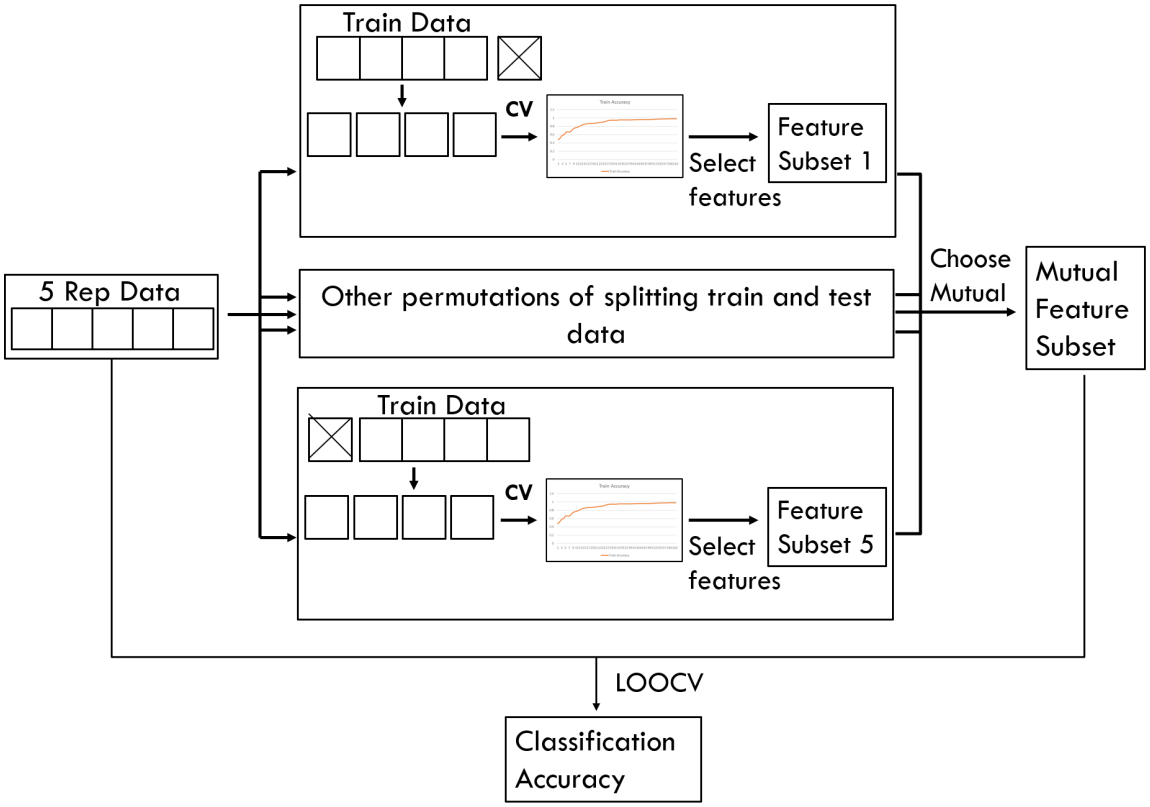

Figure 4.5: Feature selection process used in this study. Reproduced from [114] with permission.

Stability As Defined by Chandrashekar et al., stability of a feature selection method is consistency of the feature subset chosen by the algorithm as new training data are introduced or when some training data are removed [100]. Stability is an important outcome measure for comparison of algorithms used in this study since it determines the algorithm's sensitivity to the size of training data. Feature subset variations observed in this study could also be affected by variability of data in different repetitions. Variability of data in applications for individuals with amputation is inevitable due to limited visual feedback. This makes stability an important measure for applications similar to the one examined here.

To compare stability of different algorithms selected for this study, selected feature subsets were compared when training data were reduced from the first four repetitions to the first three repetitions and then to the first two repetitions. For all these cases, the last repetition was used as test data. For this outcome measure, variation in feature subsets were compared using an average percentage of variation in each iteration as training data were reduced, which was obtained using the following formula:

$$Variation\% = (number of features - number of mutual features)/number of features * 100 \tag{4.4}$$

4.4 Results

In this section, results for assessment of the five feature selection methods are reported and compared with the baseline accuracies. Baseline accuracies for the 6 gestures used in this study were 86.45% ± 4.5%, 70.7% ± 10.6%, and 80.4% ± 11.4% for dataset1, dataset2, and dataset3, respectively.

4.4.1 Classification Accuracy

Accuracies obtained using LOOCV with selected features by each of the five methods for the three datasets are shown in Figures 4.6, 4.7, and 4.8. Each method produced a feature subset with a different number of features which are shown in Table 4.1.

GA was run 10 times and reported values in Table 1 indicate the average of the 10 times. The lowest numbers of features selected by GA were 10, 14, and 10 for dataset1, dataset2,

and dataset3, respectively. These feature subsets resulted in classification accuracies of 78.4%, 71.5%, and 71.4%, respectively.

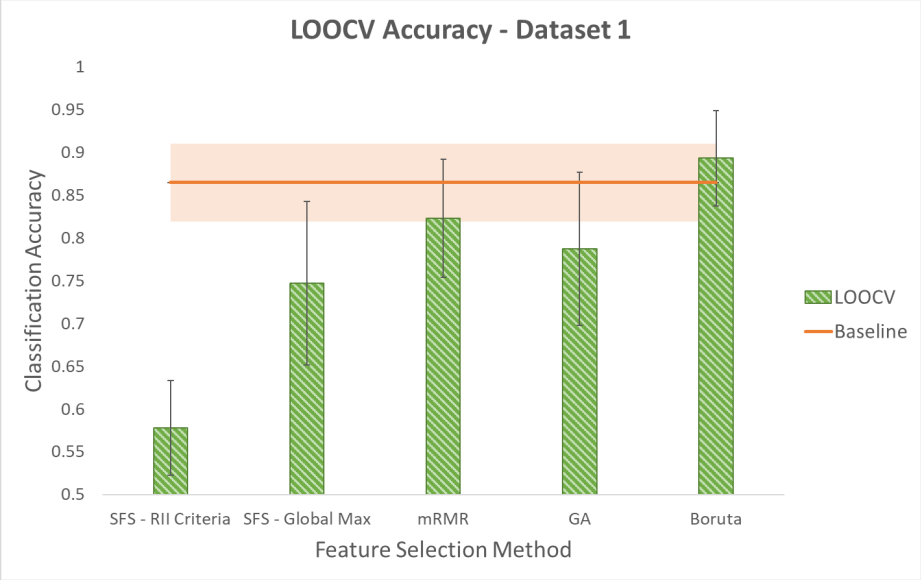

Figure 4.6: Leave-One-Out Cross Validation accuracy using different feature selection methods for dataset1. Shaded area around the baseline indicates its standard deviation. Reproduced from [114] with permission.

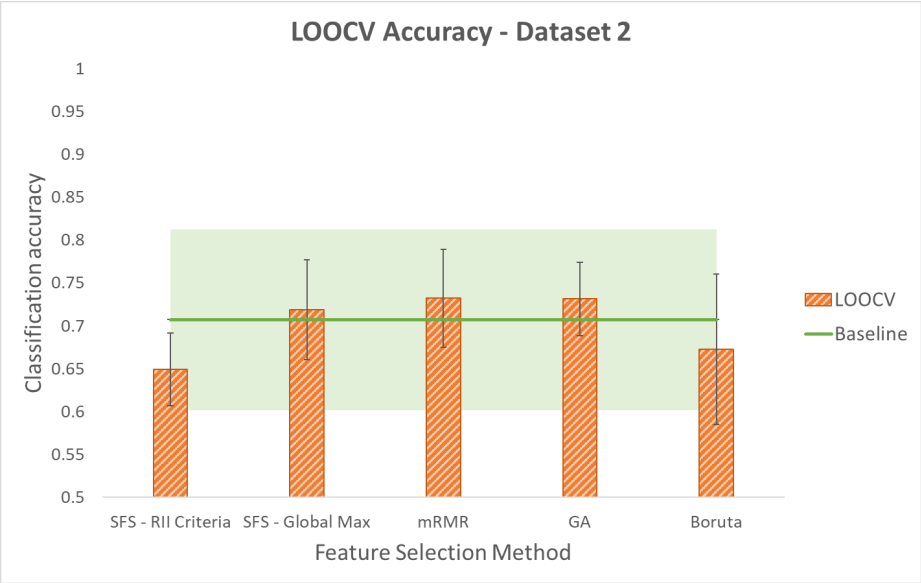

Figure 4.7: Leave-One-Out Cross Validation accuracy using different feature selection methods for dataset2. Shaded area around the baseline indicates its standard deviation. Reproduced from [114] with permission.

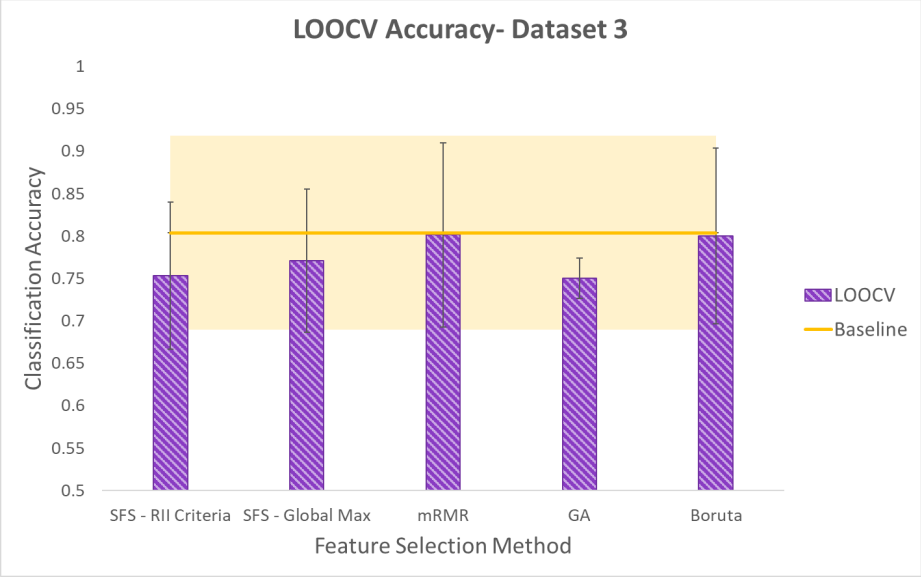

Figure 4.8: Leave-One-Out Cross Validation accuracy using different feature selection methods for dataset3. Shaded area around the baseline indicates its standard deviation. Reproduced from [114] with permission.

	SFS - RII Criteria	SFS - Global Max.	mRMR	GA	Boruta
Dataset1	2	12	23	11.6 ± 1.3	27
Dataset2	8	14	35	16 ± 1.8	32
Dataset3	11	15	30	11.8 ± 1.0	29

Table 4.1: Number of features selected in LOOCV using different feature selection methods. Adapted from [114] with permission.

To determine whether reduction in the number of input channels caused a significant decrease in classification accuracy, the Student's paired t-test at significance level of 5% was used. It is worth noting that this is an exploratory study with one participant and five repetitions of the protocol for each dataset. Each reported classification accuracy is the average of five permutations of LOOCV. Each of these five values are the average classification accuracy of 6 gestures that are performed in each repetition. The values used in the t-test are the five LOOCV accuracies. Given that this was a pilot study, there is dependency of data and therefore the assumptions underlying statistical analysis cannot be fully met and results of the statistical analysis should be taken with caution. These results should be confirmed with more participants in future work. Despite this issue, looking at the average and standard deviation values, it seems that in populations that do not prove

to be significantly different using t-test, the difference between averages is not considerable considering standard deviations.

It was found that using SFS with either of the two stopping criteria resulted in accuracies that were significantly lower than the baseline in dataset1. However, in this dataset, no significant difference was determined for the other three methods: mRMR, GA, and Boruta. In dataset2, no significant difference was observed comparing the baseline accuracy with the accuracies obtained using smaller feature subsets produced by any of the five feature selection methods. In dataset3, SFS with RII criteria lowered accuracy with significant difference. However, no significant difference was observed comparing accuracies produced by the other four methods and the baseline accuracy. It is worth noting that although GA resulted in a lower average accuracy compared to SFS - RII criteria, due to the small difference in the average accuracies of these two methods (0.31%) and GA's smaller standard deviation, the Student's t-test could not reject the null hypothesis that it comes from a population with the same mean as the baseline, while in the case of SFS - RII criteria, the null hypothesis was rejected.

Table 4.2 shows the grips with the lowest accuracy for each dataset using each FS method. In this table, the force grip appears frequently for dynamic datasets. A closer look at the errors of prediction for this class showed that in various cases, the force grip was misclassified as either the finger point grip or the key grip. This is likely because these grips are differentiated through fine finger movements. Variations in muscle volume caused by these movements could be affected by variations in the force exerted by the prosthetic socket as the user moves his arm dynamically.

	SFS - RII Criteria	SFS - Global Max.	mRMR	GA	Boruta
Dataset1	finger point	finger point	force	finger point	tripod
Dataset2	force	force	key	force	key
Dataset3	force	force	force	force	force

Table 4.2: The grip with highest classification error for each dataset, using each FS method. Adapted from [114] with permission.

Using SFS with either of the stopping criteria, grips with the lowest accuracies were 'finger point' in dataset1 and force in dataset2 and dataset 3. Using mRMR, force was the grip with the lowest accuracy in dataset1 and dataset3, and key was the grip with lowest accuracy in dataset2.

To summarize, mRMR, GA, and Boruta were able to meet the goals defined in this study in all three datasets. Percentage decrease in number of features using each of the three methods are shown in Table 4.3.

	mRMR (%)	GA (%)	Boruta (%)
Dataset1	63.5	81.6	57.1
Dataset2	39.7	72.4	44.8
Dataset3	18.9	68.1	21.6

Table 4.3: Percentage decrease in input features using different feature selection methods. Adapted from [114] with permission.

4.4.2 Stability

Stability of the five feature selection methods was measured based on consistency of the feature subset they select when the number of samples in training data was decreased. This was done by comparing the variation percentage in feature subsets selected by different selection methods. These values for the three datasets are shown in Figure 4.9.

Out of the three algorithms that were able to achieve the goals of this experiment, GA produced the feature subsets with most feature subset variation percentage ranging from 47.7% to 58.0% in the three datasets. Comparing the other two methods, mRMR resulted in average feature subset variation of about 21% in the three datasets and Boruta resulted in average variation percentage of 24.8% in all datasets with more variability between the three datasets.

4.4.3 Running Time

The five FS methods considered in this study are different in terms of computational complexity and running time. Running times for the five methods for each dataset are shown

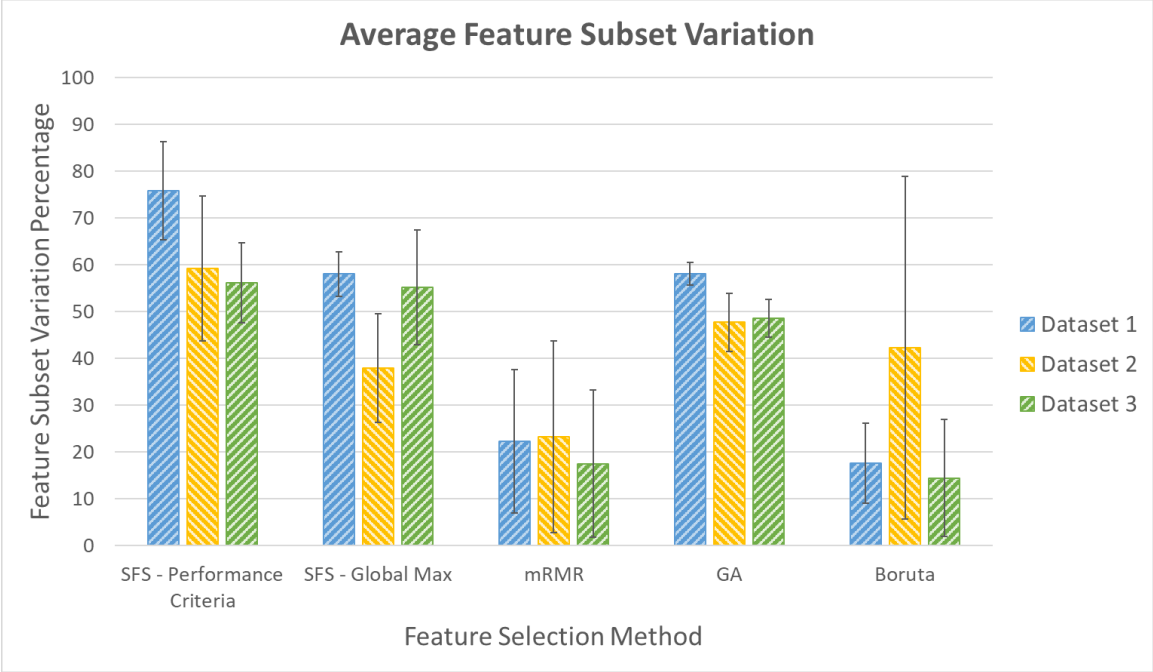

Figure 4.9: Percentage variation in feature subsets as amount of training data is decreased. Reproduced from [114] with permission.

in Table 4.4. MRMR and SFS-RII criteria have the shortest run time interchangeably for the three datastes. GA and then Boruta have the longest run times for all datasets.

	SFS - RII Criteria	SFS - Global Max.	mRMR	GA	Boruta
Dataset1	90.5	311.1	54.7	2592.3	1504.5
Dataset2	71.8	133.5	107.2	1721.2	163.5
Dataset3	42.1	53.3	42.5	2112.1	111.4

Table 4.4: Running time for each FS method for each dataset (s). Adapted from [114] with permission.

4.5 Discussion

Baseline accuracies were comparable to that of other studies. Previous studies by Cho et al. and Ferigo et al. used the same 6 grips in a static protocol on four participants and one participant with transradial amputations and reported classification accuracies of 62.61% ± 11.5% and 81.2% ± 11.3%, respectively. Ferigo et al. also used a dynamic protocol similar to the one used in dataset2 and dataset3 of this study and reported accuracy of 75.5% ±

9.2% [21], [70]. Other studies using EMG with participants with amputation have reported classification accuracies in the range of 85% to 90% for 4 to 6 classes of movement [38].

4.5.1 Classification Accuracy

This study focused on assessment of five feature selection methods on reduction of input dimension of an FMG controlled powered prosthesis without significantly sacrificing performance of the device. To determine if feature number reduction affected performance, classification accuracy was examined since it determines probability of correct prediction of user intentions.

Results showed that out of the five methods used to reduce input dimensions, while maintaining system performance, three methods were able to reduce the number of input features by 18.9% to 81% in the three datasets used in this study. This was possible since multiple sensors might produce correlated information depending on their location. Another reason is that some of the input channels could contain noisy or irrelevant signals and removing them could increase class separation and lead to higher classification accuracies [117], [118].

Elimination of irrelevant or noisy data through feature selection can also be observed by comparing standard deviations of the LOOCV accuracies over the five repetitions before and after feature selection, especially in dynamic datasets. Dynamic datasets are more prone to containing noisy or irrelevant data due to factors such as weight of the prostheses applying compressive or tensile forces as the orientation of the arm changes, slight movements of the socket, and variations in movement of the arm. In the two dynamic datasets of this study, after feature selection, LOOCV standard deviations were decreased by 4.8% and 3.3% in dataset2 and dataset3, respectively, which indicates the possibility that eliminated features were contributing to increased data variation among various repetitions.

It is worth noting that even after feature selection, data variability is still evident through average LOOCV standard deviations of 7.3% in dataset1, 5.8% in dataset2, and 8.1% in dataset3 for the five FS methods. Standard deviations of about 11% and 9% were also reported by the two studies with datasets similar to the ones used here [70], [21]. It is

likely that data variability in prostheses control applications is inevitable, especially as experimental setups become closer to the practical use case of the system.

Comparing performance of the FS methods considered in this study, out of the three methods that could successfully achieve the goal defined in this study, GA resulted in the most reduction of input features in all datasets with a chosen feature subset of about 11 sensors out of the original 63 sensors resulting in average classification accuracy of 0.78 $\pm$ 0.09 in dataset1. It also reduced feature numbers to 16 sensors out of the total of 58 sensors in dataset2 yielding an accuracy of 73.2% $\pm$ 4.3% and a chosen feature number of about 12 sensors out of the total sensor number of 37 in dataset3 with resulting classification accuracy of 75.0% $\pm$ 2.4%.

Neither of the other two methods outperformed the other drastically in terms of feature number reduction in any of the three datasets. The reduction percentage difference for Boruta and mRMR in the three datasets were from 2.7% to 6.4 % while GA outperformed them by reducing feature numbers by up to 46.5% more in dataset3. This could be because wrapper methods such as GA make their selection in each iteration based on classification accuracy. On the other hand, the other two methods (mRMR and Boruta) do not include classification in their selection decision. Thus, GA selects the feature subsets for the very specific application and tries to maximize the measure considered for it - i.e. classification accuracy. For this reason, if multiple classifiers or more generalized applications were to be considered, GA would not necessarily be able to produce similar results as the ones it produces when only one classifier is considered. Another drawback of wrapper methods such as GA compared to Boruta and mRMR is their computation complexity. Wrapper methods perform a classification task in each iteration of the algorithm which could be computationally extensive in the presence of large sample sizes [100].

Average accuracies that resulted from the three selected feature selection methods in dataset1 were within the range of "baseline accuracy - 7.7%" and "baseline accuracy + 2.9%". In this dataset, Boruta yielded the highest accuracy that was higher than the baseline accuracy. In dataset2, variation in accuracies produced by the three methods were less compared to dataset1. Contrary to dataset1, Boruta produced the feature subset with the

lowest resulting accuracy compared to the other two. Accuracy obtained using the feature subset selected by Boruta in dataset2 was less than the baseline accuracy by 3.4% while the other two methods resulted in accuracies that were about 2.5% higher than the baseline accuracy. In dataset3, Boruta and mRMR both resulted in accuracies similar to the baseline accuracy while GA reduced the accuracy by 5.4%.

None of the three methods resulted in the highest classification accuracy in all three datasets. However, it is worth noting that a decrease of up to about 7% in accuracy when the average standard deviation was about 7.1% (in the accuracies obtained using the three selected methods in all datasets), which is not considerable especially in this case where no statistically significant difference was shown.

SFS with either of the stopping criteria was not able to meet the goal defined in this study. This could be since the algorithm, in iteration i, only considers selections combining the 'selected feature subset (SF_i)' and one of the feature in the 'remaining feature subset (RF_i)'- i.e. features that are not yet selected to be in the selected feature subset. This could be a drawback since there is a chance that a combination consisting of part of the features in SF_i and more than one feature from RF_i would produce better results.

To determine sensitivity of the proposed method to the size of datasets used for model training, an analysis was conducted using selected features by the five FS methods and only half of the data from each repetition. Results showed that reducing the size of the datasets to half their size would not significantly change classification accuracies in dataset1 and dataset3. Using only half of the data significantly increased accuracies obtained using feature subsets selected by SFS-Global Max. and GA methods in dataset2. This could be due to the eliminated data being noisy. Obtained classification accuracies using the smaller datasets are reported in table 4.5 .

	SFS - RII Criteria (%)	SFS - Global Max. (%)	mRMR (%)	GA (%)	Boruta (%)
Dataset1	60.8 ± 7.5	76.7 ± 8.3	79.8 ± 5.1	75.8 ± 10.3	88.0 ± 5.0
Dataset2	66.5 ± 4.4	75.8 ± 4.5	74.6 ± 6.1	76.8 ± 3.5	71.3 ± 6.8
Dataset3	73.7 ± 9.1	77.6 ± 8.6	80.1 ± 10.0	75.8 ± 2.8	80.0 ± 8.6

Table 4.5: Classification accuracies obtained using half of the data. Adapted from [114] with permission.

Comparing this study with the studies by Wang et al. and Li et al. that performed channel selection for gesture classification (using sEMG), this study was conducted using both static and dynamic protocols with an individual with an amputation using a prosthetic socket. Experimental setup of this study was closer to the real use case of the application and was likely to be able to capture some of the possible errors introduced by the real application of the system. The aforementioned studies each investigated one FS method, while this study runs a comparison between five methods. In terms of feature number reduction, Wang et al. reported classification accuracy of 69.3% after about 35.7% decrease in channel numbers and Li et al. reported accuracy of 84.2% after about 79% decrease in the number of channels. In the study presented here, maximum percentage decrease in the number of channels varied between 57.1% to 81.6% in the three datasets [111], [112].

To summarize, all three methods resulted in inconsiderable reduction/increase in accuracy while GA resulted in the most reduction in feature number. And using only half of the data, comparable results were obtained.

Limited Feature Number

In some applications, the maximum number of features allowed by the hardware, space, or other factors may be limited. In the analysis done so far for this study however, no limitation has been placed on the maximum number of features the application allows.

Here, we consider the case where the number of sensors the feature selection method is allowed to choose is limited to floor of half of the total number of features for each dataset (i.e. 31, 29, and 18 features for dataset1, dataset2, and dataset3, respectively).

Classification accuracies obtained using the five feature selection methods for dataset1, dataset2, and dataset3 are shown in Figures 4.10, 4.11, and 4.12 respectively. The number of features selected by each of the methods are shown in Table 4.6.

To assess weather the reduction in the number of features using these methods resulted in lower performances, the Student's paired t-test at significance level of 5% was used. It was determined that for dataset1, using SFS with either of the stopping criteria, and GA resulted in classification accuracies that are significantly lower than the baseline. No significant difference was determined for the other two methods. For datset2, no significant

difference was found for any of the five feature selection methods. For dataset3, all methods resulted in significantly lower classification accuracies.

The reason why none of the methods could successfully choose a feature subset that is less than half of the total features but does not lead to a significantly lower classification accuracy in dataset3 might be the smaller number of total features. This causes the methods to limit the number of features to a maximum of 18 sensors which, from the findings of this study might not provide enough information for the application of the system under study here.

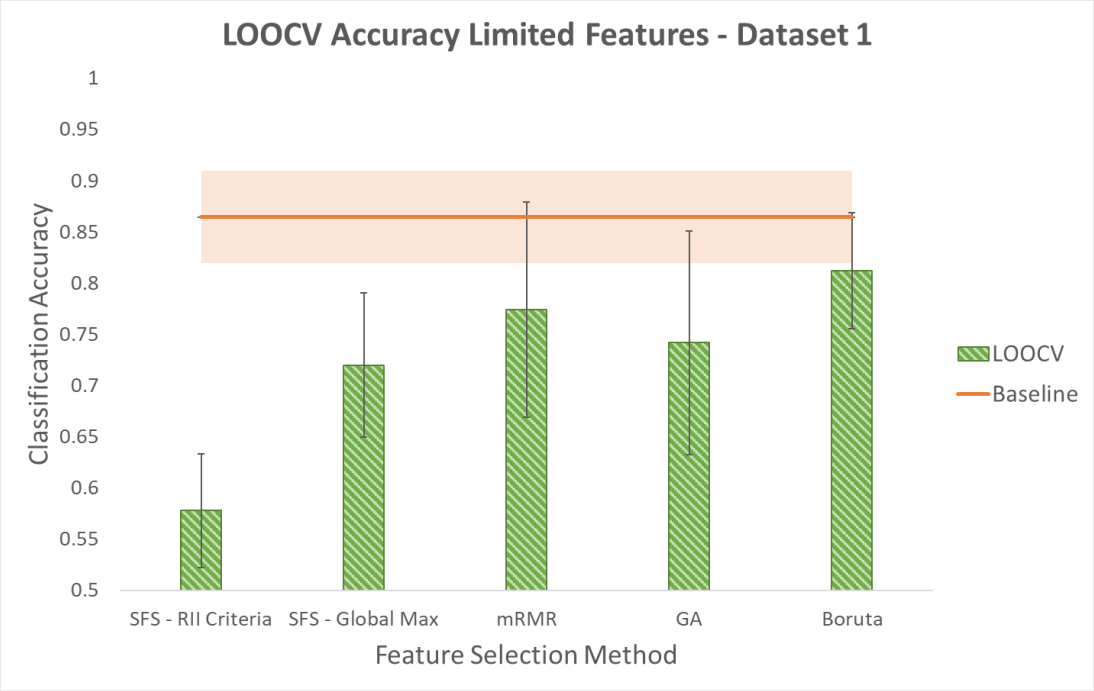

Figure 4.10: Leave-One-Out Cross Validation accuracy using different feature selection methods for dataset1 when maximum number of features is limited to half of the total features. Shaded area around the baseline indicates its standard deviation.

	SFFS - RII Criteria	SFFS - Global Max.	mRMR	GA	Boruta
Dataset 1	2	8	14	8.5	22
Dataset 2	8	10	25	13	18
Dataset 3	9	9	16	5.6	11

Table 4.6: Number of features selected in LOOCV using different feature selection methods when maximum number of features is limited to half of the total features.

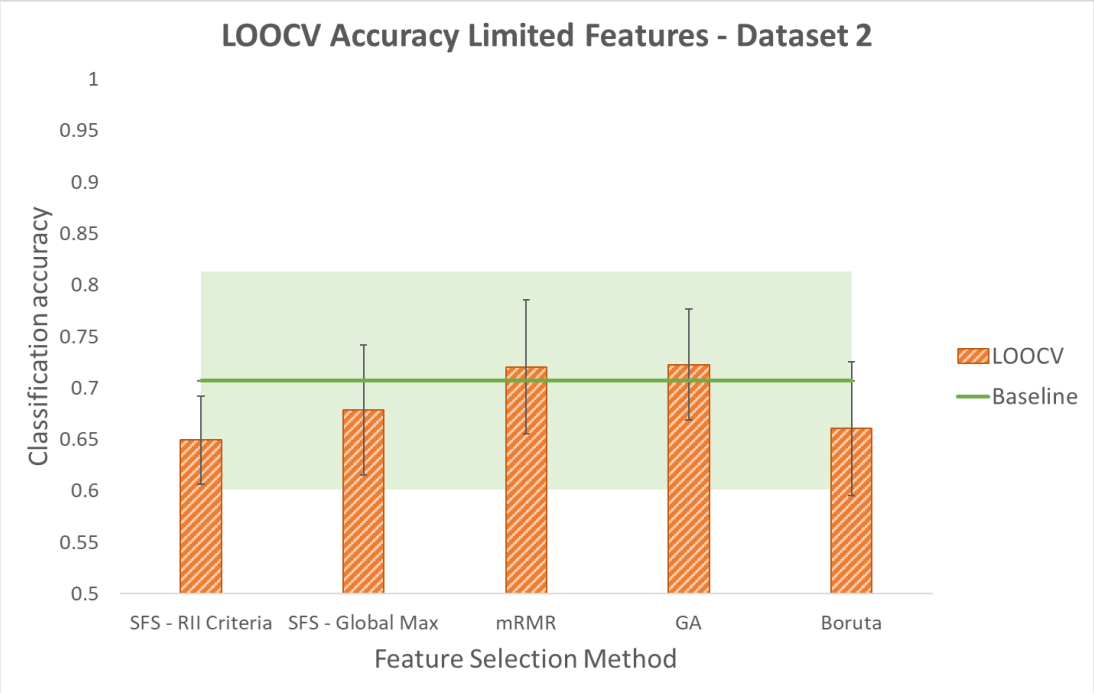

Figure 4.11: Leave-One-Out Cross Validation accuracy using different feature selection methods for dataset2 when maximum number of features is limited to half of the total features. Shaded area around the baseline indicates its standard deviation.

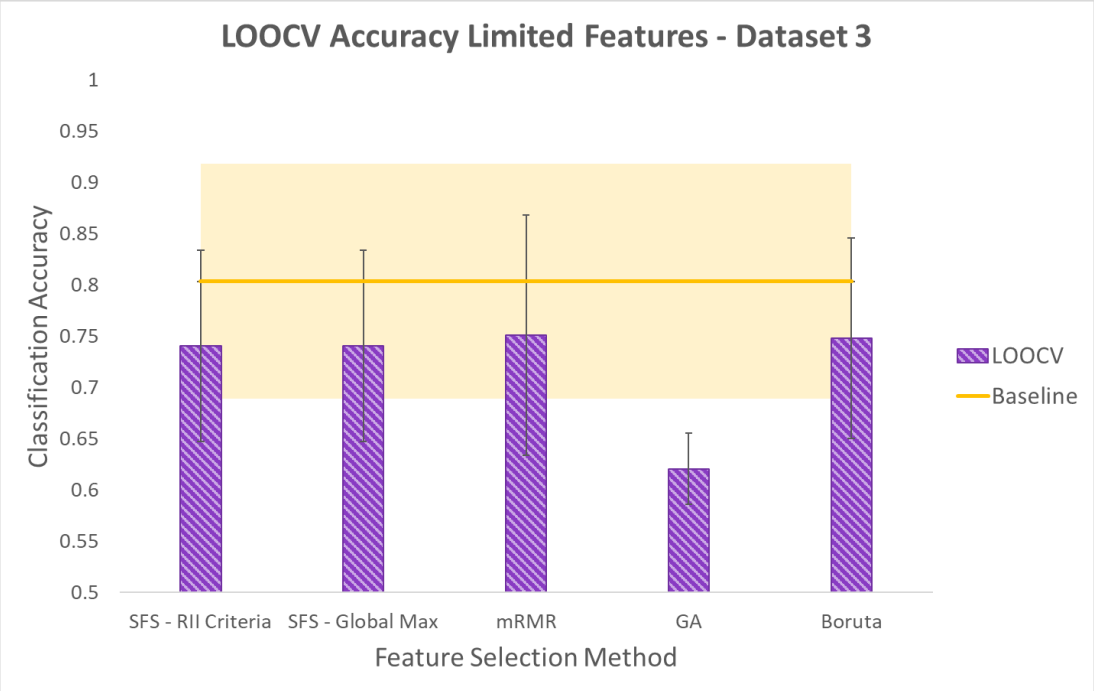

Figure 4.12: Leave-One-Out Cross Validation accuracy using different feature selection methods for dataset3 when maximum number of features is limited to half of the total features. Shaded area around the baseline indicates its standard deviation.

4.5.2 Running Time

For the different datasets, either mRMR or SFS with RII criteria was the fastest method. After these, SFS - Global Max., Boruta, and GA had increasing running times in that order. MRMR was one of the fastest method since it does not perform any classification tasks and ranks features based on solving the value of the formula stated in Equation 4.1.

The running time for SFS with the RII criteria method was less than the running time for SFS - Global Max. method. This is since the number of iterations for SFS - Global Max. is fixed and equal to the number of features as the algorithm starts with an empty set and adds one feature to it in each iteration until all features are added. On the other hand, the number of iterations of SFS - RII criteria is data dependent and is less than or equal to the number of all features.

After GA, Boruta is the method with the longest running time. Boruta's running time for dataset1 was longer compared to dataset2 and dataset3. This was because in analysis for dataset1, Boruta ran an average of above 90 runs to resolve all attributes left tentative for the five LOOCV cases, while for dataset2 and dataset3, all attributes were resolved in an average of about 13 runs. This is due to fluctuations of importance of some of the attributes requiring more runs for the algorithm to either confirm or reject them. There is also shuffling of values of shadow variables that is performed when shadow variables are created. Based on the result of this shuffling, running time of the algorithm could be affected. Although there are methods that fix convergence issues of the algorithm due to tentative attributes, these methods use weaker tests for attribute judgement. To summarize, the run time of Boruta is data dependent.

GA has the longest run time compared to all the other methods since it ran an average of about 84, 81, and 69 iterations for the five LOOCV cases of dataset1, dataset2, and dataset3, respectively. In each iteration, a classification task was performed in addition to the steps of the genetic algorithm. As mentioned before, in this study, feature selection using GA was performed 10 times for each datasset and each outcome measure. The run time reported in Table 4.4 is for one processing of the method for the 'classification accuracy' outcome measure.

4.5.3 Stability

Stability of a feature selection method was the second outcome measure assessed in this study. It is worth noting that the variations shown in this measure did not affect the accuracies reported in the previous section since the accuracy results were obtained using only the features that appeared in all iterations of cross validation and features accounting for the variability were discarded.

Out of the three algorithms that selected feature subsets capable of producing classification accuracies comparable to the baseline (namely mRMR, GA, and Boruta), GA was more sensitive to the volume of the training data or the variability in data that were collected in different repetitions of the experiment. This could be due to the randomness that is inherent to this algorithm. The measure used for stability was comparable for the other two methods.

It is worth noting that in this experiment, as the size of training data was reduced, the total number of samples in training data was decreased by 25% in the first iteration, 33% in the second iteration, and 50% of the remaining data in the last iteration. As a result, the stability measure considered here represented sensitivity of methods to high variations in the size of training data. In applications where variability in the size of training data was not considerable, these methods might yield less instability, which is only due to sensitivity to variations of data in different repetitions.

Chapter 5

The Effect of Bending of Force Sensitive Resistors on Signals Used in FMG Controlled Prostheses

The material presented in this chapter is excerpted, reproduced, and modified with permission from the following paper:

C. Ahmadizadeh and C. Menon, "Investigation of Regression Methods for Reduction of Errors Caused by Bending of FSR-Based Pressure Sensing Systems Used for Prosthetic Applications," Sensors, vol. 19, no. 24, p. 5519, 2019.

Sections of this chapter are reprinted or adapted from the above article for clarification and to fit the formatting and scope of this document.

5.1 Chapter Overview

This chapter outlines the study conducted to fulfil **objective 3.a** of this thesis which is to investigate the effect of bending of the FSR sensors on the signals used in FMG controlled prosthesis. To assess this effect, accuracy of mapping of FSR readings to known pressure values is assessed when the sensors are placed in various curved conditions.

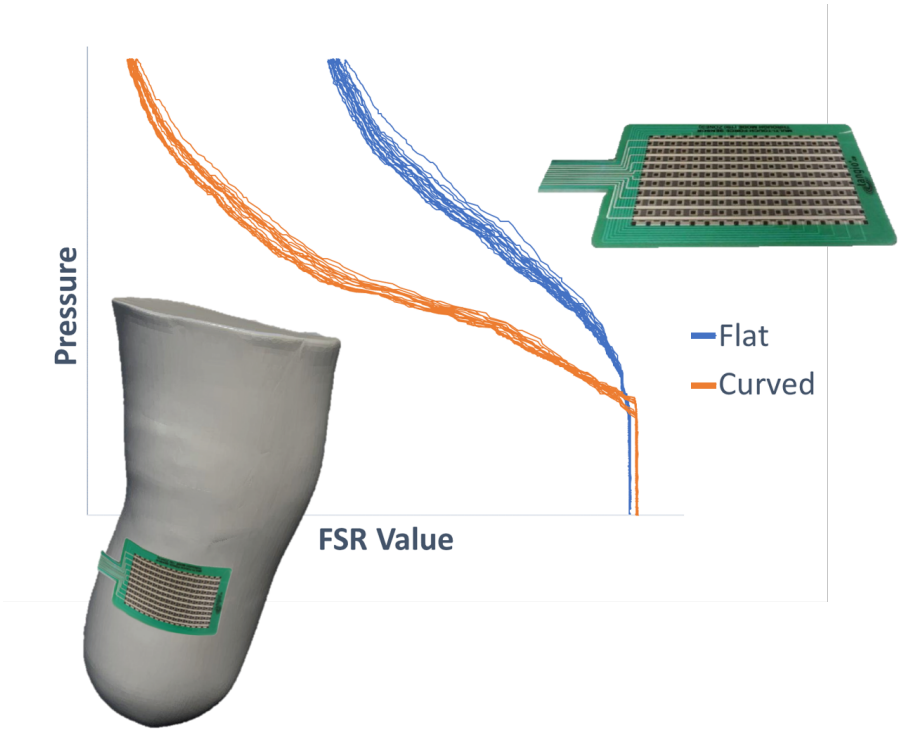

Figure 5.1: Illustration of the variations in the response of FSRs when they are curved

5.2 Introduction

The pressure profile at the interface of the prosthetic socket and the residual limb contains important information that can be used for various applications in the field of prostheses. One of the most common prosthetic applications for which the use of this pressure map has been explored is control of powered prostheses using Force Myography (FMG) [70], [20], [52].

FMG for prosthetic control has been explored for both upper extremity and lower extremity prostheses [35], [119] . For the upper limb, FMG has been mostly used for gesture classification to control externally-powered prosthetic hands [54], [34]. The feasibility of using FMG for continuous finger movement control has also been investigated [119], [120]. In lower limb prostheses, the use of FMG has been explored for locomotion mode detection. Information about the mode of locomotion can be used for the ankle's angle correction as the user walks over ramps, flat surfaces, or stairs [35], [45]. Moreover, studies have shown

promising results using FMG for gait phase detection [121] which can be used for lower limb prostheses control [122].

Various force/pressure measurement techniques can be used to acquire the pressure map used in FMG controlled prostheses. Strain gauges and load cells are used in different forms and for various applications such as measurement of ground reaction forces for gait analysis using instrumented shoes [123] and prosthetic interface pressure measurement [124]. Force plates are also commonly used in such applications due to their accuracy of measurement [123]. [125], [126]. Other force/pressure measurement methods for biomedical applications include the use of piezoelectric sensors for measurement of normal forces in shoe insoles [123], instrumented implants for telemetric measurement of forces [127], dynamometers [128], and electromyography for measurement of muscle activation forces [126].

The measurement method is determined based on the application for which the results are to be used. For example, despite the high accuracy of measurements by a shoe insole instrumented with strain gauge transducers, it is not a suitable measurement system for gait analysis due to the interference of the thickness of the sensors with parameters of the experiment [123]. For pressure measurement within prosthetic sockets, various techniques are investigated including the use of strain gauge transducers, capacitive sensors, and piezoresistive sensors [129]. The use of strain gauge-based sensors are amongst the most accurate methods that can measure both normal and shear forces. However, factors such as the high cost of these sensors and their dimensions limit their practicality for the real use case of the applications considered in this study. The use of such sensors for prosthetic pressure measurement requires modification of the prosthetic socket to make embedment of the sensors possible. Such alterations to the prosthetic socket may affect the interface pressure distribution[130], [131], [132].

Capacitive sensors are used both in single point form and as sensor arrays for prosthetic pressure measurement. The rigid substrates of the single point capacitive sensors prevented them from complying with the geometry of the socket, which in addition to their costly fabrication prevented them from being an optimal technique for prosthetic pressure measurement [129]. The Pliance system by Novel Electronics (Minneapolis, US) uses capacitive

sensor arrays for this application, however, the measurements are limited to direct pressure and are uni-directional [133], [134].

Design and development of sensors that are thin, less costly, and can measure shear forces have been investigated in the research community. Chase et al. fabricated and tested a flexible capacitive force sensor that was able to measure normal and shear forces [135]. Razian et al. designed and developed a miniature triaxial piezoelectric copolymer film pressure transducer with thickness of 2.7 mm that can be embedded in shoe insoles [136]. Although these sensory systems can potentially be used for prosthetic pressure map registration, their development methods are still in their early stages and are bound to the research laboratories.

FSR-based pressure measurement systems are amongst the most common methods for prosthetic pressure map registration for use in FMG controlled prostheses. Despite their inability to measure shear forces which is undesirable for some prosthetic applications, their thin profile, flexibility, cost effectiveness, computationally affordable signal pre-processing [124], [134], [137] , and commercially established development have made them a practical solution for prosthetic pressure measurement. The F-scoket system by Tekscan (Boston, US) has been one of the most commonly preferred solutions for pressure measurement inside prosthetic sockets [132], [124], [129], [137], [138], [133]. Various studies have demonstrated high accuracies of user intention recognition using FSR-based FMG systems despite their inability to register shear forces [54], [20], [21], [51].

Despite availability of FSR-based prosthetic pressure measurement systems in the market and their wide use in research communities, when these systems are evaluated in practical situations, higher errors are reported compared to their performance in constrained environments of the labs. In prostheses control using FMG, higher errors are reported for inter-participant and inter-trial cases [111], [121]. In other studies concerning accuracy of measurement of FSR-based sensory systems in prosthetic applications, higher errors are reported when FSR sensors are placed on moulds of the limbs [134], [139], [133].

Factors affecting stability of FSR responses have been investigated in multiple studies. Chegani et al. assessed the effect of sensor placement and spatial coverage on stability

of FMG signals used for gesture classification through studying their effect on obtained classification accuracy. It was determined that increasing spatial coverage improved accuracy when two custom FMG bands were used instead of one. However, increasing spatial coverage beyond that did not further improve the results. They also reported that optimal placement of sensors can potentially compensate for the lower spatial coverage [119]. Delva et al. investigated the effect of anthropometry and grip strength on stability of FMG signals and determined that these factors do not contribute to variability in FMG signals. They also demonstrated that FMG signal's stability was not decreased in non-stationary tasks [140].

Another factor that can decrease the stability of FSR signals is the curvature of sensors. In the use of FSR-based pressure sensing systems for prosthetic applications, as sensors are embedded inside a prosthetic socket, they are inevitably bent. When FSRs are bent, their neutral value changes and as the sensor responses are usually non-linear, this could considerably affect sensors' responses.

Multiple studies have assessed the effect of bending on stability of FSR readings by studying the effect of placement of FSR sensor arrays on moulds of the limb on the sensors' error compared with when they were laid flat [139], [133]. These assessments showed that when the sensors were placed on moulds of residual limbs, their errors increased significantly compared with when they were laid flat. Three off-the-shelf FSR-based pressure sensing systems were assessed in these studies: the Rincoe SFS system, the F-Socket, and the Pliance system. Their reported accuracy error increased from 24.7% to 32.9% for the Rincoe SFS system [139], 8.5% to 11.2% for the F-Socket [139], and from 2.42% to 9.96% for the Pliance system [133].

The objective of the study outlined in this chapter is to determine the effect of bending of FSR sensors on their response and to asses the possibility of reducing errors introduced in sensor readings due to them being bent using information about the values of curvature of the sensors. To the best of authors' knowledge, no study has been conducted to solve the problem of instability of FSR-based pressure sensing systems due to bending. Proposed methods in this study can be applied to any system of sensor matrices that are prone to decreased accuracy when bent.

The proposed approach for this study was to test sensor readings in a chamber with varying pressure when sensors were laid flat or when they were bent with known curvatures. Recorded data was then analyzed offline. In order to reduce the error due to bending, four regression-based error compensation methods were investigated. These error compensation methods required the use of a regression algorithm to form a model for pressure prediction based on FSR data and sensors' curvatures. To determine which regression algorithm to use in these error compensation methods, three algorithms, namely, linear regression (LR), general regression neural network (GRNN), and random forest (RF) were assessed on the data collected from the sensors in the pressure chamber. The data that were used for assessment of the three regression algorithms was the combination of sensor data in all curved conditions in addition to the flat condition. Data were split into 5 repetitions, and five-fold leave-one-out cross validation was used to choose one of the regression algorithms be used in the four regression-based error compensation methods proposed in this study. The assessment was performed based on two outcome measures: R^2 and $RMSE\%$.

The three regression algorithms that were assessed for this study are amongst the most frequently used for regression purposes for FSR signals used in biomedical applications [119], [53], [141], [57]. Linear machine learning algorithms are commonly used for various types of signals for a multitude of applications due to their capability of prediction and their computational efficiency [53], [113], [54], [114]. These characteristics make LR suitable for applications that are sensitive to processing time such as the ones that require repetitions of data processing, and the applications that require real-time data processing.

GRNN is a probabilistic, memory-based neural network with a highly parallel structure. This algorithm learns in a single pass through available data and converges to the optimal regression surfaces with availability of more samples. It is capable of forming acceptable regression surfaces based on limited data and is known to work with sparse data in real-time environments. GRNN is fast learning and computationally efficient as it does not need back propagation. Moreover, its implementation is relatively simple and easy to use. [141], [142]. These characteristics of GRNN make it suitable for the analysis of this study, especially considering sparsity of curvature values.

RF is a non-conventional machine learning algorithm that is commonly used for classification and regression of FSR signals. It improves on individual decision trees by using an aggregation of weakly pruned trees to prevent over-fitting to training data. This enhances generalization of the models created by RF [143]. These characteristics of the three aforementioned algorithms, common application of them to FSR signals, and their performance for the baseline condition of this study, which is when data from the flat condition and various curved conditions were combined, are the reasons they were chosen for assessment of the dataset of this study.

The selected regression algorithm was used in the four regression-based error compensation methods that were investigated. The objective of the error compensation methods was to take into account the variability introduced in the sensors' responses due to their bending. A common method to account for such variability in different conditions is to calibrate sensors separately for each condition [144]. Method1 does so by separating data based on the curvature of the sensors and making a separate model for each condition using the selected regression algorithm. To predict pressure for test data using this method, the model associated with the curvature of test data would be used. Method2 uses the selected regression algorithm to make a single model for all data. In this method, the value of curvature is used as an input channel for model training and pressure prediction. Findings of method2 motivated implementation of method3 and method4. More explanation on this is provided in the "Discussion" section. Method3 splits the data to flat and curved. It then uses the selected regression algorithm to make a separate model for each of these two conditions. Pressure prediction for test data using this method is similar to the first method. Method4 is similar to method2 except that the curvature input channel in this method has binary values of 0 and 1 representing whether the sensor is curved or flat. For comparison of performance of these methods, data were split to 5 partitions and five-fold leave-one-out cross validation was used with the two aforementioned outcome measures (R^2 and $RMSE\%$).

Findings of this study showed that the curvatures of FSR sensors affected their responses. Moreover, the four error compensation methods proposed in this study proved to be effective to reduce the errors caused by bending of FSR sensors. The findings of this study in the

future, can potentially be used to further improve the performance of FMG controlled prosthesis.

5.3 Materials and Methods

To assess the effect of bending on accuracy of the response of FSRs, sensors' responses to known pressure values were examined as they were placed on structures that were flat or were curved with various curvatures. Regression methods were used to map sensor responses to pressure values. To assess whether bending the sensors significantly affected their response accuracy, two conditions were first compared: sensors' responses when only the flat condition was considered and sensors' responses when all six conditions were considered. Multiple error compensation methods were then used to decrease the errors introduced due to the bending of the sensors and their performances were compared.

To collect required data for this study, a test setup was needed that could apply pressure on sensors in the matrix while measuring the value of the applied pressure, i.e. true pressure value. The measured value would then be used to produce the regression model.

For all statistical tests, normality of data was determined using the Shapiro-Wilk test. When data were from a normal distribution, depending on the number of populations being compared, either the Student's paired t-test at significance level of 5% or a repeated measures ANOVA was employed. For these tests, 70 samples were used, each representing the outcome measure for one of the sensors in the matrix.

For cases where the assumption of normality was violated, non-parametric tests were used. When more than two populations were being compared, the Friedman test was used. For post hoc analysis in these cases, or in cases where two populations were being compared, depending on symmetry of the distribution of differences between paired variables, either the Wilcoxon signed-rank test or the paired-samples sign test with a Bonferroni correction was used. All tests were conducted with the IBM SPSS Statistics v24 software.

5.3.1 Sensor Matrices

To explore the extent of the effect of bending on accuracy of the response of FSRs, an off-the-shelf sensor matrix of FSRs was chosen for this study: the TPE-900 Series multi-touch

resistive evaluation sensor by Tangio Printed Electronics. This sensor matrix was chosen due to its independence on specific hardware or electronics. The FSR matrix used in this study was comprised of 7 rows and 10 columns of individual FSR sensors and its dimensions were approximately 7 cm x 10 cm. The sensor matrix is shown in Figure 5.2. For this experiment, the sensor matrix was sealed using Polydimethylsiloxane (PDMS) to prevent the pressurized air inside the chamber from filling the air channel that was integrated in the design of the matrix. If the air channel was filled with pressurized air, the pressure difference between the environment and the sensor matrix's air channel would be zero. This would prevent the sensors from sensing the air pressure in their surrounding environment.

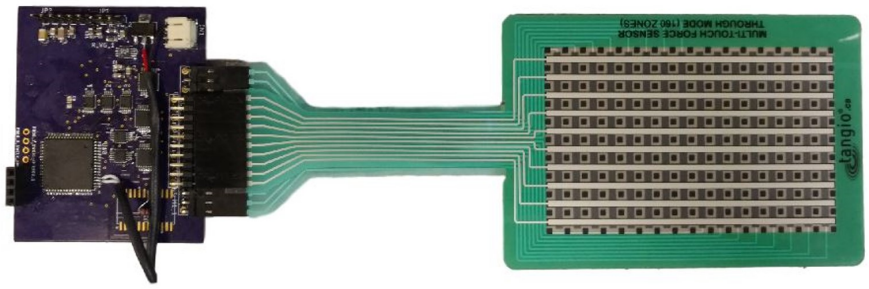

Figure 5.2: FSR matrix and the data acquisition PCB used in this study. Reproduced from [145] with permission.

5.3.2 Data Acquisition

Two-dimensional (2D) networks of matrices are used in variety of applications such as tactile sensing, pressure distribution measurements, temperature sensing, gas detection, etc. [146]. Shared signal and power lines between sensors in a row and sensors in a column allow for smaller number of traces which simplifies hardware and electronics. However, an inherent problem with the row-column fashion of these matrices is the cross-talk between adjacent elements of the matrix.

Cross talk is the unwanted effect that activation of a sensor may have on the response of other sensors in the matrix [147]. This effect is observed in 2D networks of sensors due to parasitic parallel paths that cause current leaks. This phenomenon is represented in Figure 5.3. In this figure, the circuit used to read the target FSR (RT), using a voltage divider, is

shown in part (a). This circuit is then simplified in part (b). It can be seen in this figure that as one sensor is pressed, paths form that can affect the current passing through other sensors. This phenomenon causes unreliable readings of individual sensors as other sensors in the same row or column are under pressure, i.e., are active.

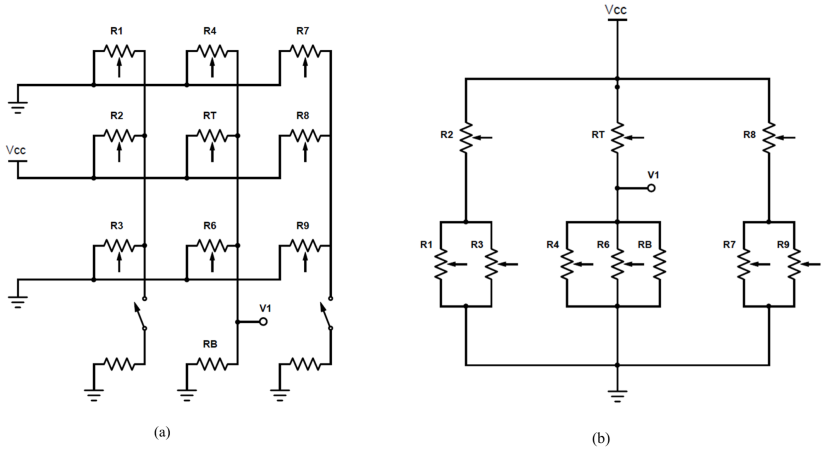

Figure 5.3: FSR matrix representation. (a) Original circuit of a 3x3 FSR matrix (b) simplified circuit.

Various circuits are proposed and used in literature for scanning of piezoresistive sensor arrays that reduce the interference of unwanted paths [146], [148], [149]. Two of the commonly used cross-talk suppression circuits are based on the Voltage Feedback method and the Zero-potential method [148].

In this study, a printed circuit board (PCB) was designed for data acquisition that used the Zero-potential circuitry shown in Figure 5.4. The data acquisition PCB used a Cypress PSoC 4 (model CY8C4247AXI-M485) microcontroller, op-amps, switches, a voltage regulator chip, a voltage reference chip, and multiplexers. Outputs of the circuit were transferred to a computer using universal asynchronous receiver-transmitter (UART) communication and were then saved on the computer for offline data analysis. The PCB could acquire data from sensor matrices of up to 10 columns and 16 rows. PCB is shown in Figure 5.2.

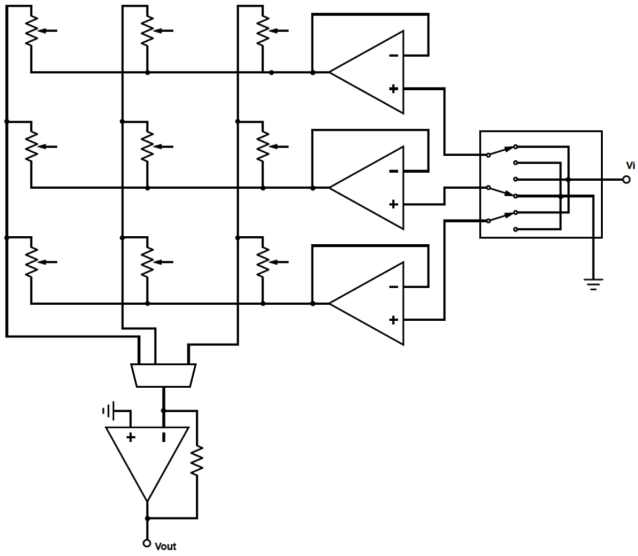

Figure 5.4: Cross talk compensation circuit used in this study. Reproduced from [145] with permission.

True pressure values also needed to be measured and recorded. This was done using a digital pressure transducer by Omega Engineering (model PX309) whose data was acquired using a National Instrument (NI) Data Acquisition Unit (DAQ)(model USB-6001). Recordings of sensor readings and pressure sensor values were synchronized using NI LabVIEW software.

5.3.3 Test Setup

Sensors' responses were assessed in six conditions: when sensors were laid flat and when they were placed on each of the five structures that were designed with varying curvatures. The curved structures were 3D printed and are shown in Figure 5.5. Each structure was part of a cylinder with a different radius, namely 5, 7, 9, 11, and 13 cm, with corresponding curvatures of approximately 0.20, 0.14, 0.11, 0.091, and 0.077 cm^{-1}, respectively. As transtibial amputations account for majority of the major lower limb amputations [150], [151], and transhumeral amputations account for majority of the upper limb amputations [150], chosen curvatures are based on measurements of the lower transtibial residual limb reported by Persson et al. [152] and the average circumference of the arm reported by Holzbaur et al. [153].

Persson et al. studied dimensions of 93 lower residual limbs to construct a standard formula of their classification into cylindrical (ordinary), conical, and club-shaped as well as short, ordinary ($breadth < length < 2 * breadth$), or long. In this study, they tested the constructed classification formula on 96 residual limbs of 86 volunteers in 135 examinations and determined that 80% of them were ordinary in both size and shape. Measurements of the breadth of the residual limbs were not reported, however, considering the ordinary length of the majority of the residual limbs and the range reported for their length, breadth of the stump of majority of participants can be approximated to be larger than 9 cm which corresponds to the curvature of about 0.2 cm^{-1} [152].

Holzbaur et al. used magnetic resonance imaging for measurement of the features of 32 upper limbs and reported an average of approximately 31 cm for the circumference of the arm which corresponds to the curvature of about 0.2 $m^{-}1$. Based on the measurements reported by the aforementioned studies, the highest curvature used in this study was 0.2 $m^{-}1$. The rest of the curvatures were chosen with 2cm variations in the radius of the cylinders up to the radius of 13 cm. The reason lower curvatures were not considered is that they were not expected to have considerable effects on sensors' responses [153]. As this was a preliminary study, it did not consider double curvatures which would be more important for the conical and club-shaped stumps which account for about 20% of the stumps according to the above study [152]. This should be considered in future work.

Design of the curved structures included fixtures to assure fixed placement of sensor matrices that was normal to the horizontal cross section of the cylinders. Fixtures were also added to the structures to ensure their mechanical stability under pressure. For the experiments in this study, to bend sensor matrices to specific, known curvatures, they were placed on these structures.

Figure 5.5: Curved structured used to bend the sensor matrix. From left to right, top to bottom, 5, 7, 9, 11, 13 cm. Reproduced from [145] with permission.

A test setup was required to apply and measure known values of pressure to the sensor matrix as it was bent. The setup included an air pressure chamber rated at 793 kPa built to American Society of Mechanical Engineers' specifications, a pressure transducer with ±0.25% best straight-line accuracy and range of approximately -103 to 1034 kPa, and an electrical feed-through to allow for powering the system and reading output values. This setup was similar to the one used in literature to evaluate sensory systems for prosthetic fitting [139], [133]. The test setup is shown in Figure 5.6.

Figure 5.6: Experimental setup using a pressure chamber. Reproduced from [145] with permission.

5.3.4 Data Collection

The sensor matrix was placed on a flat or curved surface and was placed inside the chamber. Sensors were then tested by increasing air pressure inside the chamber up to about 620 kPa and decreasing it back to room pressure in a cyclic manner. This was repeated for each condition (five curved surfaces and the flat surface) for up to 10 cycles. This method was similar to what has been done in literature for assessment of accuracy of similar systems [139].

Frequency of data collection was 10 Hz. At each frame, both sensor values and the pressure inside the chamber were recorded. Total number of data samples (observations) for the 6 sets combined was about 45000.

5.3.5 Regression Methods

To determine which regression algorithm to use in this study, three algorithms, GRNN, LR, and RF, were applied to collected data, and their performance was compared using two outcome measures.

Linear regression uses a linear combination of input data to create the regression model as shown in the equation below [154]:

$$y = \omega_0 + \sum_{i=1}^{N} \omega_i x_i \tag{5.1}$$

Where ω_i represents the weight of input feature i, x_is are the input features, N is the number of features, y is the predicted value, and ω_0 is the intercept of the linear model. In this study Matlab's implementation of LR was used. No parameter turning was required.

GRNN functions based on two layers other than the input and output layers: a pattern layer and a summation layer. First, the pattern layer assesses the relationship between each input feature and the corresponding prediction value. Then, the summation layer performs a dot product of a vector containing produced signals in the previous layer and a weight vector. This layer consists of two neurons: a numerator neuron that is the summation of weighted target values; and the denominator neuron which is the summation of weight values. The mathematical representation is the following [141], [142]:

$$align \qquad Y(x) = \frac{\sum_{j=1}^{N} Y_j L(x, x_j)}{\sum_{j=1}^{N} L(x, x_j)} \qquad (5.2)$$
$$L(x, x_j) = exp[\frac{-D_j^2}{2\sigma^2}]$$

Where $Y(x)$ is the prediction value, x is the new input, x_js are the training samples, D_j^2 is the Euclidean distance between x and x_j, and σ is the spread constant that was tuned to 2^{-7} using a grid search . The smaller the distance between new test data x and the training sample X_j is, the larger the value of $L(x, x_j)$ becomes. This makes the effect of training samples that are more similar to the new test data greater on its predicted value.

RF algorithm functions based on a modified version of decision trees. It creates an ensemble of weakly pruned trees. In a standard decision tree, each split is based on all available features while in RF trees, decision splits are based on comparisons of guesses among randomly selected input features. To perform prediction on a data point after RF model is learned, the aggregation of prediction of all decision trees are used. In the implementation used in this study, the mean of prediction of trees are used as the predicted pressure [119], [143]. Matlab's implementation of RF was used in this study. A grid search was performed to tune the number of trees to 150. The default option was used for the number of features used for each decision split which is one third of the number of variables.

The two outcome measures used in this study were: coefficient of determination (R^2) and Root Mean Square Error Percentage ($RMSE\%$) that are calculated using the following formulas:

$$R^2 = 1 - \frac{\sum_{k=1}^{n}(y_k - y'_k)^2}{\sum_{k=1}^{n}(y_k - \overline{y_k})^2} \qquad (5.3)$$

$$RMSE\% = \frac{\sqrt{\frac{1}{n}\sum_{k=1}^{n}(y_k - y'_k)^2}}{range_y} * 100 \qquad (5.4)$$

Where y_k is the expected value of the reading, y'_k is the predicted value, $\overline{y_k}$ is the mean of expected values, n is the number of observations, and $range_y$ is the range of values in

observations of expected values. R^2 and $RMSE\%$ are commonly used for assessment of performance of regression methods [108]. Based on these outcome measures, one of the regression algorithms was chosen to be used in this study.

Four different regression-based error compensation methods were examined to reduce the error caused in sensors' responses due to their bending. These methods were compared with each other and the baseline results based on the two aforementioned outcome measures. Baseline values were obtained by combining data from all 6 conditions (flat and curved). In the baseline method, one regression model was created and used for the combined data. In order to eliminate any bias based on the number of samples used in different regression methods, data were down-sampled in any of the methods that were using data from multiple conditions. The four error compensation methods are described in Table 5.1:

Method1	A separate model was made for each curvature and data for each curve was assessed separately. A total of 6 models were used in this method.
Method2	The value of curvature for each of the curved or flat structures was inputted as an extra channel to the model. Data was down sampled to 1/6 of total observations so that the number of observations was comparable to the one for Method1.
Method3	All curved structures were grouped together, and two models were made in total: one for when the matrix was laid flat, and one for all the curved conditions. Data was down sampled so that the total amount of data for each of the two groups was comparable to the one in method1.
Method4	Similar to method2, an input was added for curvature values. However, value of curvature was set to 0 for flat, and 1 for all the curved conditions. Data was down sampled similar to method3.

Table 5.1: Regression-based error compensation methods used to reduce the errors introduced due to bending of the sensors. Adapted from [145] with permission.

In all methods data were normalized based on the mean and the standard deviation of training data before model was made. This was done since in practice, test data is unknown

and cannot affect these factors. Each sensor was analyzed separately in all methods and the means of outcome measures for the 70 sensors were reported to represent the outcome measures for each method.

Five-fold leave-one-out cross validation method was used for all assessments done in this study. Data were split to 5 sections. Five repetitions of the assessment were done, in each, one of the 5 sections of data was held out as test data and the rest was used as training data. Obtained values of the outcome measures for each sensor was the average of the five repetitions.

5.4 Results

Figure 5.7 illustrates how the curvature of an FSR sensor affects its response to applied force or pressure. Since such variations can negatively impact the stability of sensor readings in practical situations, we propose a regression-based calibration system that takes into account the information about the curvature of a sensor in addition to its pressure measurements. In this section, results of our proposed method are explained in detail.

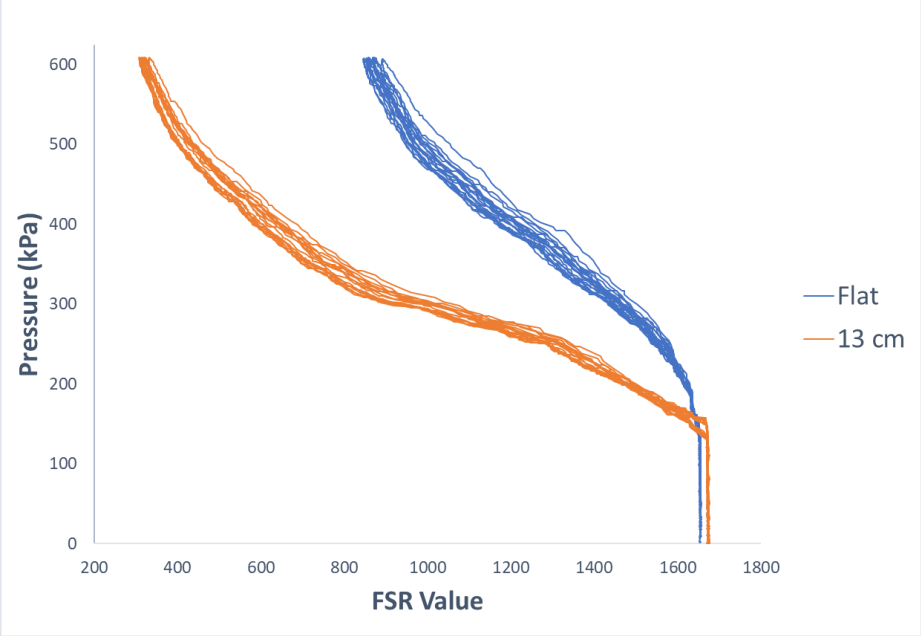

Figure 5.7: Comparison of the response of one of the FSRs when sensor was laid flat vs. when it was placed on the curved structure with radius of 13 cm. Reproduced from [145] with permission.

5.4.1 Algorithm Selection

Results of the two outcome measures using the three regression algorithms assessed in this study are shown in Figure 5.8.

Statistical analysis showed significant differences between results of the three algorithms in terms of both R^2 ($\chi^2(2) = 107.31, p < 0.001$) and $RMSE\%$ ($\chi^2(2) = 109.83, p < 0.001$). Post hoc analysis determined that LR had significantly worse performance in terms of both outcome measures. Means of R^2 values obtained using GRNN and RF were also significantly different. However, significance of the difference between GRNN's and RF's performances in terms of $RMSE\%$ was not determined.

GRNN was chosen as the regression algorithm to be used moving forward due to its better performance, lower standard deviations of errors and ease of use.

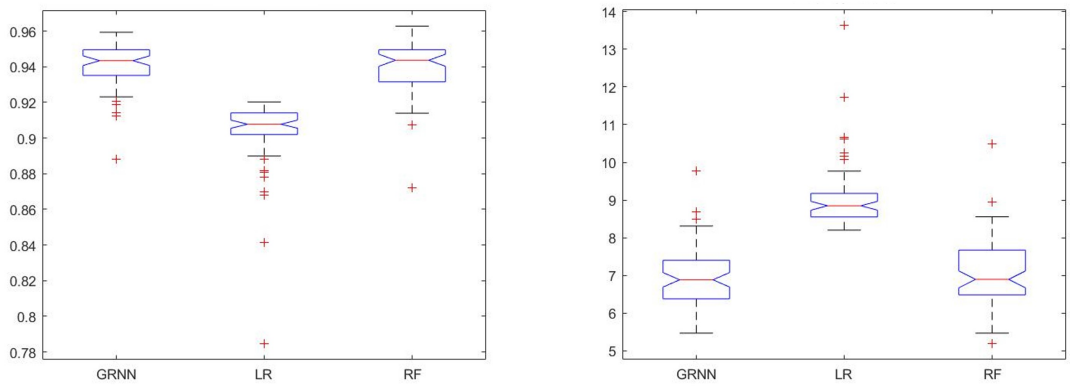

Figure 5.8: Comparison of performance of three regression algorithms: GRNN, LR, and RF. Reproduced from [145] with permission.

5.4.2 Method Selection

The comparison of when only flat condition was considered vs. when data from all six conditions were combined yielded results shown in Table 5.2.

Method	R^2	$RMSE\%$
Flat	0.99 ± 0.0012	3.51 ± 0.19
All Curvatures	0.94 ± 0.013	6.93 ± 0.81

Table 5.2: Comparison of when sensors were laid flat vs. when all 6 conditions were considered. Adapted from [145] with permission.

These results determined that inclusion of varying curvatures statistically reduced accuracy of prediction based on both outcome measures. To compensate for this effect, the four error compensation methods explained in Table 5.1 were used. Results obtained using these methods are shown in Figure 5.9 and Table 5.3.

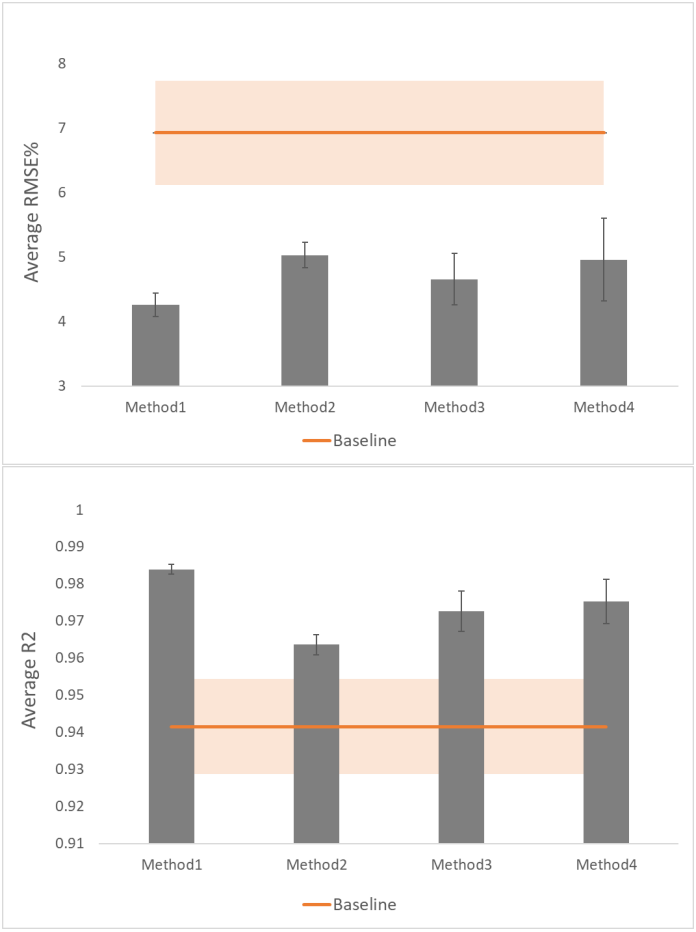

Figure 5.9: Outcome measures for the four proposed methods. Reproduced from [145] with permission.

Method	R^2	$RMSE\%$
Baseline	0.94 ± 0.013	6.93 ± 0.81
Method1	0.98 ± 0.0014	4.26 ± 0.18
Method2	0.96 ± 0.0027	5.03 ± 0.20
Method3	0.97 ± 0.0055	4.66 ± 0.40
Method4	0.98 ± 0.0060	4.96 ± 0.64

Table 5.3: Results of method selection. Adapted from [145] with permission.

The baseline method had the worst performance compared to all the other methods. Method1 yielded the best results. Method2 made significant improvement compared to the baseline results, however, its performance was significantly worse than method1. Method3 showed improvement over both the baseline and method2 with significant difference for both R^2 and $RMSE\%$ outcome measures. Yet it did not achieve as much improvement as method1. Method4 also showed improvement over method2 but could not reach the amount of improvement obtained using method1. Means of the average values for both outcome measures for this method were statistically significantly different from both method2 and method3. This method performed better in terms of R^2 but worse in terms of $RMSE\%$ compared with method3 with significant difference.

Statistical analysis using the Friedman test determined significant differences between results of all methods including the baseline in terms of both R^2 ($\chi^2(4) = 270.09, p < 0.001$) and $RMSE\%$ ($\chi^2(4) = 246.83, p < 0.001$). Post hoc analysis of means of both outcome measures showed significant differences between all methods.

5.5 Discussion

Bending FSR sensors can affect their neutral state value which is their response in the minimum pressure of the system. The effect of bending on the neutral state value of sensors is shown in Figure 5.10 by comparing the response of one of the sensors in a low range of pressure when the sensor matrix was laid flat vs. when it was placed on the structure with the radius of 13 cm. This phenomenon, in addition to other factors such as the non-

linearity of sensors' response to applied pressure, can considerably affect the response of FSRs when they are positioned with various curvatures. To better highlight this point, Figure 5.11 shows how applied pressure can be inaccurately interpreted from FSR readings if the sensor's curvature is not taken into account. Figure 5.11 also shows how a regression-based calibration method can resolve this issue.

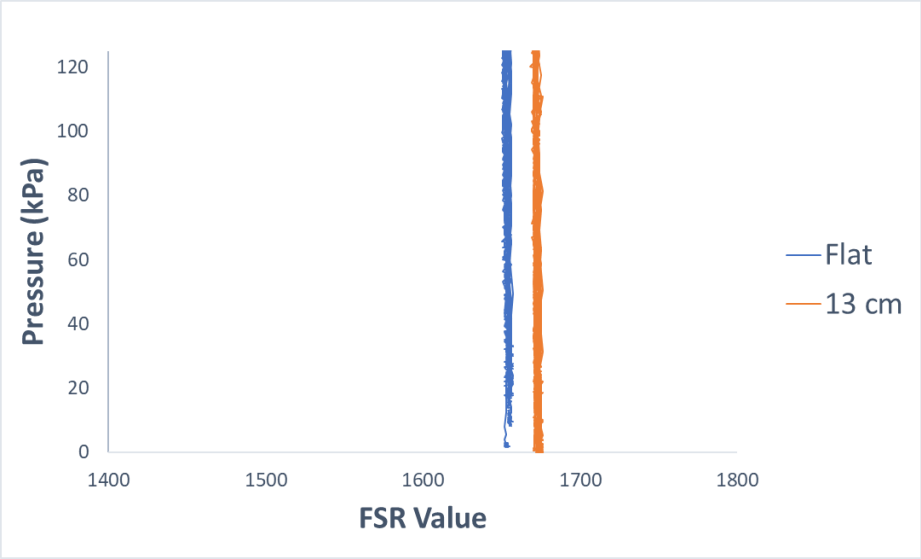

Figure 5.10: Comparison of the response of one of the FSRs when sensors were laid flat vs. when they were placed on the curved structure with radius of 13 cm. Response of the sensors in low pressure values is shown. Reproduced from [145] with permission.

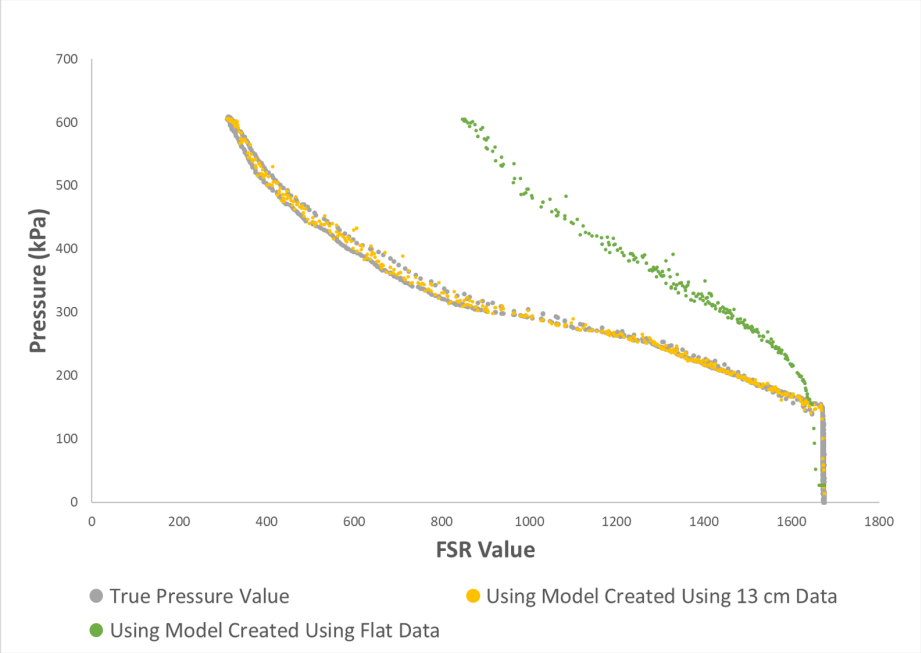

Figure 5.11: Comparison of predicting pressure from output of one of the sensors without and with considering sensor's curvature information. Sensor was curved with a curvature of approximately 0.77 cm^{-1}. GRNN regression algorithm was applied to predict pressure values from the measurements of one of the sensors. Reproduced from [145] with permission.

The goodness of fit of the regression models was compared in two cases: when only the flat condition was considered vs. when varying curvatures were also included. This comparison determined that the effect of variation in curvatures of the sensors on their responses was statistically significant. In this step of the experiment, statistical significance was determined using the Student's paired t-test.

Four regression-based error compensation methods were used to compensate for this effect. These methods were compared with the baseline. The baseline method yielded values for errors without any attempt to compensate for the bending errors in the sensor matrix. As expected, this method had the worst performance compared to all the other methods.

Method1 classified data to six classes of matrix positioning: one for flat and five for bent with different curvatures and created a separate model for each class. This method resulted in the best accuracy of prediction based on both of the outcome measures used in this study. This was likely because in this method, data from each condition was considered separately without any effect from data from other conditions. In this method, variation of data used

for training and testing of each model was minimal compared to other methods. The main disadvantage of this method was its difficulty of implementation in practice. This is because, in practice, curvature values are continuous while this method requires classification of data into discrete curvature conditions. A solution for this is to classify data based on ranges of curvatures and to use separate models for each of the classes of curvature range.

Method2 used values of curvatures of the sensor matrix as an added input channel to the regression algorithm. Compared to method1, this method performed significantly worse. A closer look at the data indicated that similarities between the data when sensors were curved with different curvatures was much more than similarity of the data between any of the curved conditions and the flat condition. This can be seen in Figure 5.12.

Looking at the physics and operation of FSRs may help in understanding why their behaviour changes when they are curved. It may also clarify the reason for similarity of sensors' responses when curved with various curvatures. Force sensitive resistors are resistive polymer-thick-film (RPTF) sensors comprised of multiple layers including semi-conductive layers and electrode layers. These sensors often employ a spacer mechanism such as spacer layers or air channels to control the spacing between the substrates of the sensors. This layer ensures high resistance of the sensors in the absence of external forces. When force is applied to the sensors, their resistance decreases due to two main factors. The first factor is the comprising layers of the sensors becoming in contact with each other. The other factor is variation in the geometry of the semi-conductive layer in a way that reduces sensors' resistance [53].

When sensors are bent, their physics that play an important role in their responses to pressure also change. Curving FSRs causes their comprising layers to become closer to each other which can be considered similar to pre-loading the sensors. Moreover, since the forces due to bending are not distributed evenly across the sensors [142], their curvature affects their responses not only by pre-loading the sensors, but also by changing the rate of the change of their responses to increasing pressure. It is likely that the similarity of the responses of curved sensors regardless of the value of their curvatures is because of the

similarity in distribution of bending forces across sensors in these conditions compared to when they are laid flat.

The reason method2 did not make as much improvement as expected is likely that the differences between curvature values are not good representatives of the variation in data in corresponding conditions. The model likely assumes that the difference between the value of the curvatures of two conditions determines the difference between the sensors' responses in those conditions. However, this is not the case according to the data collected for this study. For example, the difference between the curvatures of the flat condition and the curved condition with the radius of 13 cm is about 0.08 cm^{-1} and the difference between the curvatures of the curved condition with the radius of 13 cm and the one with the radius of 7 cm is about 0.07 cm^{-1}. The differences between the value of curvatures in these cases are comparable, so the model likely assumes that the variations of the sensors' responses in these cases would also be similar. However, looking at the graph in Figure 5.12, it can be seen that the sensors' responses are much more different in the former case compared to the latter one.

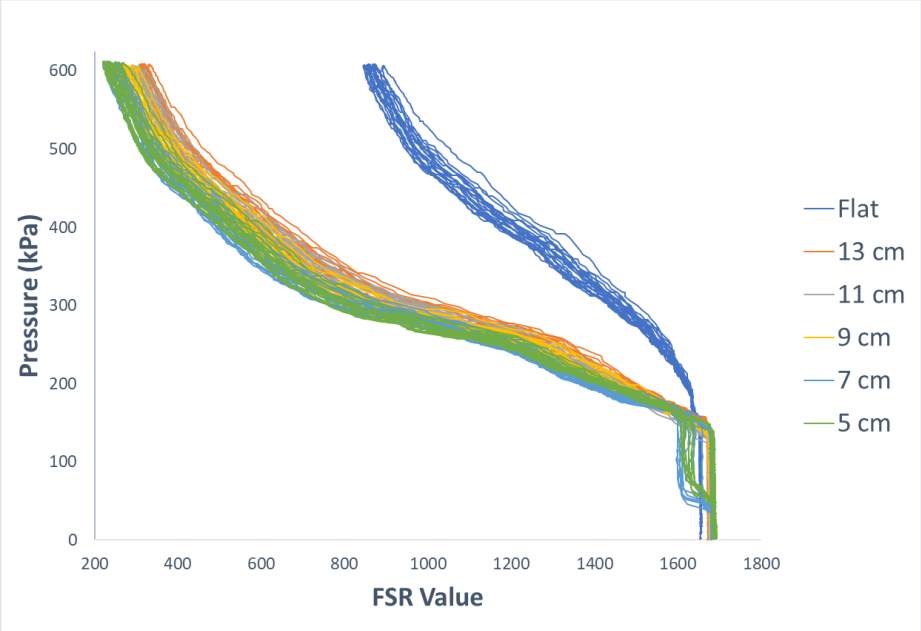

Figure 5.12: Comparison of the response of one of FSRs when sensors are positioned on structures with varying curvatures. Reproduced from [145] with permission.

A solution for this could be to use binary inputs for curvatures. This would imply using 6 extra input channels for model creation. In each of the 6 conditions, a unique binary sequence consisting of a single 1 and five 0s would be used. This solution was implemented for the dataset of this experiment. Obtained results were 0.96 $\pm$ 0.003 and 5.05% $\pm$ 0.19% for the R^2 and $RMSE\%$ respectively. Both outcome measures were improved compared to method2, however, significant improvement was not determined using the Student's t-test for either of the outcome measures. To further improve on this, categorical inputs could be used for curvature. However, in that case, curvature values would need to be classified to curvature ranges which would entail similar problems as the ones explained for method1.

Another solution to improve on method2 would be to determine a mapping of curvatures to continuous values that would be able to accurately represent the extent of their effect on variation of FSR responses. This should be investigated in future work.

The similarity between all curved conditions compared to the flat condition brought up the possibility of grouping all curved data and simply separating the two situations when the sensor matrix was laid flat and when it was curved, regardless of the amount of its curvature. This led to method3 and method4. Both method3 and method4 improved on the results obtained using method2 significantly.

Method3 made two different models, one for flat and one for curved. This method yielded improvement over method2 with significant statistical difference for both R2 and RMSE% outcome measures. This is likely because the error caused by ignoring variations in data when sensors were bent with various curvatures is smaller than the error caused by assuming that the value of curvatures were accurate representatives of the amount of variation introduced in data as sensors were bent. This was expected as discussed before. Method3 did not achieve as much improvement as method1 since, in method1 the error caused by assuming no variation in data from various curvatures was also omitted.

Method3 is easier to implement in practical situations compared to both previous methods. This is because there is no need to know the exact or even approximate value of curvatures, as long as it is known that the matrix is curved. It is reasonable to assume that sensors are bent in most locations when the matrix is embedded in a prosthetic socket.

Method4 inputted an extra channel to the algorithm. The value of this channel was 0 when the sensors were laid flat, and it was 1 when they were curved regardless of the amount of bend. This method, similar to method3 groups all curved data together. Method4 also showed improvement over method2 but could not reach the amount of improvement obtained using method1 for the same reasons explained for method3.

It is worth noting that since only two values, 0 and 1, were used as the second input for method4, this method is similar to binary curvature inputs that was discussed for method2. This is likely the reason why method3 and method4 have comparable performances (each outperforms the other based on one of the outcome measures). Method3 performed significantly better than method4 in terms of $RMSE\%$, however, it performed significantly worse than method4 in terms of R^2. In comparison of the last two methods, i.e. method3 and method4, it was determined that method3 outperformed method4 based in $RMSE\%$ while method4 outperformed method3 based on the other outcome measure (R^2). Because we only considered two outcome measures in this study, neither of which was considered more important than the other, and due to the fact that each of these methods performed better that the other based on one of these outcome measures, we cannot conclude superiority of one of these methods compared with the other. As a result, we cannot consider one of them to have had better overall performance for the dataset of this study.

In terms of computing power and running time, variations for testing using these methods are not considerable. This is because in all methods, the model is produced using offline data. In online testing, at each sample and for each sensor, one prediction is performed using the pre-built model. The main difference among different methods would be in the training time. However, this is not an important factor in applications considered in this study since model production would be performed offline.

In order to use the proposed methods of this study, information about curvature of the limb is required. Various methods are used for geometric assessments of a residual limb that can be used for this purpose. Some possible methods include circumferential measurements and contacting methods utilizing digitizing methods of the cast of the limb or the residual limb itself [155], [156]. Since in common practice, for fabrication of prosthetic sockets, casts

are made in one of the initial steps, cast of the limb is available and can be used for geometric assessment of the limb [157]. Three-dimensional (3D) scanning is another method that has recently gained attention in the field of prosthesis for various applications. 3D scans of the limb can be used for extraction of information required for the methods proposed in this study. Another option would be to place sensors on the cast of the limb and calibrate them as they are curved and placed on the location of the limb that they would later be positioned on for measurements.

Bend sensors can also potentially be used to measure the value of curvature of sensors. Compared to the aforementioned methods, the use of bend sensors can be faster and easier but less accurate. Another method that could be valuable for this purpose in the settings similar to the one used in this study, is to use the value of FSRs in specific states to determine their curvature value. To achieve this, values of sensors in room pressure or another known state could be considered. Another option would be to determine the curvature value based on the response of sensors to cyclic variations of pressure. In either of these cases, features should be extracted from time windows with optimized lengths. For more reliable prediction of curvatures, values of multiple adjacent sensors can be considered. This method should be investigated in future work.

Chapter 6

The Effect of Variations in the Volume of the Residual Limb on Signals Used in FMG Controlled Prostheses

The material presented in this chapter is excerpted, reproduced, and modified with permission from the following paper:

C. Ahmadizadeh, B. Pousett, and C. Menon, "Towards Management of Residual Limb Volume: Monitoring the Prosthetic Interface Pressure to Detect Volume Fluctuations - a Feasibility Study," Applied Sciences, vol. 10, no. 19, p. 6841, 2020.

Sections of this chapter are reprinted or adapted from the above article for clarification and to fit the formatting and scope of this document.

6.1 Chapter Overview

The study conducted towards fulfilment of **objective 3.b** of this thesis is explained in this chapter. In this study the effect of fluctuations in the volume of the residual limb on signals used in FMG controlled prostheses is assessed through evaluations of FSR readings at the distal end of the prosthetic sockets of 7 participants with lower limb amputations.

Although volume variations occur in both upper and lower residual limbs, this effect is more considerable in the lower extremity residual limbs due to their weight bearing nature. Therefore, the study outlined in this chapter focuses on lower residual limbs.

6.2 Introduction

Variations in the shape and volume of the residual limb are common amongst individuals with amputations. Some of the causes of such variations are the residual limb's fluid volume changes, the user's weight variations, limb's muscle activity, and muscle atrophy and edema in immature residual limbs - defined as less than a year post amputation [158], [159]. Even in mature residual limbs, both diurnal and long term fluctuations in the volume of the limb may occur. The amount of volume variations in mature residual limbs varies considerably amongst individuals depending on their activity level, socket fit, dietary habits, etc. [160], [161], [162].

Changes in the volume of the limb may lead to problems in various aspects of prostheses use, such as control of externally powered prostheses. Volume variations cause inaccuracies in signals extracted from various human machine interfaces (HMIs) used for prosthetic control. One of the most widely explored HMIs for externally powered prosthesis control is force myography (FMG) [51], [2]. In FMG controlled prostheses, residual limb volume fluctuations cause variations in the pressure map at the interface of the limb and the socket which is the primary signal used for user intention interpretation in these devices [54], [20], [70].

Sanders et al. conducted a study that monitored positioning of the residual limb inside a prosthetic socket. In this study, they reported that a larger volume of the residual limb would cause a more proximal placement inside the socket [163]. Based on the results reported by Sanders et al. and the experience of the collaborating certified prosthetist, the effect of the variations in the volume of the residual limb is most significant on the interface pressure at the distal location. The interface pressure at the bottom of the socket is expected to change with variations in the volume of the limb because an increase in the limb's volume would cause the limb to get pushed upward inside the socket which would lead to a decrease in the interface pressure at the bottom of the socket. Therefore, the study outlined in this chapter investigated the effect of limb's volume variations on FMG signals by assessing this effect on signals acquired from the distal end of prosthetic sockets of individuals with amputations.

Moreover, this study proposes a method to gain information about variations in the volume of the residual limb. Such information can potentially be used to mitigate some of the negative effects of limb's volume variations on signals used in FMG controlled prostheses. Information about variations in the volume of the residual limb can be used in various manners to compensate for the changes they introduce in signals used for prosthesis control. For instance, the HMI could have multiple calibration settings each using a different machine learning model for user intention recognition. Each model would be pre-trained based on signals recorded in a specific state of the volume of the limb from the user, e.g. one model for low volume, one for medium volume of the limb, and one for high volume of the limb. In this method, when the device is being used, information about the current state of the limb's volume can be used to determine the closest pre-trained model which would be used for control of the device. This method could especially be practical for FMG controlled prosthesis since various pressure maps, and consequently different machine learning models, would be produced as the volume of the limb varies. [164], [159].

Various methods are available for measurement of the volume of the residual limb such as water displacement, anthropometric measurements, contact probes, optical scanning, ultrasound, spiral X-ray imaging, 3D scanning, and bioimpedence [159], [165], [166]. Among available methods, only a few can be employed for volume measurement within the prosthetic socket which is a requirement for most of the solutions discussed above. Bioimpedence and radiological imaging methods are the ones that can measure limb's volume within the socket. Out of these two methods, bioimpedence has the potential to monitor limb's volume as the user performs their daily activities [164]. Bioimpedence measures limb's volume by monitoring its resistance to electrical current which is then used to determine changes in fluid volume of the limb [167]. Sanders et al. tested this method on eight able-bodied participants and three participants with lower limb amputations and showed promising results for fluid volume measurements.

Although the bioimpedence method has shown promise for limb volume measurement within the socket, it requires contact between electrodes and the skin. To ensure proper electrical contact between electrodes and the skin, a layer of hydrogel is recommended

which may make this method less favorable for everyday use [164]. In this study, an alternative method is proposed that uses the distal limb-socket interface pressure to determine variations in the volume of the limb. This method is simple, easy to incorporate into the socket, inexpensive, and does not rely on electrical contact with the skin. Moreover, to use this method to enhance accuracy of control in FMG controlled prostheses, the distal limb-socket interface pressure can be accessed either using the available hardware in these devices or with minor modifications to the hardware.

This chapter presents a study to determine the effect of variations in the volume of the lower residual limb on FMG signals acquired from the distal end of the socket and to assess whether signals recorded from FSR sensors embedded at the bottom of the prosthetic socket can be used to gain information about variations in the volume of the limb. In the study outlined in this chapter variations in the volume of the residual limb were simulated by changes in the number of sock plies worn by volunteers.

This study was carried out in two phases. The first phase was conducted to determine the effect of variations in the volume of the residual limb on limb-socket interface pressure. To investigate this effect, variations of as large as three sock plies - which was determined by the collaborating prosthetist based on their expertise - in the volume of the limb were considered. The first phase was also to demonstrate the possibility of detecting variations in limb's volume using the proposed method. To test this possibility, the locations at the bottom of the socket at which the variations of pressure would be representative of the changes in the volume of the limb were identified. Results of this phase were based on data collected from four participants with transtibial amputations. Each participant was asked to walk a marked distance of 3 meters back and forth 5 times in three conditions of sock plies. Readings of FSR sensors were then compared in the three conditions. Findings of this experiment motivated proceeding to the second phase of the study.

Having established the effectiveness of the proposed method in phase 1, the second phase was carried out to determine the resolution, i.e. the smallest variations of the limb's volume that could be detected using the proposed method under simulated conditions. The experiment carried out in this phase involved three volunteers with transtibial amputations.

The protocol and setup were similar to the first phase. FSR readings were compared in increments of one and two plies.

Findings of this study determined that variations in the volume of the residual limb affected signals used in FMG controlled prosthesis. Moreover, it was shown that using a sensor at the distal end of the prosthetic socket enabled variations in the volume of the limb to be determined. This information can potentially be used to enhance the performance of FMG controlled prostheses in the future.

6.3 Materials and Methods

Materials and methods used in the experiments conducted in the two phases of the study are explained in this section. An FSR sensory system was installed inside the prosthetic sockets of volunteers and data were collected as they walked a marked distance. Collected data were then analyzed offline.

Experiments conducted in this study were approved by the Office of Research Ethics at Simon Fraser University and informed consents were provided by participants. All experiments were conducted in collaboration with a Certified Prosthetist.

6.3.1 Participants

In the first phase of this study, data were collected from four participants with transtibial amputations. For the second phase of this study data were collected from three participants with transtibial amputations. All participants used their prosthesis on a daily basis. More information about participants can be found in Table 6.1. The volunteers were recruited by Barber Prosthetics Clinic (BPC) (Vancouver, BC, Canada).

6.3.2 Hardware

The sensory systems used for data collection in this study contained FSR sensors from Tangio Printed Electronics (North Vancouver, Canada), model TPE-502 round sensors with the diameter of approximately 2 cm. FSRs were connected to an Arduino model Pro Mini that would register their responses through a voltage divider circuit where the FSR sensor was connected between V_{dd} - that was provided by the Arduino - and V_{out}, and a base

	Participant	Weight Range (kg)	Amputation Side	Prosthesis
Phase 1	1	65-70	right	TSB socket with a TPE cushion liner and a suspension sleeve
	2	85-90	left	PTB socket with a sock fit and sleeve suspension
	3	90-95	left	TSB socket with a hybrid locking liner
	4	110-115	right	TSB socket with a silicone cushion liner and a sleeve suspension
Phase 2	1	100-105	right	TSB socket with a hybrid locking liner
	2	80-85	right	Hybrid socket with a gel sock and sleeve suspension
	3	105-110	left	TSB socket with a silicone cushion liner and sleeve suspension

Table 6.1: Summary of weight range, amputation side, and prosthesis type of participants of this study. TSB: Total Surface Bearing, TPE: Thermoplastic Elastomer, PTB: Patellar Tendon Bearing. Adapted from [168] with permission.

resistor was connected between V_{out} and ground. All sensors were connected to the same resistor on one side, and a separate Arduino output on the other side. The voltage at the Arduino side of each sensor was raised to V_{dd} when the other sensors were not supplied with a voltage. As a result, only one sensor was activated at each point in time. Analog sensor readings obtained through this method were converted to digital values to be read by the Arduino. Sensor readings were transferred to a computer by the Arduino board wirelessly using a Bluetooth module. The system was powered using a 3.7 V Lithium Polymer (LiPo) battery. The main components of the system are shown in Figure 6.1.

In phase 1, four sensors were placed in the distal, anterior distal, medial distal, and lateral distal locations inside the prosthetic sockets that participants used on a daily basis. The distal end of the socket was selected since it was expected that an increase in the volume of the residual limb would cause the limb to be pushed upward inside the socket. This would cause the interface pressure at the distal location to be considerably affected by such variations in limb's volume. This hypothesis was based on literature and experience of the collaborating prosthetist [163]. Posterior distal pressure was not considered as less pressure variation was expected at this location compared to the other distal locations due to higher ratio of soft tissues at this location in most individuals. Placement of sensors

inside the prosthetic socket in phase 1 is shown in Figure 6.1. Number of sensors and their placement in phase 2 were determined based on results of phase 1 and are explained in the 'Results' section.

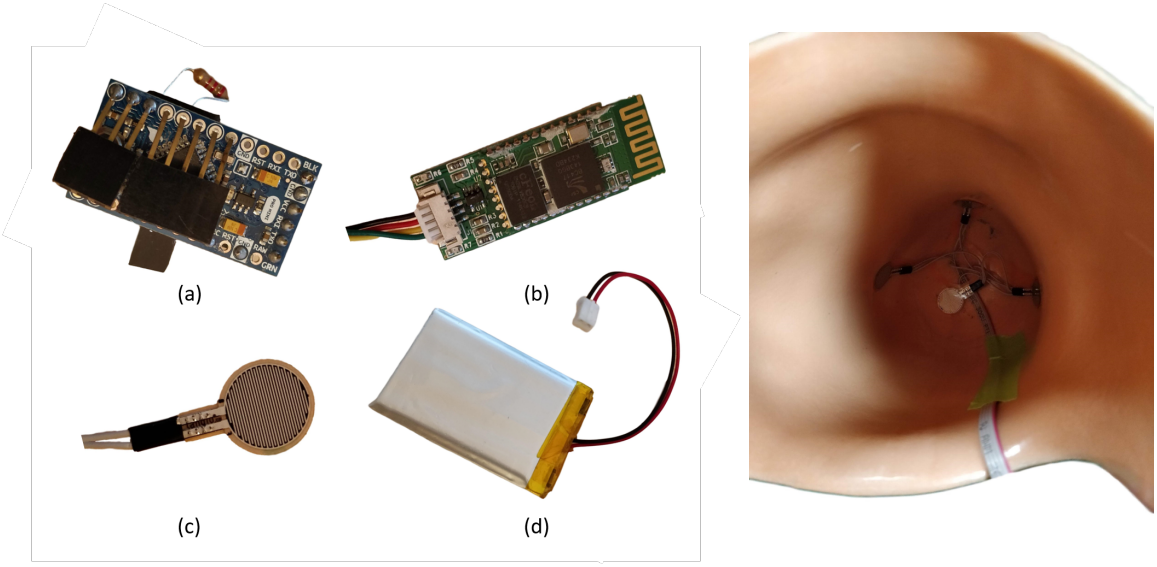

Figure 6.1: The figure on the left shows the main components of the system: (a) an Arduino Pro Mini board, (b) a Bluetooth module, (c) an FSR sensor, (d) a LiPo battery. The figure on the right shows the placement of the four FSRs inside the socket in the distal, anterior distal, lateral distal, and medial distal locations. The image shows the lower limb prosthetic socket from the top. The bottom of the image shows the posterior side of the socket. Reproduced from [168] with permission.

6.3.3 Protocol

Experimental protocols used in the two phases of this study are explained in this section. Each phase of this study contained one experiment. The first experiment was designed to demonstrate that variations in the volume of the residual limb affect the FSR signals obtained from sensors placed at the bottom of the prosthetic socket. In this phase, the possibility of our proposed method to determine variations in the volume of the residual limb was also tested. To test the possibility of determining limb's volume variations based on distal interface pressure, four locations at the bottom of the socket were examined and the locations of the sensors that were able to determine variations in the volume of the limb were determined. The second experiment was to determine if smaller variations in

the volume of the residual limb could be detected using signals from sensors placed in the locations determined in the first experiment.

To collect data, FSRs were placed in the four aforementioned locations inside the participants' sockets. This was performed in the beginning of the data collection session for each participant. The locations of the sensors were not modified throughout the session.

In the experiments conducted for both phases of the study, prosthetic socks were used to simulate variations in the volume of the limb. Prosthetic socks were added to increase the volume, conversely socks were removed to reduce the volume. Three sock ply conditions were considered in both phases: 'normal plies', 'less plies', and 'extra plies'. The number of sock plies that would be considered normal for each participant was determined by the collaborating prosthetist based on information provided by the participant regarding their level of comfort and socket fit. The difference between the number of sock plies worn by participants in different sock ply conditions varied for the two phases as larger variations in the volume of the limb were considered in the first phase compared to the second phase. More details regarding the amount of variation between the sock plies worn in different conditions are provided in following subsections.

For each sock ply condition of each experiment, after adjustment of sock plies based on the condition being investigated, the participant would don their prosthesis without any further preparation and perform the protocol of the test.

The protocol consisted of the participants walking a marked distance of approximately 3 m on a flat surface back and forth. Five repetitions of this was performed for each sock ply condition (test). FSR signals were obtained and saved as the participant was performing the task of the protocol. Video was also recorded for data labelling. The sampling rate of FSR data collection was 10 Hz.

Phase 1 For this phase, in the 'less plies' condition, the participant would wear three sock plies less compared to the 'normal plies' condition, and in the 'extra plies ' condition, they would wear three plies more than the 'normal plies' condition.

Phase 2 In the second phase, each condition differed from the next/previous condition by variation of one sock ply. To reduce the effect of variations of thickness of sock plies due to the sock's age, manufacturer, etc., in each condition, a 1-ply sock was either added or removed to ensure the increase/decrease in the thickness.

6.3.4 Data Analysis

Data collected during the two phases of this study were saved on a computer and processed offline. The goal of data analysis was to determine if signals or features extracted from signals recorded from sensors placed in the prosthetic socket varied in correlation with changes in the number of sock plies worn by users.

To separate sections of data that corresponded to the time volunteers were performing the 'walking' task of the protocol, recorded videos were used. This task was performed manually for each individual, and for each test condition. Then raw FSR signals were filtered using a second order Butterworth low pass filter to remove noise. The cut-off frequency for the Butterworth filter was determine based on the Welch's power spectral density estimate of the signal being filtered. Peaks of filtered signals were extracted. Each peak corresponds to one step as pressure/force at the distal end of the socket peaks once in every step taken by the foot being monitored - the leg with amputation in this case - at the time when the maximum amount of user's weight is loaded on the foot during the mid-stance phase of a gait cycle. To obtain a single measurement per sensor, for each participant, and for each condition, the values of peaks of FSR signals were averaged. This was to avoid pseudoreplication in statistical tests [169].

The average peak values of FSR readings were converted to force. To convert FSR readings to force, a calibration method was used in which sensors' readings in response to known values of applied force were measured for multiple FSR sensors as the applied force increased and decreased in a cyclic manner. In this experiment, the value of applied force was known based on measurements of load cells. Using measurements obtained in this experiment, an exponential curve was fitted to map sensors' responses to force values. The reason exponential fitting was used for this calibration was based on the documentation of FSR sensors used in this study.

In order to generalize the results, average peaks of force values were normalized with respect to the values obtained in the 'normal plies' condition for each participant. Normalized means of peaks of force were the final measure that were compared in the different conditions of sock plies. The process of data analysis is shown in Figure 6.2.

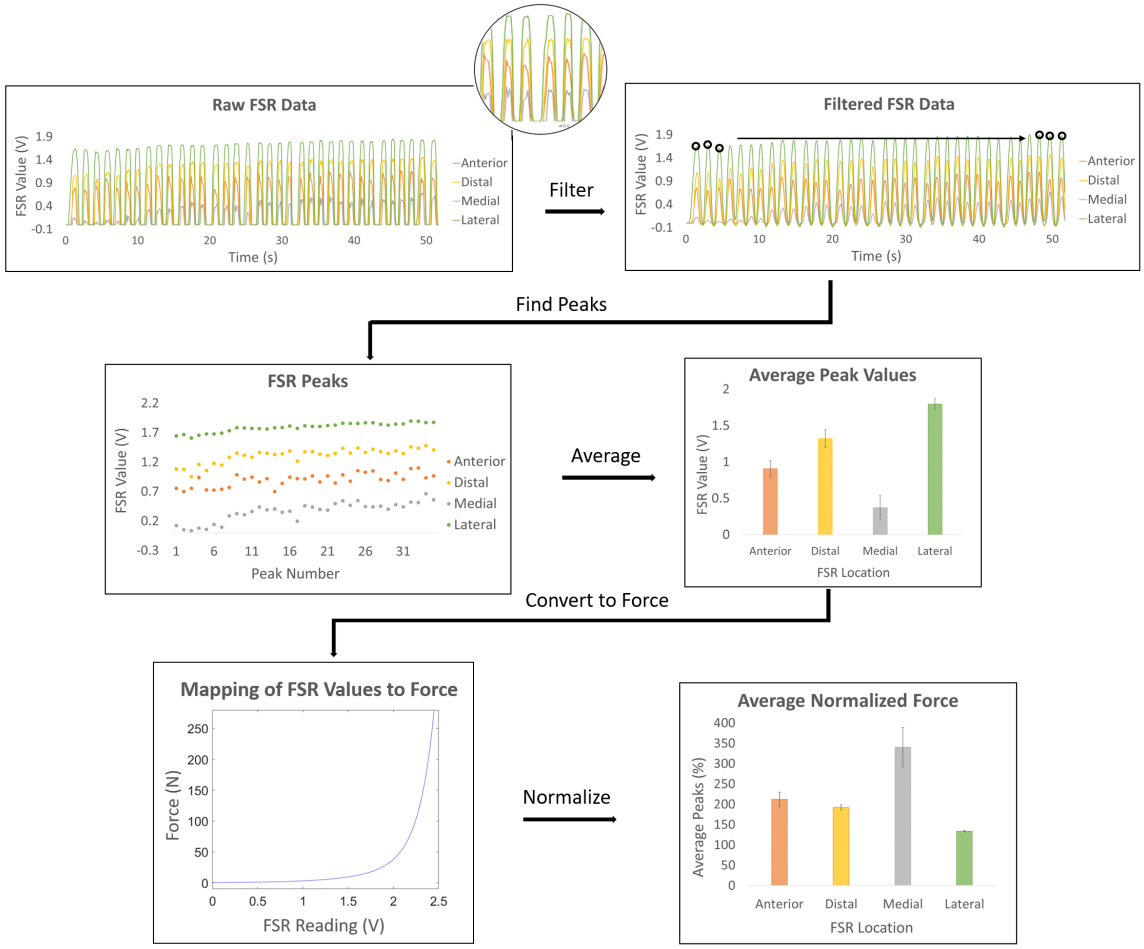

Figure 6.2: Data analysis process used in this study that consisted of filtering the raw signals, finding peaks of the filtered signals, averaging the peaks, converting mean peaks to force, and normalizing the average peaks of force. Reproduced from [168] with permission.

It is worth noting that in the beginning of each test, after donning the socket, there was a transient period when the user's residual limb and the prosthetic socket were adjusting to the test conditions. The length of this time in each test depended on the socket fit, the shape of the residual limb, the number of sock plies, and other variables such as the user's weight. For the purpose of this study, this transient section - about 4 steps on average -

was removed from the beginning of the protocol in each test condition as present only in the beginning of the tests and not representative of normal operations of the socket.

For statistical analysis, randomized complete block experimental design with mixed-model analysis was used where volunteers were considered random effects. This was to remove the effect of variations of data due to variables associated with conditions of each individual [170]. In this repeated measures design, normalized means of peaks of force obtained from different participant for each sock ply condition, for each phase were considered as repeated measures. statistical analysis performed for this study were done using JMP statistical analysis software from the Statistical Analysis System (SAS) institute (Cary, NC, US).

6.4 Results

This section reports the results obtained from the experiments of the two phases of the study based on the measure explained before - i.e. the normalized average of peaks of force.

6.4.1 Phase 1

In this phase, the effect of variations in the volume of the residual limb on readings of the sensors embedded in the distal end of participants' prosthetic sockets was investigated. The obtained normalized means of peaks of force for the four participants of phase 1 are shown in Figure 6.3 and Table 6.2. Results showed that the force read by all four sensors were affected by the variation in the residual limb.

In the first phase, the possibility of the proposed method to gain information about variations in limb's volume from distal limb-socket interface force was also investigated. This method functions based on a correlation between variations of the interface pressure at the bottom of the prosthetic socket and changes in the volume of the residual limb. The possibility of determining variations in the volume of the limb through measurements of the interface pressure in four locations at the bottom of the socket was tested.

As shown in Figure 6.3, the force measured by the sensor placed at the distal location decreased as the volume increased in all participants in the first phase which followed the

expected pattern of variation in interface pressure as a result of fluctuations in the volume of the residual limb.

In two of the other locations considered, namely the lateral distal and the anterior distal locations, the force measured by sensors followed the expected pattern in all participants except in participant 2.

The normalized average peak of force at the medial distal location did not follow the expected pattern in both participants 2 and 3. This measure increased between the 'less plies' and the 'normal plies' conditions and then decreased between the 'normal plies' and the 'extra plies' conditions in these participants at this location. However, the differences in the force values between the three conditions in participant three were very small considering the standard deviations. Moving forward with this study, we chose to use the distal location as it was consistent in all participants. Results of phase 1 motivated proceeding to the second phase of the study.

Participant #	Sock Ply Condition	Distal	Lateral Distal	Medial Distal	Anterior Distal
1	Less Plies	192.2 ± 6.3	133.4 ± 1.9	340.3 ± 48.3	212.2 ± 17.2
	Normal Plies	100 ± 7.5	100 ± 2.1	100 ± 63.7	100 ± 18.0
	Extra Plies	39.5 ± 8.2	76.0 ± 2.0	49.4 ± 47.9	29.5 ± 16.3
2	Less Plies	122.1 ± 44.9	53.7 ± 3.9	29.7 ± 9.4	64.8 ± 64.8
	Normal Plies	100 ± 41.1	100 ± 3.8	100 ± 8.0	100 ± 78.4
	Extra Plies	85.3 ± 43.8	76.5 ± 3.9	79.8 ± 8.0	114.6 ± 78.8
3	Less Plies	415.6 ± 18.7	118.0 ± 0.8	97.7 ± 1.0	270.5 ± 6.7
	Normal Plies	100 ± 22.6	100 ± 0.8	100 ± 1.0	100 ± 7.4
	Extra Plies	67.1 ± 18.6	91.7 ± 0.8	96.8 ± 1.0	20.6 ± 6.8
4	Less Plies	156.7 ± 9.6	134.3 ± 0.8	120.2 ± 1.0	142.4 ± 1.1
	Normal Plies	100 ± 9.8	100 ± 0.8	100 ± 1.0	100 ± 0.9
	Extra Plies	17.1 ± 13.3	30.9 ± 1.1	38.7 ± 1.3	24.3 ± 1.4

Table 6.2: Mean peaks of FSR signals obtained in the first phase of this study.

To determine if normalized mean of distal force peaks changed significantly in response to variations in the volume of the limb, simulated by addition and removal of sock plies, mixed-model analysis was performed on results of the first phase. In this analysis, the null hypothesis was that normalized mean of distal force peaks remained the same in different sock ply conditions. As a result, rejecting the null hypothesis would determine that normal-

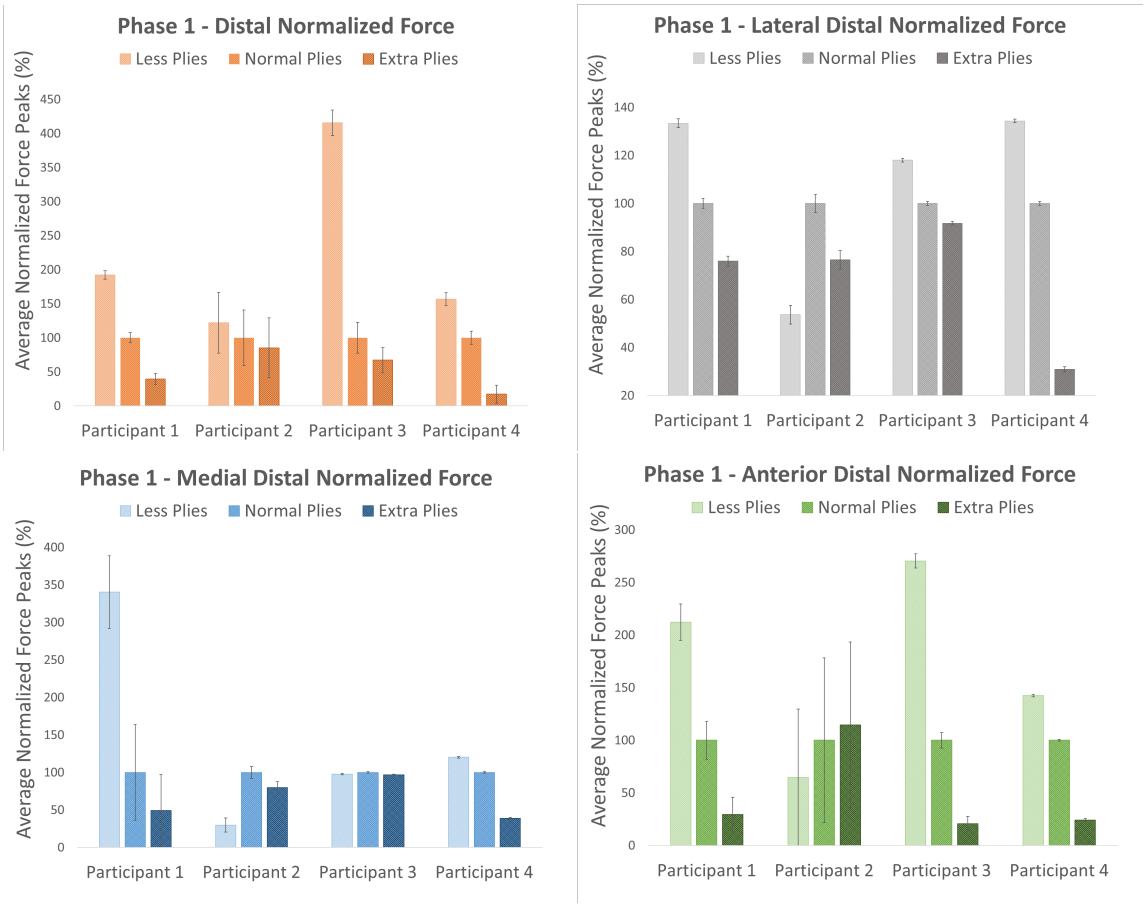

Figure 6.3: Average peaks of normalized force in four location at the bottom of the prosthetic sockets of the four participants in Phase 1. Reproduced from [168] with permission.

ized mean of distal force peaks changed in response to variations in the volume of the limb, thus proving that there is a relationship between distal force and volume of the limb. This would confirm that volume variations can be determined by monitoring distal force.

Results of mixed model analysis rejected the null hypothesis, proving the feasibility of our proposed method. Results of this analysis determined significant difference for the normalized means of peaks of force in the distal location in different sock ply conditions ($F(2,6) = 5.1742$, $p = 0.0494$).

Results of the two phases are also shown in Figure 6.5. This figure shows adjusted means and standard errors as predicted by the model fit to data from all individuals, as repeated measures, of each phase during mixed model analysis. Using adjusted means of the different sock ply conditions was deemed appropriate for quantitative representation of the results

of this study since it isolated the effect of sock plies by eliminating the effect of individual-specific variables, such as body weight and socket fit. This effect isolation was achieved by setting participants to be random effects in mixed model analysis.

6.4.2 Phase 2

In this phase, normalized means of force peaks at the location that was determined to be effective in the first phase, i.e. the distal location, were compared in three conditions varying by one prosthetic sock ply. To determine the effect of increments of as large as two sock plies on the distal FSR values, the first and the third conditions that varied in the number of sock plies by two were also compared. Results are shown in Figure 6.4 and Table 6.3.

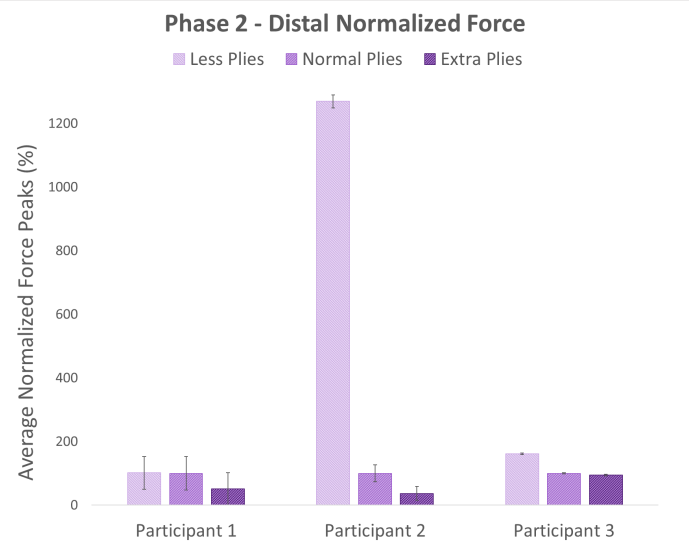

Figure 6.4: Normalized average peaks of force in the distal location of the prosthetic sockets of the three participants in Phase 2. Reproduced from [168] with permission.

As volume increased by either one ply or two plies, normalized average peak of force decreased in this location for all participants. This was the expected pattern and was consistent with the results of the first phase of the study. Adjusted normalized means across participants are shown in Figure 6.5.

Participant #	Sock Ply Condition	Distal
1	Less Plies	101.3 ± 51.9
	Normal Plies	100 ± 52.5
	More Plies	51.4 ± 50.6
2	Less Plies	1269.2 ± 20.6
	Normal Plies	100 ± 26.3
	More Plies	36.8 ± 21.5
3	Less Plies	161.7 ± 2.3
	Normal Plies	100 ± 2.2
	More Plies	94.8 ± 2.2

Table 6.3: Mean peaks of FSR signals obtained in the second phase of this study.

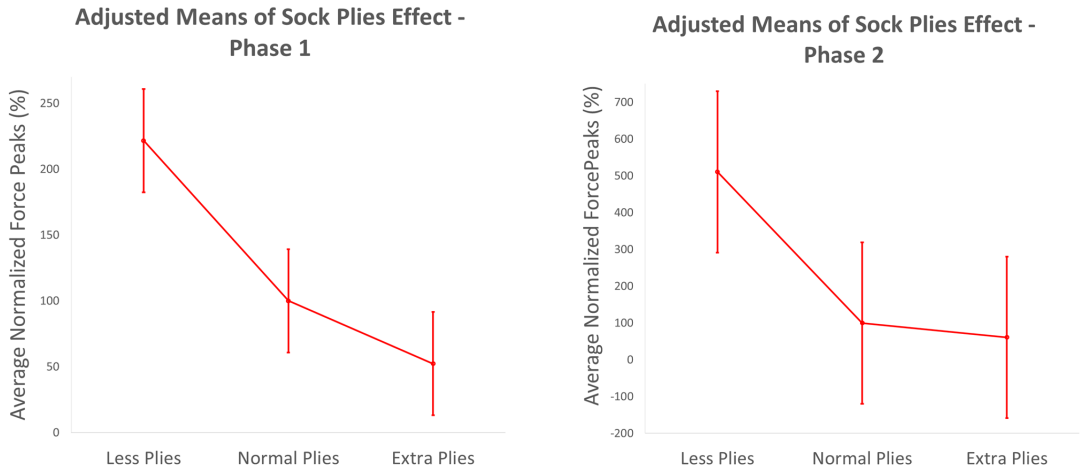

Figure 6.5: Adjusted normalized means of peaks of force in the distal location across participants in the two phases of the study. Reproduced from [168] with permission.

6.5 Discussion

As explained in the 'Results' section, the normalized means of peaks of force were affected as the volume of the residual limb varied in all four locations in all participants. Although the changes in force as a result of an increase in the volume of the residual limb did not follow the same trend in all locations in all participants, the presence of variations in the normalized means of peaks of force show that the factor being investigate in this objective introduces unexpected changes in the signals used in FMG controlled prosthesis. These

changes, if not accounted for, decrease the accuracy of intention recognition based on FMG signals.

To test the proposed method to gain information about variations in the volume of the residual limb based on distal limb-socket interface pressure, four locations at the distal end of the socket were considered. The normalized means of peaks of distal force decreased as the volume increased in all participants in the first phase. This decrease in the distal force as a consequence of an increase in the volume of the limb followed the expected pattern of variation in pressure at the bottom of the socket. This pattern is expected because as the volume of the limb increases, the limb gets pushed upward inside the socket which consequently relieves some of the distal pressure. The decrease in pressure in the distal location occurred between every two sock ply conditions that varied by at least three plies. This demonstrated the possibility of using the proposed method by facilitating the FSR readings at the distal location to determine variations in the volume of the residual limb.

In the first phase, in the lateral distal and the anterior distal locations, the results obtained from all participants were consistent with expected pattern except for participant 2. In this participant, as the number of sock plies increased, the pressure at the anterior distal location also increased. This pattern contradicts measurements at the distal location.

A closer look at the variables that could have led to this variation in the pattern of pressure change in participant 2 revealed that this participant, unlike all other participants, did not use a prosthetic liner underneath the socks. Although this could be the factor making this participant an outlier in those locations, it is important to note that such conclusions cannot be derived based on a single participant. For instance, the fact that participant 2 did not wear a liner could be indicative of variation in his socket fit compared to the rest of volunteers. To determine whether wearing a liner affects results obtained using the lateral distal and the anterior distal pressures, investigations with more participants is required.

The reason that the force at the anterior distal, medial distal, and lateral distal locations did not follow the expected pattern in phase 1 is likely that for those locations, sensors were placed more proximal compared to the distal location. This makes these locations more prone to variations in interface pressure that are caused by user's socket fit, style of socket,

and movements of the limb inside the socket. For example, depending on the shape of the residual limb and the relative location of the Tibia bone, the pressure distribution at the anterior location could vary in different individuals. On the other hand, all users were using non-distal-bearing sockets which made the pressure at the distal location more consistent. Moreover, an increase in the volume of the limb results in an increased width/diameter of the limb which could affects these locations that are more proximal compared to the distal location.

It is worth noting that although the pattern of variations in the distal normalized force peaks was consistent among participants, the absolute value of this measure or the amount of reduction in it with an increase of 3 sock plies is not the same in all participants. This is likely because multiple factors such as user's weight and socket fit influence the distal pressure in an individual. Moreover, the number of sock plies that were considered normal was selected based on information from the user. Since this selection was not automated using quantifiable measures, a certain degree of variation is expected between what different users consider to be the 'normal' socket fit or the 'normal' interface pressure.

The small sample sizes used in the two phases of this study are amongst its limitation and lead to low powers of statistical tests which result in higher probabilities of making type II errors. However, despite the small sample size used, results of statistical analysis for the first phase are valid. This is because significant difference was determined in the analysis performed in that phase, and when significance is determined, one does not need to worry about type II errors as they only occur when significance cannot be determined [171]. On the other hand, because significance was not determined in the second phase, statistical analysis was not valid for this phase as their results might have been compromised by type II errors. Thus, results of statistical analysis of the second phase were not reported. Results of the second phase should only be considered quantitatively as reported in the 'Results' section and need to be confirmed by future studies with larger sample sizes.

Various solutions are available for problems caused by volume fluctuations in the residual limb. The method proposed in this study is novel since unlike most other methods, it easily incorporates into the user's prosthesis with minimal modifications. The sensory system

requires one time installation and can be used seamlessly afterward. Using this method, volume variations can be detected as the user carries out their daily activities using the prosthetic socket without a need for doffing the socket. This method is simple to use and does not require extensive calibration before use. Signals used in this method can potentially be acquired throughout extended periods of time. FSR signals are easy to process which makes this method computationally efficient [114], [51]. Another advantage of this methods is that it does not require direct contact with the skin and is less prone to errors due to environmental changes compared to some of the alternative methods. Moreover, this method does not depend on the reason of volume change while some alternatives do. For instance, bioimpedence measures variations in the fluid volume of the limb rather than directly measuring the volume of the limb itself.

Signals acquired using the method proposed in this study can also be analyzed using machine learning algorithms. With data from more participants and in more sock ply conditions, regression algorithms can potentially be used for absolute discretized measurements of the residual limb. Another approach could be to use classification algorithms with features extracted from time windows to determine volume variations.

To use the proposed method in the real use case of the application, the sensory system needs to be embedded in the prosthetic socket of users and data should be recorded continuously throughout the day. In this scenario, an algorithm would be required to detect the 'walking' action during which FSR signals would be used to determine variations in the residual limb's volume. Various methods can be used for detection of the 'walking' action, one of which is the use of classification algorithms. The system used for this study facilitated rechargeable LiPo batteries which allows for it to be used in the real use case considered here.

In the case of applications for impaired individuals, case-by-case variability is an important factor and should be considered. The proposed method of this study was tested using different types of sockets as shown in Table 6.1. Two of the sockets had cut outs at the distal end for extrusion of the rod attached to locking liners, another one of the sockets had foam placed at its distal end for cushioning (this is not uncommon in prosthetic practice).

In this study, there were also variations in the types of the liners used, for instance, one of the participants did not use any silicone liners, and another one used a sheath instead of a liner while others used silicone liners. Moreover, there were variations in weights, ages, amounts of experience in using a prosthetic socket, and other factors in participants of the study. Despite these case-by-case variations in the participants and the devices used by them, a similar trend of variation in sensor readings as a result of changes in the volume of the residual limb was determined. From results of this study, we believe that the proposed method is not sensitive to such case-by-case variations and that the same method could be used to achieve the goal regardless of such variations. However, in future work with more participants, if otherwise is determined, adjustment of the proposed method based on the specific devices used and the user's conditions should be investigated.

Chapter 7

Conclusions and Future Works

The material presented in this chapter is excerpted, reproduced, and modified with permission from the following papers:

 C. Ahmadizadeh, L.-K. Merhi, B. Pousett, S. Sangha, and C. Menon, "Toward Intuitive Prosthetic Control: Solving Common Issues Using Force Myography, Surface Electromyography, and Pattern Recognition in a Pilot Case Study," IEEE Robot. Autom. Mag., no. December, pp. 102-111, 2017.

C. Ahmadizadeh, B. Pousett, and C. Menon, "Investigation of Channel Selection for Gesture Classification for Prosthesis Control Using Force Myography: a Case Study," Frontiers in Bioengineering and Biotechnology, vol. 7, no. December, pp. 1-15, 2019.

C. Ahmadizadeh and C. Menon, "Investigation of Regression Methods for Reduction of Errors Caused by Bending of FSR-Based Pressure Sensing Systems Used for Prosthetic Applications," Sensors, vol. 19, no. 24, p. 5519, 2019.

C. Ahmadizadeh, B. Pousett, and C. Menon, "Towards Management of Residual Limb Volume: Monitoring the Prosthetic Interface Pressure to Detect Volume Fluctuations - a Feasibility Study," Applied Sciences, vol. 10, no. 19, p. 6841, 2020.

Sections of this chapter are reprinted or adapted from the above article for clarification and to fit the formatting and scope of this document.

7.1 Chapter Overview

This chapter concludes the four studies conducted for fulfillment of the objectives of this thesis:

- Objective 1: To assess the use of FMG for control of powered prostheses in the following conditions:
  - HMI embedded in the prosthetic socket of an individual with an amputation using a powered prosthesis
  - Prosthesis controlled in a dynamic protocol
- Objective 2: To investigate a design method that reduces complexity of high density FMG based systems for control of powered prosthesis
- Objective 3: To investigate possible factors contributing to errors in signals used in FMG controlled prostheses
  - Objective 3.a: the effect of bending of force sensitive resistors on signals used in FMG controlled prostheses
  - Objective 3.b: the effect of variations in the volume of the residual limb on signals used in FMG controlled prostheses

This chapter also outlines some of the future works that could continue the work carried out in this thesis towards advancement of FMG controlled prostheses.

7.2 Challenges in the Field

Some of the main challenges in the field of FMG controlled prostheses research, leading to the small sample sizes used in most studies including the ones outlined in this thesis, are the high cost of custom socket fabrication for each participant with an amputation, the difficulty of finding clinicians to collaborate with, the limited time of clinicians, and the limited availability of participants, especially for multi-session experiments.

Challenges limiting the size of data collected in studies focused on prosthesis control using pattern recognition including the ones outlined in this thesis, include the instability of HMIs such as EMG and FMG upon doffing and donning of the prosthesis, and factors such as muscle fatigue affecting signals over time. EMG and FMG HMIs used for prosthesis control, in their current states, require re-training upon every donning of the device due

to the shifting of the sensors as the device is taken off and donned again. This limitation eliminates the option of data collections over several days to expand the size of data used in a classification or regression model. The collection of data over long sessions in a day without doffing the device would not provide stable FMG signals either as factors such as swelling and muscle fatigue over time would affect these signals. Future works should investigate methods to address these challenges.

7.3 Conclusions and Future Works

Despite advancements in both the mechatronics and the control aspects of powered prostheses, the rejection rate for these devices remain high [20]. One of the issues preventing such advancements from being adopted in practical situations is that the development and testing of novel prosthetic technology is often performed in constrained environments of the labs. In the case study conducted for fulfillment of **objective 1** of this thesis, the performance of FMG controlled prosthesis was assessed in conditions that are relatively close to the practical application of the system.

The system that was introduced in this study can be used in daily life without requiring modifications. In fact, this system was used by an individual with an amputation to compete in the Cybathlon - a competition in which individuals with disabilities use state-of-the-art technologies to complete tasks resembling those of daily life. The results of the study outline in chapter 3 showed the possibility of using an FMG controlled prosthesis in conditions that are relatively close to the real use case of the system, i.e. in a real prosthesis worn by an individual with an amputation as he was performing a dynamic protocol.

Future works building on findings of the first objective would investigate whether the use of features extracted from FMG signals rather than using raw signals would enhance the performance of the device. Moreover, the effect of donning and doffing of the prosthesis on FMG signals, and the degradation of signals over time should be investigated. To ensure satisfaction of users' needs, future work should include surveys to take into account users' feedback.

The study conducted for **objective 2** of this thesis is outline in chapter 4. This study examined and showed the possibility of using a high density FMG apparatus to determine the number and location of sensors required for customized prostheses for each individual. This aimed at design of a simpler and lower cost FMG controlled prosthesis with performance comparable to that of high density FMG systems.

Five feature selection methods were examined using data collected on a pilot participant with transradial amputation: SFS with two different stopping criteria, mRMR, GA, and Boruta. Three of the five feature selection methods were able to reduce the number of FSR sensors while maintaining vital information for gesture classification in all three datasets examined in this study.

Out of the three selected methods, none outperformed the others in all datasets in terms of classification accuracy, however, GA produced the smallest feature subsets in all datasets without significantly sacrificing performance defined by classification accuracy. MRMR and Boruta were more stable than GA in all datasets which means that GA was most sensitive to variations in training data. The results reported for this study showed the possibility of the proposed design method to produce a system with performance comparable to that of the high density FMG systems with lower cost and less complexity.

The two studies conducted towards fulfilment of the first two objectives of this thesis were case studies. This is because the socket was custom-made for the participant of these studies and also due to the difficulty of recruiting individuals with amputations to participate in such studies. Given that these were pilot studies, there is dependency of data and therefore the assumptions underlying statistical analysis cannot be fully met. In future work, the results of these studies should be confirmed with more participants and statistical analysis. Moreover, the methods proposed and tested for these objectives should be tested for the lower limb in the future work.

Objective 3 of this thesis was to assess possible factors contributing to errors in signals used in FMG controlled prostheses. Two factors were considered for this objective the first one of which was the effect of bending of FSR sensors on signals read from them and used in FMG controlled prosthesis. Chapter 5 outlines the study conducted towards this assessment.

In this study, it was confirmed that when FSR sensors were bent, the error in their mapping to pressure values significantly increased compared to when they were laid flat. This would affect the signals used in FSR-based FMG controlled prosthesis since when these sensors are embedded inside a prosthetic socket, they are inevitably bent.

Four regression-based error compensation methods were proposed to solve the problem of instability of FSR sensor matrices when placed on a curved structure. All proposed methods significantly improved the accuracy of mapping of sensor readings to pressure values. It was determined that by just knowing when the sensor was curved without any knowledge about the value of its curvature, results could be improved using proposed methods in this study.

The best performance was achieved by making separate models based on the value of curvature of sensors. The second best performance was obtained by grouping all curved conditions and separating them from the flat condition. The former method would require classifying curvature values to pre-defined ranges. The latter method is simpler and more practical since no knowledge about the value of the curvature is required, however, the amount of improvement obtained using this method is significantly less than the former method.

Based on findings of this study, for practical use of the proposed methods, method1 is recommended due to its better performance in terms of both outcome measures. To use this method with continuous curvature values, curvatures would be grouped into classes of different ranges and a model would be made for each group. Depending on the range that the sensor's curvature falls into when placed on the limb, the regression model for its calibration would be selected.

In this study, experimental conditions such as sensor sealing with PDMS may have affected the reported results. Various types of FSR sensors, e.g. sensors that don't need to be sealed, should be tested in different experimental conditions to confirm findings of this study in future work.

In order to fully control the experiments carried out in this study, the sensors were not removed in between tests. Future work should assess the effect of removing and re-positioning sensors between multiple repetitions of data collection. This would be to assess

the effect of variability of data due to re-positioning on accuracy of pressure prediction using the methods proposed in this study.

The second factor considered in **objective 3** of this thesis was the effect of fluctuations in the volume of the residual limb on signals used in FMG controlled prosthesis. Fluctuations in the volume of the residual limb lead to problems in various aspects of prostheses use. One of the aspects that is negatively affected by this factor is the accuracy of prostheses control. Due to the weight bearing nature of the lower limb prosthesis, this effect is more significant in the lower limb. Therefore, the study conducted towards fulfilment of **Objective 3.b** focused on lower residual limbs. This study also proposed a method to determine variations in the volume of the residual limb based on limb-socket interface pressure. Information about these variations can help mitigate some of the problems they cause. The study conducted towards fulfilment of this objective is outline in chapter 6.

In this study, it was determined that the output of the sensors that were embedded inside the prosthetic sockets of participants were affected by variations in the volume of the residual limbs. The possibility of using the proposed method that monitors the pressure at the bottom of the lower extremity socket as the user walks to provide information about variations in the volume of the limb was also demonstrated in this study. Two phases of experiments were designed to test the proposed method. The first phase demonstrated the possibility of using this method to detect variations in the volume of the limb and also determined the location at the bottom of the socket where the residual limb-socket interface pressure was representative of the variations in the limb's volume to be the distal location. The second phase was to determine if smaller variations, as much as one or two sock plies, could be detected using this method. It was determined that the sensor readings followed the expected pattern as the volume changed. Test with more participants will be needed to confirm the resolution of this method using statistical analysis.

To build on results reported for objective 3, the use of proposed methods for sensors incorporated into both upper limb and lower limb prosthetic systems should be investigated and clinical tests of these systems should be conducted.

Future work should also investigate the effect of creep in prolonged use of the sensors. If findings of future work determine that sensors' creep influence performance of the proposed method, periodic calibration can potentially be used to mitigate this problem.

To sum up, the four objectives of this thesis were fulfilled in four studies outlined in chapters 3, 4, 5, and 6. These studies showed the possibility of using FMG controlled prosthesis in conditions that are relatively close to the real use case of the system. Moreover, the possibility of using a design method that reduces complexity of such FMG controlled prostheses was determined. The last two studies investigated two possible factors that contribute to errors in signals used in this type of powered prostheses. In the study outlines in chapter 5, it was determined that bending of FSR sensors negatively affects their accuracy of pressure measurement. Multiple regression-based methods were shown effective to reduce the errors caused by bending of the sensors in signals used in FSR-based FMG controlled prostheses. The last study determined the effect of fluctuations in the residual limb on signals used in FMG controlled prostheses. This study also proposed and proved the possibility of using a method based on the distal limb-socket interface pressure to gain information about variations in the volume of the residual limb. Such information can potentially be used towards compensation for errors caused by such volume variations in the signals used in FMG controlled powered prosthesis.

Bibliography

[1] Kathryn Ziegler-Graham, Ellen J MacKenzie, Patti L Ephraim, Thomas G Travison, and Ron Brookmeyer. Estimating the prevalence of limb loss in the united states: 2005 to 2050. *Archives of physical medicine and rehabilitation*, 89(3):422–429, 2008.

[2] Francesca Cordella, Anna Lisa Ciancio, Rinaldo Sacchetti, Angelo Davalli, Andrea Giovanni Cutti, Eugenio Guglielmelli, and Loredana Zollo. Literature review on needs of upper limb prosthesis users. *Frontiers in neuroscience*, 10:209, 2016.

[3] Dipak Datta, Kanther Selvarajah, and Nicola Davey. Functional outcome of patients with proximal upper limb deficiency–acquired and congenital. *Clinical rehabilitation*, 18(2):172–177, 2004.

[4] K Fisher, R.S Hanspal, and L Marks. Return to work after lower limb amputation. *Disability and Rehabilitation*, 26(17):51–56, 2003. ISSN 09638288. doi: 10.1080/09638280701320797.

[5] W. S. Journeay, T. Pauley, M. Kowgier, and M. Devlin. Return to work after occupational and non-occupational lower extremity amputation. *Occupational Medicine*, 68(7):438–443, 2018. ISSN 14718405. doi: 10.1093/occmed/kqy091.

[6] Thomas W Wright, Arlene D Hagen, and Michael B Wood. Prosthetic usage in major upper extremity amputations. *Journal of Hand Surgery*, 20(4):619–622, 1995.

[7] D Datta and V Ibbotson. Prosthetic rehabilitation of upper limb amputees: a five year review. *Clinical rehabilitation*, 5(4):311–316, 1991.

[8] Tanneke Schoppen, Annemarijke Boonstra, Johan W. Groothoff, Eric van Sonderen, Ludwig N. Goumleken, and Willem H. Eisma. Factors related to successful job reintegration of people with a lower limb amputation. *Archives of Physical Medicine and Rehabilitation*, 82(10):1425–1431, 2001. ISSN 00039993. doi: 10.1053/apmr.2001.26074.

[9] Javad H Kashani, RG Frank, SR Kashani, SA Wonderlich, and JC Reid. Depression among amputees. *The Journal of clinical psychiatry*, 1983.

[10] Judith Davidson. A survey of the satisfaction of upper limb amputees with their prostheses, their lifestyles, and their abilities. *Journal of Hand Therapy*, 15(1):62–70, 2002.

[11] D G K Madusanka, L N S Wijayasingha, R A R C Gopura, Y W R Amarasinghe, and G K I Mann. A Review on Hybrid Myoelectric Control Systems for Upper Limb Prosthesis. *2015 Moratuwa Engineering Research Conference (MERCon)*, pages 136–141, 2015. doi: 10.1109/MERCon.2015.7112334.

[12] John W Michael and John H Bowker. *Atlas of amputations and limb deficiencies: surgical, prosthetic, and rehabilitation principles*. American Academy of Orthopaedic Surgeons Rosemont, IL, 2004.

[13] Custom silicone arm cover, 2019. URL https://www.ottobockus.com/prosthetics/upper-limb-prosthetics/solution-overview/custom-silicone-arm-cover/.

[14] Body-powered prosthetics, 2019. URL https://www.ottobockus.com/prosthetics/upper-limb-prosthetics/solution-overview/body-powered-prosthetics/.

[15] Michelangelo prosthetic hand, 2019. URL https://www.ottobockus.com/prosthetics/upper-limb-prosthetics/solution-overview/michelangelo-prosthetic-hand/.

[16] Custom silicone foot prosthesis, 2019. URL https://www.ottobockus.com/prosthetics/lower-limb-prosthetics/solution-overview/prosthetics_lower_limb_solution_silicone_partial_foot_prosthesis_2-contentupdate/.

[17] Meridium, 2019. URL https://www.ottobockus.com/prosthetics/lower-limb-prosthetics/solution-overview/meridium/.

[18] C-leg above knee prosthetic leg, 2019. URL https://www.ottobockus.com/prosthetics/lower-limb-prosthetics/solution-overview/c-leg-above-knee-system/.

[19] Brenna D Argall. Autonomy in rehabilitation robotics: An intersection. *Annual Review of Control, Robotics, and Autonomous Systems*, 1:441–463, 2018.

[20] Chakaveh Ahmadizadeh, Lukas-Karim Merhi, Brittany Pousett, Sohail Sangha, and Carlo Menon. Toward intuitive prosthetic control: solving common issues using force myography, surface electromyography, and pattern recognition in a pilot case study. *IEEE robotics & automation magazine*, 24(4):102–111, 2017.

[21] Erina Cho, Richard Chen, Lukas-karim Merhi, Zhen Xiao, Brittany Pousett, and Carlo Menon. Force Myography to Control Robotic Upper Extremity Prostheses: A Feasibility Study. *Frontiers in Bioengineering and Biotechnology*, 4 (March):1–12, mar 2016. ISSN 2296-4185. doi: 10.3389/fbioe.2016.00018. URL http://journal.frontiersin.org/article/10.3389/fbioe.2016.00018http://journal.frontiersin.org/Article/10.3389/fbioe.2016.00018/abstract.

[22] Otto Bock HealthCare LP. The world ' s most lifelike bionic hand. URL https://www.ottobock.ca/media/local-media/prosthetics/upper-limb/files/15667-bebionic-user-guide.pdf.

[23] Ottobock. Fascinated with Michelangelo. URL http://oc4assets.azurewebsites.net/library/39300.

[24] Touch Bionics Ossur. i-limb access.

[25] Empower, 2017. URL https://www.ottobock.ca/en/prosthetics/lower-limb-prosthetics/solution-overview/empower-ankle/.

[26] Kenevo above knee prosthetic leg, 2017. URL https://www.ottobock.ca/en/prosthetics/lower-limb-prosthetics/solution-overview/kenevo-microprocessor-knee/.

[27] Erik Scheme. Electromyogram pattern recognition for control of powered upper-limb prostheses: State of the art and challenges for clinical use. 48(6):643–660, 2011. doi: 10.1682/JRRD.2010.09.0177.

[28] Claudio Castellini, Emanuele Gruppioni, Angelo Davalli, and Giulio Sandini. Fine detection of grasp force and posture by amputees via surface electromyography. *Journal of Physiology-Paris*, 103(3-5):255–262, may 2009. ISSN 09284257. doi: 10.1016/j.jphysparis.2009.08.008. URL http://www.sciencedirect.com/science/article/pii/S0928425709000497.

[29] L. J. Hargrove, H. Huang, A. E. Schultz, B. A. Lock, R. Lipschutz, and T. A. Kuiken. Toward the development of a neural interface for lower limb prosthesis control. *Proceedings of the 31st Annual International Conference of the IEEE Engineering in Medicine and Biology Society: Engineering the Future of Biomedicine, EMBC 2009*, pages 2111–2114, 2009. doi: 10.1109/IEMBS.2009.5334303.

[30] Aaron J. Young, Ann M. Simon, and Levi J. Hargrove. A training method for locomotion mode prediction using powered lower limb prostheses. *IEEE Transactions on Neural Systems and Rehabilitation Engineering*, 22(3):671–677, 2014. ISSN 15344320. doi: 10.1109/TNSRE.2013.2285101.

[31] Aimee Cloutier and James Yang. Design, control, and sensory feedback of externally powered hand prostheses: a literature review. *Critical reviews in biomedical engineering*, 41(2):161–181, 2013. ISSN 0278-940X. doi: 10.1615/CritRevBiomedEng.2013007887. URL http://www.ncbi.nlm.nih.gov/pubmed/24580569.

[32] Michele Xiloyannis, Constantinos Gavriel, Andreas AC Thomik, and A Aldo Faisal. Dynamic forward prediction for prosthetic hand control by integration of emg, mmg and kinematic signals. In *2015 7th International IEEE/EMBS Conference on Neural Engineering (NER)*, pages 611–614. IEEE, 2015.

[33] Michael R Tucker, Jeremy Olivier, Anna Pagel, Hannes Bleuler, Mohamed Bouri, Olivier Lambercy, José del R Millán, Robert Riener, Heike Vallery, and Roger Gassert. Control strategies for active lower extremity prosthetics and orthotics: a review. *Journal of neuroengineering and rehabilitation*, 12(1):1, 2015.

[34] Mahdi Rasouli, Rohan Ghosh, Wang Wei Lee, Nitish V Thakor, and Sunil Kukreja. Stable force-myographic control of a prosthetic hand using incremental learning. In *37th Annual International Conference of the IEEE Engineering in Medicine and Biology Society (EMBC)*, pages 4828–4831. IEEE, aug 2015. ISBN 978-1-4244-9271-8. doi: 10.1109/EMBC.2015.7319474. URL http://ieeexplore.ieee.org/lpdocs/epic03/wrapper.htm?arnumber=7319474.

[35] Anoop Kant Godiyal, Hemant Kumar Verma, Nitin Khanna, and Deepak Joshi. A force myography-based system for gait event detection in overground and ramp walking. *IEEE Transactions on Instrumentation and Measurement*, 67(10):2314–2323, 2018. ISSN 00189456. doi: 10.1109/TIM.2018.2816799.

[36] Yinfeng Fang, Student Member, Nalinda Hettiarachchi, and Dalin Zhou. Multi-Modal Sensing Techniques for Interfacing Hand Prostheses : A Review. *IEEE Sensors Journal*, 15(11):6065–6076, 2015. doi: 10.1109/JSEN.2015.2450211.

[37] Christoph Guger, Werner Harkam, Carin Hertnaes, and Gert Pfurtscheller. Prosthetic control by an eeg-based brain-computer interface (bci). pages 3–6, 1999.

[38] Bart Peerdeman, Daphne Boere, Heidi Witteveen, Hermie Hermens, Stefano Stramigioli, Hans Rietman, Peter Veltink, Sarthak Misra, et al. Myoelectric forearm prostheses: state of the art from a user-centered perspective. *Journal of Rehabilitation Research & Development*, 48(6), 2011.

[39] Paul J Dougherty. Long-term follow-up study of bilateral above-the-knee amputees from the vietnam war. *JBJS*, 81(10):1384–90, 1999.

[40] Elaine A Biddiss and Tom T Chau. Upper limb prosthesis use and abandonment: a survey of the last 25 years. *Prosthetics and orthotics international*, 31(3):236–257, 2007.

[41] S Bilodeau, R Hébert, and J Desrosiers. Lower limb prosthesis utilisation by elderly amputees. *Prosthetics and Orthotics International*, 24(2):126–132, 2000.

[42] Elaine Biddiss, Dorcas Beaton, and Tom Chau. Consumer design priorities for upper limb prosthetics. *Disability and Rehabilitation: Assistive Technology*, 2(6):346–357, 2007.

[43] Marti L Riemer-Reiss and Robbyn R Wacker. Factors associated with assistive technology discontinuance among individuals with disabilities. *Journal of Rehabilitation*, 66(3), 2000.

[44] Amol M Karmarkar, Diane M Collins, Todd Wichman, Allison Franklin, Shirley G Fitzgerald, Brad E Dicianno, Paul F Pasquina, and Rory A Cooper. Prosthesis and wheelchair use in veterans with lower-limb amputation. *Journal of Rehabilitation Research & Development*, 46(5), 2009.

[45] Huseyin Atakan Varol, Frank Sup, and Michael Goldfarb. Multiclass real-time intent recognition of a powered lower limb prosthesis. *IEEE Transactions on Biomedical Engineering*, 57(3):542–551, 2009.

[46] Myo plus pattern recognition, 2017. URL `https://www.ottobock.ca/en/prosthetics/upper-limb-prosthetics/solution-overview/myo-plus/`.

[47] Dapeng Yang, Yikun Gu, Li Jiang, Luke Osborn, and Hong Liu. Dynamic training protocol improves the robustness of pr-based myoelectric control. *Biomedical Signal Processing and Control*, 31:249–256, 2017.

[48] Cheng-Kung Cheng, Hsiao-Shu Hsiung, and Jin-Shin Lai. The use of surface emg in knee extensor moment prediction. *PROCEEDINGS-NATIONAL SCIENCE COUNCIL REPUBLIC OF CHINA PART B LIFE SCIENCES*, 18:179–179, 1994.

[49] Kevin H Ha, Huseyin Atakan Varol, and Michael Goldfarb. Volitional control of a prosthetic knee using surface electromyography. *IEEE Transactions on Biomedical Engineering*, 58(1):144–151, 2010.

[50] Vikram Ravindra and Claudio Castellini. A Comparative Analysis of Three Non-Invasive Human-Machine Interfaces for the Disabled. *Frontiers in Neurorobotics*, 8 (October):1–10, 2014. ISSN 1662-5218. doi: 10.3389/fnbot.2014.00024. URL `http://journal.frontiersin.org/article/10.3389/fnbot.2014.00024/abstract`.

[51] Alexander T Belyea, Kevin B Englehart, and Erik J Scheme. A proportional control scheme for high density force myography. *Journal of neural engineering*, 15(4):046029, 2018.

[52] Anoop Kant Godiyal, Upinderpal Singh, Sneh Anand, and Deepak Joshi. Analysis of force myography based locomotion patterns. *Measurement: Journal of the International Measurement Confederation*, 140:497–503, 2019. ISSN 02632241. doi: 10.1016/j.measurement.2019.04.009. URL `https://doi.org/10.1016/j.measurement.2019.04.009`.

[53] Zhen Gang Xiao and Carlo Menon. A review of force myography research and development. *Sensors*, 19(20):4557, 2019.

[54] Ashkan Radmand, Erik Scheme, and Kevin Englehart. High-density force myography: A possible alternative for upper-limb prosthetic control. *Journal of Rehabilitation Research & Development*, 53(4):443–456, 2016.

[55] Mathilde Connan, Eduardo Ruiz Ramírez, Bernhard Vodermayer, and Claudio Castellini. Assessment of a wearable force-and electromyography device and comparison of the related signals for myocontrol. *Frontiers in neurorobotics*, 10:17, 2016.

[56] Xianta Jiang, Lukas-Karim Merhi, Zhen G Xiao, and Carlo Menon. Exploration of force myography and surface electromyography in hand gesture classification. *Medical Engineering & Physics*, 41:63–73, 2017. doi: 10.1016/j.medengphy.2017.01.015.

[57] Maram Sakr and Carlo Menon. Study on the force myography sensors placement for robust hand force estimation. In *2017 IEEE International Conference on Systems, Man, and Cybernetics (SMC)*, pages 1387–1392. IEEE, 2017.

[58] Anoop Kant Godiyal, Milton Mondal, Shiv Dutt Joshi, and Deepak Joshi. Force myography based novel strategy for locomotion classification. *IEEE Transactions on Human-Machine Systems*, 48(6):648–657, 2018. ISSN 21682291. doi: 10.1109/THMS.2018.2860598.

[59] Claudio Castellini and Risto Koiva. Using a high spatial resolution tactile sensor for intention detection. *IEEE Rehabilitation Robotics (ICORR)*, pages 1–7, 2013. ISSN 1945-7901. doi: 10.1109/ICORR.2013.6650365. URL `http://www.ncbi.nlm.nih.gov/pubmed/24187184`.

[60] By Matthew S Fifer, Soumyadipta Acharya, Heather L Benz, Mohsen Mollazadeh, Nathan E Crone, and Nitish V Thakor. Toward Electrocorticographic Control of a Dexterous Upper Limb Prosthesis: Building Brain-Machine Interfaces. *IEEE Pulse*, 3(FEBRUARY):38–42, 2012. doi: 10.1109/MPUL.2011.2175636.

[61] Don A Yungher, Michael T Wininger, JB Barr, William Craelius, and A Joseph Threlkeld. Surface muscle pressure as a measure of active and passive behavior of muscles during gait. *Medical engineering & physics*, 33(4):464–471, 2011.

[62] Dapeng Yang, Li Jiang, Qi Huang, Rongqiang Liu, and Hong Liu. Experimental study of an emg-controlled 5-dof anthropomorphic prosthetic hand for motion restoration. *Journal of Intelligent & Robotic Systems*, 76(3-4):427–441, 2014.

[63] F Riillo, L R Quitadamo, F Cavrini, E Gruppioni, C A Pinto, N Cosimo Pastò, L Sbernini, L Albero, and G Saggio. Biomedical Signal Processing and Control Optimization of EMG-based hand gesture recognition : Supervised vs . unsupervised data preprocessing on healthy subjects and transradial amputees. *Biomedical Signal Processing and Control*, 14:117–125, 2014. ISSN 1746-8094. doi: 10.1016/j.bspc.2014.07.007. URL `http://dx.doi.org/10.1016/j.bspc.2014.07.007`.

[64] Yanjuan Geng, Ping Zhou, and Guanglin Li. Toward attenuating the impact of arm positions on electromyography pattern-recognition based motion classification in transradial amputees. *Journal of neuroengineering and rehabilitation*, 9(1):74, 2012.

[65] He Huang, Todd A. Kuiken, and Robert D. Lipschutz. A strategy for identifying locomotion modes using surface electromyography. *IEEE Transactions on Biomedical Engineering*, 56(1):65–73, 2009. ISSN 00189294. doi: 10.1109/TBME.2008.2003293.

[66] Claudio Castellini and Vikram Ravindra. A wearable low-cost device based upon Force-Sensing Resistors to detect single-finger forces. *5th IEEE RAS/EMBS International Conference on Biomedical Robotics and Biomechatronics*, pages 199–203, 2014. ISSN 21551774. doi: 10.1109/BIOROB.2014.6913776. URL `http://ieeexplore.ieee.org/lpdocs/epic03/wrapper.htm?arnumber=6913776`.

[67] Anita Kadkhodayan, Xianta Jiang, and Carlo Menon. Continuous Prediction of Finger Movements Using Force Myography. *Journal of Medical and Biological Engineering*, 36(4):594–604, 2016. ISSN 2199-4757. doi: 10.1007/s40846-016-0151-y.

[68] Zhen Gang Xiao and Carlo Menon. Performance of Forearm FMG and sEMG for Estimating Elbow, Forearm and Wrist Positions. *Journal of Bionic Engineering*, 14(2):284–295, 2017. ISSN 16726529. doi: 10.1016/S1672-6529(16)60398-0. URL `http://dx.doi.org/10.1016/S1672-6529(16)60398-0`.

[69] Michael Wininger, Nam-Hun Kim, and William Craelius. Pressure signature of forearm as predictor of grip force. *Journal of Rehabilitation Research & Development*, 45 (6), 2008.

[70] Diego Ferigo, Lukas Karim Merhi, Brittany Pousett, Zhen Gang Xiao, and Carlo Menon. A Case Study of a Force-myography Controlled Bionic Hand Mitigating Limb Position Effect. *Journal of Bionic Engineering*, 14(4):692–705, 2017. ISSN 16726529. doi: 10.1016/S1672-6529(16)60435-3. URL `http://dx.doi.org/10.1016/S1672-6529(16)60435-3`.

[71] Jacopo Carpaneto, Annarita Cutrone, Silvia Bossi, P Sergi, Luca Citi, Jacopo Rigosa, Paolo Maria Rossini, and Silvestro Micera. Activities on pns neural interfaces for the control of hand prostheses. In *2011 Annual International Conference of the IEEE Engineering in Medicine and Biology Society*, pages 4637–4640. IEEE, 2011.

[72] Enzo Mastinu, Pascal Doguet, Yohan Botquin, Bo Håkansson, and Max Ortiz-Catalan. Embedded system for prosthetic control using implanted neuromuscular interfaces accessed via an osseointegrated implant. *IEEE transactions on biomedical circuits and systems*, 11(4):867–877, 2017.

[73] Paolo M Rossini, Silvestro Micera, Antonella Benvenuto, Jacopo Carpaneto, Giuseppe Cavallo, Luca Citi, Christian Cipriani, Luca Denaro, Vincenzo Denaro, Giovanni Di Pino, et al. Double nerve intraneural interface implant on a human amputee for robotic hand control. *Clinical neurophysiology*, 121(5):777–783, 2010.

[74] Silvestro Micera, Paolo M Rossini, Jacopo Rigosa, Luca Citi, Jacopo Carpaneto, Stanisa Raspopovic, Mario Tombini, Christian Cipriani, Giovanni Assenza, Maria C Carrozza, et al. Decoding of grasping information from neural signals recorded using peripheral intrafascicular interfaces. *Journal of neuroengineering and rehabilitation*, 8(1):53, 2011.

[75] Chou-Ching K Lin, Ming-Shaung Ju, and Hang-Shing Cheng. Model-based ankle joint angle tracing by cuff electrode recordings of peroneal and tibial nerves. *Medical & biological engineering & computing*, 45(4):375–385, 2007.

[76] Emma Brunton, Christoph Blau, Carolina Silveira, and Kianoush Nazarpour. Identification of sensory information in mixed nerves using multi-channel cuff electrodes for closed loop neural prostheses. In *2017 8th International IEEE/EMBS Conference on Neural Engineering (NER)*, pages 391–394. IEEE, 2017.

[77] Natasha Alves and Tom Chau. Uncovering patterns of forearm muscle activity using multi-channel mechanomyography. *Journal of Electromyography and Kinesiology*, 20 (5):777–786, 2010. ISSN 1050-6411. doi: 10.1016/j.jelekin.2009.09.003. URL `http://dx.doi.org/10.1016/j.jelekin.2009.09.003`.

[78] J Silva, W Heim, and T Chau. MMG-Based Classification of Muscle Activity for Prosthesis Control. *The 26th Annual International Conference of the IEEE Engineering in Medicine and Biology Society*, 1:968–971, 2004. doi: 10.1109/IEMBS.2004.1403322.

[79] Haifeng Wu, Daqing Wang, Qing Huang, and Lifu Gao. Real-time continuous recognition of knee motion using multi-channel mechanomyography signals detected on clothes. *Journal of Electromyography and Kinesiology*, 38:94–102, 2018.

[80] Tobias Pistohl, Andreas Schulze-bonhage, Ad Aertsen, Carsten Mehring, and Tonio Ball. NeuroImage Decoding natural grasp types from human ECoG. *NeuroImage*, 59(1):248–260, 2012. ISSN 1053-8119. doi: 10.1016/j.neuroimage.2011.06.084. URL `http://dx.doi.org/10.1016/j.neuroimage.2011.06.084`.

[81] Douglas P Murphy, Ou Bai, Ashraf S Gorgey, John Fox, William T Lovegreen, Brian W Burkhardt, Roozbeh Atri, Juan S Marquez, Qi Li, and Ding-Yu Fei. electroencephalogram-based brain–computer interface and lower-limb prosthesis control: A case study. *Frontiers in neurology*, 8:696, 2017.

[82] Justin A Brantley, Trieu Phat Luu, Sho Nakagome, and Jose L Contreras-Vidal. Towards the development of a hybrid neural-machine interface for volitional control of a powered lower limb prosthesis. In *2017 International Symposium on Wearable Robotics and Rehabilitation (WeRob)*, pages 1–1. IEEE, 2017.

[83] Arnab Rakshit, Anwesha Khasnobish, and DN Tibarewala. A naïve bayesian approach to lower limb classification from eeg signals. In *2016 2nd International Conference on Control, Instrumentation, Energy & Communication (CIEC)*, pages 140–144. IEEE, 2016.

[84] Andrew B Schwartz, X Tracy Cui, Douglas J Weber, and Daniel W Moran. Brain-controlled interfaces: movement restoration with neural prosthetics. *Neuron*, 52(1): 205–220, 2006.

[85] Johanna Ruescher, Olga Iljina, Dirk-Matthias Altenmüller, Ad Aertsen, Andreas Schulze-Bonhage, and Tonio Ball. Somatotopic mapping of natural upper-and lower-extremity movements and speech production with high gamma electrocorticography. *Neuroimage*, 81:164–177, 2013.

[86] Kai J Miller, Eric C Leuthardt, Gerwin Schalk, Rajesh PN Rao, Nicholas R Anderson, Daniel W Moran, John W Miller, and Jeffrey G Ojemann. Spectral changes in cortical surface potentials during motor movement. *Journal of Neuroscience*, 27(9):2424–2432, 2007.

[87] Colin M McCrimmon, Po T Wang, Payam Heydari, Angelica Nguyen, Susan J Shaw, Hui Gong, Luis A Chui, Charles Y Liu, Zoran Nenadic, and An H Do. Electrocorticographic encoding of human gait in the leg primary motor cortex. *Cerebral Cortex*, 28 (8):2752–2762, 2018.

[88] Claudio Castellini and Giulio Sandini. Gaze tracking for robotic control in intelligent teleoperation and prosthetics. (November 2014), 2017. doi: 10.13140/2.1.4591.3285.

[89] Chengkun Cui, Gui-Bin Bian, Zeng-Guang Hou, Jun Zhao, and Hao Zhou. A multimodal framework based on integration of cortical and muscular activities for decoding human intentions about lower limb motions. *IEEE transactions on biomedical circuits and systems*, 11(4):889–899, 2017.

[90] David P Mcmullen, Student Member, Guy Hotson, Student Member, Kapil D Katyal, Brock A Wester, Matthew S Fifer, Student Member, Timothy G Mcgee, Andrew Harris, Matthew S Johannes, R Jacob Vogelstein, Alan D Ravitz, William S Anderson, Nitish V Thakor, Nathan E Crone, and Senior Member. Demonstration of a Semi-Autonomous Hybrid Brain - Machine Interface Using Human Intracranial EEG , Eye Tracking , and Computer Vision to Control a Robotic Upper Limb Prosthetic. *IEEE Transactions on Neural Systems and Rehabilitation Engineering*, 22(4):784–796, 2014. doi: 10.1109/TNSRE.2013.2294685.

[91] Rafael Barea, Luciano Boquete, Manuel Mazo, and E López. Wheelchair guidance strategies using eog. *Journal of intelligent and robotic systems*, 34(3):279–299, 2002.

[92] Matthieu Duvinage, Thierry Castermans, and Thierry Dutoit. Control of a lower limb active prosthesis with eye movement sequences. In *2011 IEEE Symposium on*

Computational Intelligence, Cognitive Algorithms, Mind, and Brain (CCMB), pages 1–7. IEEE, 2011.

[93] Qian Yu, Peng Gong, Nick Clinton, Greg Biging, Maggi Kelly, and Dave Schirokauer. Object-based Detailed Vegetation Classification with Airborne High Spatial Resolution Remote Sensing Imagery. *Photogrammetric Engineering & Remote Sensing*, 72(7):799–811, 2006. ISSN 00991112. doi: 10.14358/PERS.72.7.799. URL `http://openurl.ingenta.com/content/xref?genre=article{&}issn=0099-1112{&}volume=72{&}issue=7{&}spage=799`.

[94] S Thiemjarus, B P L Lo, K V Laerhoven, and G Z Yang. Feature Selection for Wireless Sensor Networks. *1st International Workshop on Wearable and Implantable Body Sensor Networks*, 2004. URL `http://vip.doc.ic.ac.uk/benlo/public/Feature{_}Selection{_}for{_}Wireless{_}Sensor{_}Networks.pdf`.

[95] Chris Ding and Hanchuan Peng. Minimum redundancy feature selection from microarray gene expression data. *Journal of bioinformatics and computational biology*, 3(02):185–205, 2005.

[96] Xuelian Deng, Yuqing Li, Jian Weng, and Jilian Zhang. Feature selection for text classification: A review. *Multimedia Tools and Applications*, 78(3):3797–3816, 2019.

[97] Zenglin Xu, Irwin King, Michael Rung-Tsong Lyu, and Rong Jin. Discriminative semi-supervised feature selection via manifold regularization. *IEEE Transactions on Neural networks*, 21(7):1033–1047, 2010.

[98] Mahesh Pal and Giles M. Foody. Feature selection for classification of hyperspectral data by SVM. *IEEE Transactions on Geoscience and Remote Sensing*, 48(5):2297–2307, 2010. ISSN 01962892. doi: 10.1109/TGRS.2009.2039484.

[99] Ke Yan and David Zhang. Feature selection and analysis on correlated gas sensor data with recursive feature elimination. *Sensors and Actuators, B: Chemical*, 212:353–363, 2015. ISSN 09254005. doi: 10.1016/j.snb.2015.02.025. URL `http://dx.doi.org/10.1016/j.snb.2015.02.025`.

[100] Girish Chandrashekar and Ferat Sahin. A survey on feature selection methods. *Computers and Electrical Engineering*, 40(1):16–28, 2014. ISSN 00457906. doi: 10.1016/j.compeleceng.2013.11.024. URL `http://dx.doi.org/10.1016/j.compeleceng.2013.11.024`.

[101] Huiqing Liu, Jinyan Li, and Limsoon Wong. A comparative study on feature selection and classification methods using gene expression profiles and proteomic patterns. *Genome Informatics*, 13:51–60, 2002. ISSN 0919-9454. doi: 10.11234/gi1990.13.51. URL `https://www.jstage.jst.go.jp/article/gi1990/13/0/13{_}0{_}51/{_}article`.

[102] Dennis C Duro, Steven E Franklin, and Monique G Dubé. Multi-scale object-based image analysis and feature selection of multi-sensor earth observation imagery using random forests. *International Journal of Remote Sensing*, 33(14):4502–4526, 2012.

[103] Fernando Vidal-Verdú, Maria Jose Barquero, Julián Castellanos-Ramos, Rafael Navas-González, Jose Antonio Sánchez, Javier Serón, and Alfonso García-Cerezo. A large area tactile sensor patch based on commercial force sensors. *Sensors*, 11(5): 5489–5507, 2011. ISSN 14248220. doi: 10.3390/s110505489.

[104] Yingen Xiong and Francis Quek. Hand motion gesture frequency properties and multimodal discourse analysis. *International Journal of Computer Vision*, 69(3):353–371, 2006.

[105] Ashkan Radmand, Erik Scheme, and Kevin Englehart. On the suitability of integrating accelerometry data with electromyography signals for resolving the effect of changes in limb position during dynamic limb movement. *JPO: Journal of Prosthetics and Orthotics*, 26(4):185–193, 2014.

[106] Stuart Geman, Elie Bienenstock, and René Doursat. Neural networks and the bias/variance dilemma. *Neural computation*, 4(1):1–58, 1992.

[107] Ganesh R Naik, Ali H Al-Timemy, and Hung T Nguyen. Transradial amputee gesture classification using an optimal number of semg sensors: an approach using ica clustering. *IEEE Transactions on Neural Systems and Rehabilitation Engineering*, 24 (8):837–846, 2015.

[108] Rana Sadeghi Chegani and Carlo Menon. Regressing grasping using force myography: an exploratory study. *BioMedical Engineering OnLine*, 17 (1):159, 2018. ISSN 1475-925X. doi: 10.1186/s12938-018-0593-2. URL `https://biomedical-engineering-online.biomedcentral.com/articles/10.1186/s12938-018-0593-2`.

[109] Mahdi Rasouli, Karthik Chellamuthu, John John Cabibihan, and Sunil L. Kukreja. Towards enhanced control of upper prosthetic limbs: A force-myographic approach. *Proceedings of the IEEE RAS and EMBS International Conference on Biomedical Robotics and Biomechatronics*, 2016-July:232–236, 2016. ISSN 21551774. doi: 10.1109/BIOROB.2016.7523629.

[110] Hongda Wang, Weiwei Shi, and Chiu-sing Choy. Integrating channel selection and feature selection in a real time epileptic seizure detection system. *2017 39th Annual International Conference of the IEEE Engineering in Medicine and Biology Society (EMBC)*, pages 3206–3211, 2017. doi: 10.1109/EMBC.2017.8037539.

[111] Zheng Wang, Yinfeng Fang, Gongfa Li, and Honghai Liu. Facilitate semg-based human-machine interaction through channel optimization. *International Journal of Humanoid Robotics*, 2019.

[112] Xiangxin Li, Oluwarotimi Williams Samuel, Xu Zhang, Hui Wang, Peng Fang, and Guanglin Li. A motion-classification strategy based on sEMG-EEG signal combination for upper- limb amputees. *Journal of NeuroEngineering and Rehabilitation*, pages 1–13, 2017. ISSN 1743-0003. doi: 10.1186/s12984-016-0212-z. URL `http://dx.doi.org/10.1186/s12984-016-0212-z`.

[113] Zhen Gang Xiao and Carlo Menon. Counting Grasping Action Using Force Myography: An Exploratory Study With Healthy Individuals. *JMIR Rehabilitation and*

Assistive Technologies, 4(1):e5, 2017. ISSN 2369-2529. doi: 10.2196/rehab.6901. URL http://rehab.jmir.org/2017/1/e5/.

[114] Chakaveh Ahmadizadeh, Carlo Menon, and Brittany Pousett. Investigation of channel selection for gesture classification for prosthesis control using force myography: a case study. *Frontiers in Bioengineering and Biotechnology*, 7:331, 2019.

[115] Peng Hanchuan, Long Fuhui, and Ding Chris. Feature Selection Based on Mutual Information : Criteria of Max-Dependency, Max-Relevance and Min-Redundancy. *IEEE Transactions on Pattern Analysis and Machine Intelligence*, 27(8):1226–1238, 2005. ISSN 01628828. doi: 10.1109/TPAMI.2005.159.

[116] Pavitra Krishnaswamy, Emery N. Brown, and Hugh M. Herr. Human leg model predicts ankle muscle-tendon morphology, state, roles and energetics in walking. *PLoS Computational Biology*, 7(3), 2011. ISSN 1553734X. doi: 10.1371/journal.pcbi.1001107.

[117] Isabelle Guyon and André Elisseeff. An introduction to variable and feature selection. *Journal of machine learning research*, 3(Mar):1157–1182, 2003.

[118] Rajiv Kumar, Vaidyanathan K Jayaraman, and Bhaskar D Kulkarni. An svm classifier incorporating simultaneous noise reduction and feature selection: illustrative case examples. *Pattern Recognition*, 38(1):41–49, 2005.

[119] Ra'Na Chengani, Mona L. Delva, Maram Sakr, and Carlo Menon. Pilot study on strategies in sensor placement for robust hand/wrist gesture classification based on movement related changes in forearm volume. *2016 IEEE Healthcare Innovation Point-of-Care Technologies Conference, HI-POCT 2016*, pages 46–49, 2016. doi: 10.1109/HIC.2016.7797693.

[120] Nan Li, Dapeng Yang, Li Jiang, Hong Liu, and Hegao Cai. Combined use of fsr sensor array and svm classifier for finger motion recognition based on pressure distribution map. *Journal of Bionic Engineering*, 9(1):39–47, 2012.

[121] X. Jiang, L. Tory, M. Khoshnam, K. H.T. Chu, and C. Menon. Exploration of Gait Parameters Affecting the Accuracy of Force Myography-Based Gait Phase Detection. *Proceedings of the IEEE RAS and EMBS International Conference on Biomedical Robotics and Biomechatronics*, 2018-Augus:1205–1210, 2018. ISSN 21551774. doi: 10.1109/BIOROB.2018.8487790.

[122] Pierre Cherelle, Victor Grosu, Louis Flynn, Karen Junius, Marta Moltedo, Bram Vanderborght, and Dirk Lefeber. The Ankle Mimicking Prosthetic Foot 3—Locking mechanisms, actuator design, control and experiments with an amputee. *Robotics and Autonomous Systems*, 91:327–336, 2017. ISSN 09218890. doi: 10.1016/j.robot.2017.02.004. URL http://dx.doi.org/10.1016/j.robot.2017.02.004.

[123] Andrea Ancillao, Salvatore Tedesco, John Barton, and Brendan O'Flynn. Indirect measurement of ground reaction forces and moments by means of wearable inertial sensors: A systematic review. *Sensors*, 18(8):2564, 2018.

[124] A F Mak, M Zhang, and D A Boone. State-of-the-art research in lower-limb prosthetic biomechanics-socket interface: a review. *Journal of rehabilitation research and development*, 38(2):161–74, 2001. ISSN 0748-7711. URL `http://www.ncbi.nlm.nih.gov/pubmed/11392649`.

[125] Pascal Schütz, William R Taylor, Barbara Postolka, Sandro F Fucentese, Peter P Koch, Michael AR Freeman, Vera Pinskerova, and Renate List. Kinematic evaluation of the gmk sphere implant during gait activities: a dynamic videofluoroscopy study. *Journal of Orthopaedic Research®*, 37(11):2337–2347, 2019.

[126] Deepak Kumar, Kurt T Manal, and Katherine S Rudolph. Knee joint loading during gait in healthy controls and individuals with knee osteoarthritis. *Osteoarthritis and cartilage*, 21(2):298–305, 2013.

[127] Georg Bergmann, Alwina Bender, Jörn Dymke, Georg N Duda, and Philipp Damm. Physical activities that cause high friction moments at the cup in hip implants. *JBJS*, 100(19):1637–1644, 2018.

[128] Andrea Ancillao, Stefano Rossi, and Paolo Cappa. Analysis of knee strength measurements performed by a hand-held multicomponent dynamometer and optoelectronic system. *IEEE Transactions on Instrumentation and Measurement*, 66(1):85–92, 2016.

[129] Ebrahim A. Al-Fakih, Noor Azuan Abu Osman, and Faisal Rafiq Mahmad Adikan. Techniques for interface stress measurements within prosthetic sockets of transtibial amputees: A review of the past 50 years of research. *Sensors (Switzerland)*, 16(7), 2016. ISSN 14248220. doi: 10.3390/s16071119.

[130] M Zhang, a R Turner-Smith, a Tanner, and V C Roberts. Clinical investigation of the pressure and shear stress on the trans-tibial stump with a prosthesis. *Medical engineering & physics*, 20(3):188–198, 1998. ISSN 13504533. doi: 10.1016/S1350-4533(98)00013-7.

[131] RB Williams, D Porter, VC Roberts, and JF Regan. Triaxial force transducer for investigating stresses at the stump/socket interface. *Medical and Biological Engineering and Computing*, 30(1):89–96, 1992.

[132] K Hachisuka, M Takahashi, H Ogata, S Ohmine, H Shitama, and K Shinkoda. Properties of the flexible pressure sensor under laboratory conditions simulating the internal environment of the total surface bearing socket. *Prosthetics and Orthotics International*, 22(3):186–192, 1998. ISSN 0309-3646. doi: 10.3109/03093649809164483. URL `http://poi.sagepub.com/content/22/3/186.abstract`.

[133] A. Polliack, D. Craig, R C Sieh, S Landsberger, and D R McNeil. Laboratory and clinical tests of a prototype pressure sensor for clinical assessment of prothetic socket fit. *Prosthetics and Orthotics International*, 26:23–34, 2002. ISSN 03093646. doi: 10.3109/03093649909071625.

[134] Candy H.Y. Lai and Cecilia W.P. Li-Tsang. Validation of the Pliance X System in measuring interface pressure generated by pressure garment. *Burns*, 35(6):845–851, 2009. ISSN 03054179. doi: 10.1016/j.burns.2008.09.013.

[135] Troy A Chase and Ren C Luo. A thin-film flexible capacitive tactile normal/shear force array sensor. In *Proceedings of IECON'95-21st Annual Conference on IEEE Industrial Electronics*, volume 2, pages 1196–1201. IEEE, 1995.

[136] Mohammad A Razian and Matthew G Pepper. Design, development, and characteristics of an in-shoe triaxial pressure measurement transducer utilizing a single element of piezoelectric copolymer film. *IEEE Transactions on Neural Systems and Rehabilitation Engineering*, 11(3):288–293, 2003.

[137] Z P Luo, L J Berglund, and K N An. Validation of F-Scan pressure sensor system: a technical note. *Journal of rehabilitation research and development*, 35(2):186–191, 1998. ISSN 0748-7711.

[138] A W Buis and P Convery. Calibration problems encountered while monitoring stump/socket interface pressures with force sensing resistors: techniques adopted to minimise inaccuracies. *Prosthetics and orthotics international*, 21(3): 179–182, 1997. ISSN 0309-3646. doi: 10.3109/03093649709164552. URL `http://informahealthcare.com/doi/pdf/10.3109/03093649709164552`.

[139] A. A. Polliack, R. C. Sieh, D. D. Craig, S. Landsberger, D. R. McNeil, and E. Ayyappa. Scientific validation of two commercial pressure sensor systems for prosthetic socket fit. *Prosthetics and orthotics international*, 24:63–73, 2000. ISSN 0309-3646. doi: 10.1080/03093640008726523.

[140] Mona Lisa Delva and Carlo Menon. Fsr based force myography (fmg) stability throughout non-stationary upper extremity tasks. In *Proceedings of the Future Technologies Conference, Vancouver, BC, Canada*, pages 29–30, 2017.

[141] Maram Sakr and Carlo Menon. Exploratory evaluation of the force myography (fmg) signals usage for admittance control of a linear actuator. In *2018 7th IEEE International Conference on Biomedical Robotics and Biomechatronics (Biorob)*, pages 903–908. IEEE, 2018.

[142] Donald Specht. A general regression neural network, 1991.

[143] Leo Breiman. Random forests. *Machine learning*, 45(1):5–32, 2001.

[144] Jonathon S Schofield, Katherine R Evans, Jacqueline S Hebert, Paul D Marasco, and Jason P Carey. The effect of biomechanical variables on force sensitive resistor error: Implications for calibration and improved accuracy. *Journal of biomechanics*, 49(5): 786–792, 2016.

[145] Chakaveh Ahmadizadeh and Carlo Menon. Investigation of regression methods for reduction of errors caused by bending of fsr-based pressure sensing systems used for prosthetic applications. *Sensors*, 19(24):5519, 2019.

[146] Jianfeng Wu, Lei Wang, and Jianqing Li. Design and crosstalk error analysis of the circuit for the 2-D networked resistive sensor array. *IEEE Sensors Journal*, 15(2): 1020–1026, 2015. ISSN 1530437X. doi: 10.1109/JSEN.2014.2359967.

[147] Hong Liu, Yuan Fei Zhang, Yi Wei Liu, and Ming He Jin. Measurement errors in the scanning of resistive sensor arrays. *Sensors and Actuators, A: Physical*, 163(1): 198–204, 2010. ISSN 09244247. doi: 10.1016/j.sna.2010.08.004. URL `http://dx.doi.org/10.1016/j.sna.2010.08.004`.

[148] Tommaso D'Alessio. Measurement errors in the scanning of piezoresistive sensors arrays. *Sensors and Actuators A: Physical*, 72(1):71–76, 1999. ISSN 09244247. doi: 10.1016/S0924-4247(98)00204-0.

[149] Fernando Vidal-Verd, Oscar Oballe-Peinado, Jose A. Sanchez-Duran, Julian Castellanos-Ramos, and Rafael Navas-Gonzalez. Three realizations and comparison of hardware for piezoresistive tactile sensors. *Sensors*, 11(3):3249–3266, 2011. ISSN 14248220. doi: 10.3390/s110303249.

[150] Katherine A Raichle, Marisol A Hanley, Ivan Molton, Nancy J Kadel, Kellye Campbell, Emily Phelps, Dawn Ehde, and Douglas G Smith. Prosthesis use in persons with lower-and upper-limb amputation. *Journal of rehabilitation research and development*, 45(7):961, 2008.

[151] Michael P Dillon, Lauren V Fortington, Muhammad Akram, Bircan Erbas, and Friedbert Kohler. Geographic variation of the incidence rate of lower limb amputation in australia from 2007-12. *PloS one*, 12(1):e0170705, 2017.

[152] BM Persson and E Liedberg. A clinical standard of stump measurement and classification in lower limb amputees. *Prosthetics and orthotics international*, 7(1):17–24, 1983.

[153] Katherine RS Holzbaur, Wendy M Murray, Garry E Gold, and Scott L Delp. Upper limb muscle volumes in adult subjects. *Journal of biomechanics*, 40(4):742–749, 2007.

[154] Christopher M Bishop. *Pattern recognition and machine learning*. Springer Science+ Business Media, 2006.

[155] TA Krouskop, M Yalcinkaya, A Muilenberg, K Holland, and E Zuniga. A measurement technique to assess residual limb volume. *Orthop Rev*, 8:69–77, 1979.

[156] Carl G Saunders, Margaret Bannon, Robert M Sabiston, Larry Panych, Sandra L Jenks, Ian R Wood, and Silvia Raschke. The canfit system: shape management technology for prosthetic and orthotic applications. *JPO: Journal of Prosthetics and Orthotics*, 1(3):122–130, 1989.

[157] Yong-Ping Zheng, Arthur FT Mak, and Aaron KL Leung. State-of-the-art methods for geometric and biomechanical assessments of residual limbs: a review. *Journal of rehabilitation research and development*, 2001.

[158] Audrey T. Tantua, Jan H.B. Geertzen, Jan J.A.M. van den Dungen, Jan Kees C. Breek, and Pieter U. Dijkstra. Reduction of residual limb volume in people with transtibial amputation. *Journal of Rehabilitation Research and Development*, 51(7): 1119–1126, 2014. ISSN 19381352. doi: 10.1682/JRRD.2013.11.0243.

[159] Joan E Sanders and Stefania Fatone. *Residual limb volume change: systematic review of measurement and management*, volume 48. NIH Public Access, 2011.

[160] Joan E. Sanders, Daniel S. Harrison, Katheryn J. Allyn, and Timothy R. Myers. Clinical utility of in-socket residual limb volume change measurement: Case study results. *Prosthetics and Orthotics International*, 33(4):378–390, 2009. ISSN 03093646. doi: 10.3109/03093640903214067.

[161] Krittika D'Silva, Brian J. Hafner, Katheryn J. Allyn, and Joan E. Sanders. Self-reported prosthetic sock use among persons with transtibial amputation. *Prosthetics and Orthotics International*, 38(4):321–331, 2014. ISSN 17461553. doi: 10.1177/0309364613499064.

[162] Engineering National Academies of Sciences, Medicine, et al. *The promise of assistive technology to enhance activity and work participation*. National Academies Press, 2017.

[163] Joan E Sanders, Ari Karchin, John R Fergason, and Elizabeth A Sorenson. A noncontact sensor for measurement of distal residual-limb position during walking. *Journal of rehabilitation research and development*, 43(4):509, 2006.

[164] Joan E Sanders, Mark A Moehring, Travis M Rothlisberger, Reid H Phillips, Tyler Hartley, Colin R Dietrich, Christian B Redd, David W Gardner, and John C Cagle. A bioimpedance analysis platform for amputee residual limb assessment. *IEEE Transactions on Biomedical Engineering*, 63(8):1760–1770, 2015.

[165] Paul K. Commean, Barry S. Brunsden, Kirk E. Smith, and Michael W. Vannier. Below-knee residual limb shape change measurement and visualization. *Archives of Physical Medicine and Rehabilitation*, 79(7):772–782, 1998. ISSN 00039993. doi: 10.1016/S0003-9993(98)90355-0.

[166] Elena Seminati, David Canepa Talamas, Matthew Young, Martin Twiste, Vimal Dhokia, and James L.J. Bilzon. Validity and reliability of a novel 3D scanner for assessment of the shape and volume of amputees' residual limb models. *PLoS ONE*, 12(9):1–16, 2017. ISSN 19326203. doi: 10.1371/journal.pone.0184498.

[167] Joan E. Sanders, Ellen L. Rogers, and Daniel C. Abrahamson. Assessment of residual-limb volume change using bioimpedence. *Journal of Rehabilitation Research and Development*, 44(4):525–535, 2007. ISSN 07487711. doi: 10.1682/JRRD.2006.08.0096.

[168] Chakaveh Ahmadizadeh, Brittany Pousett, and Carlo Menon. Towards management of residual limb volume: Monitoring the prosthetic interface pressure to detect volume fluctuations—a feasibility study. *Applied Sciences*, 10(19):6841, 2020.

[169] Robert A Heffner, Mark J Butler, and Colleen Keelan Reilly. Pseudoreplication revisited. *Ecology*, 77(8):2558–2562, 1996.

[170] Rong Cai Yang. Towards understanding and use of mixed-model analysis of agricultural experiments. *Canadian Journal of Plant Science*, 90(5):605–627, 2010. ISSN 00084220. doi: 10.4141/CJPS10049.

[171] Richard L Lieber. Statistical significance and statistical power in hypothesis testing. *Journal of Orthopaedic Research*, 8(2):304–309, 1990.

Appendix A

Raw Signal Visualization

Visualization of samples of raw force sensitive resistor (FSR) and electromyography (EMG) signals obtained in the first two objectives of this thesis are presented in this appendix. The signals demonstrated in this chapter are as acquired by the data acquisition circuit and without any further pre-processing. The content of this chapter is only to provide visualization of the signals. Colored shaded areas are used to separate samples in different classes of motion.

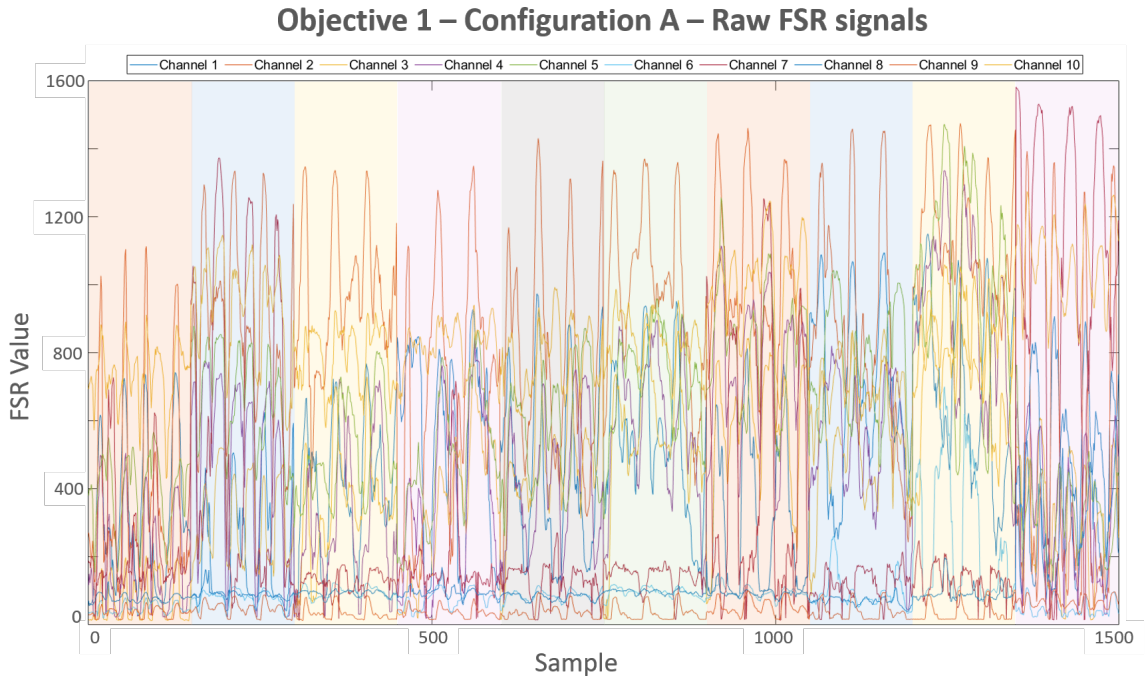

Figure A.1: Visualization of samples of force sensitive resistor (FSR) signals obtained in Objective 1 - Configuration A

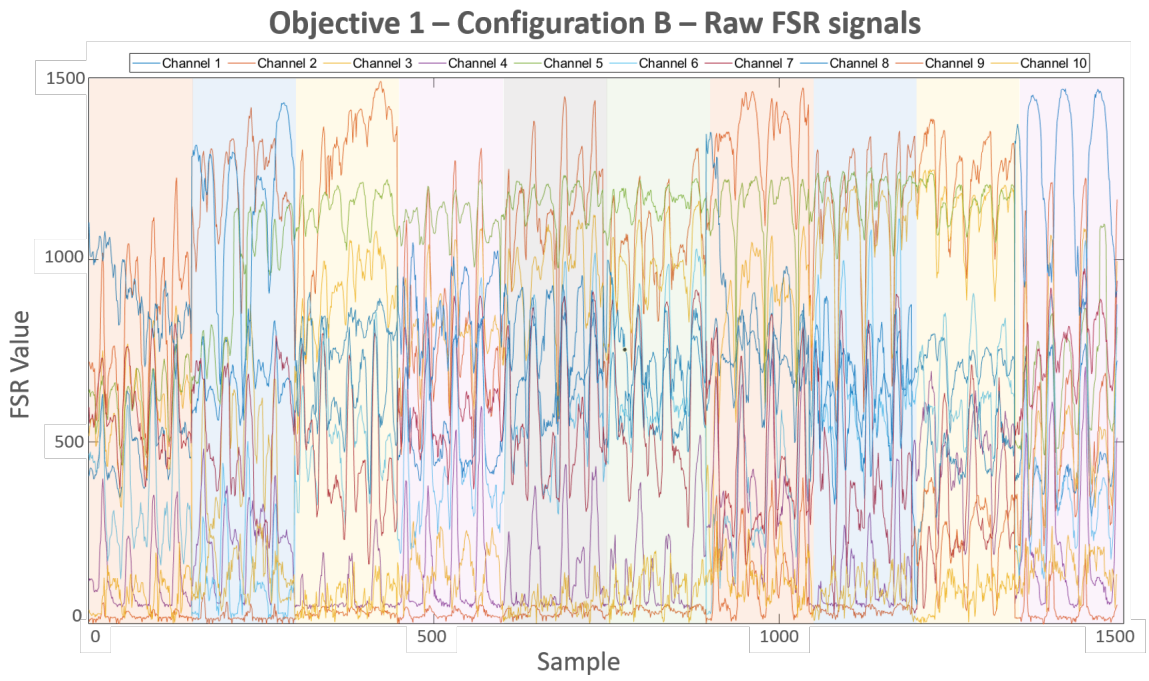

Figure A.2: Visualization of samples of force sensitive resistor (FSR) signals obtained in Objective 1 - Configuration B

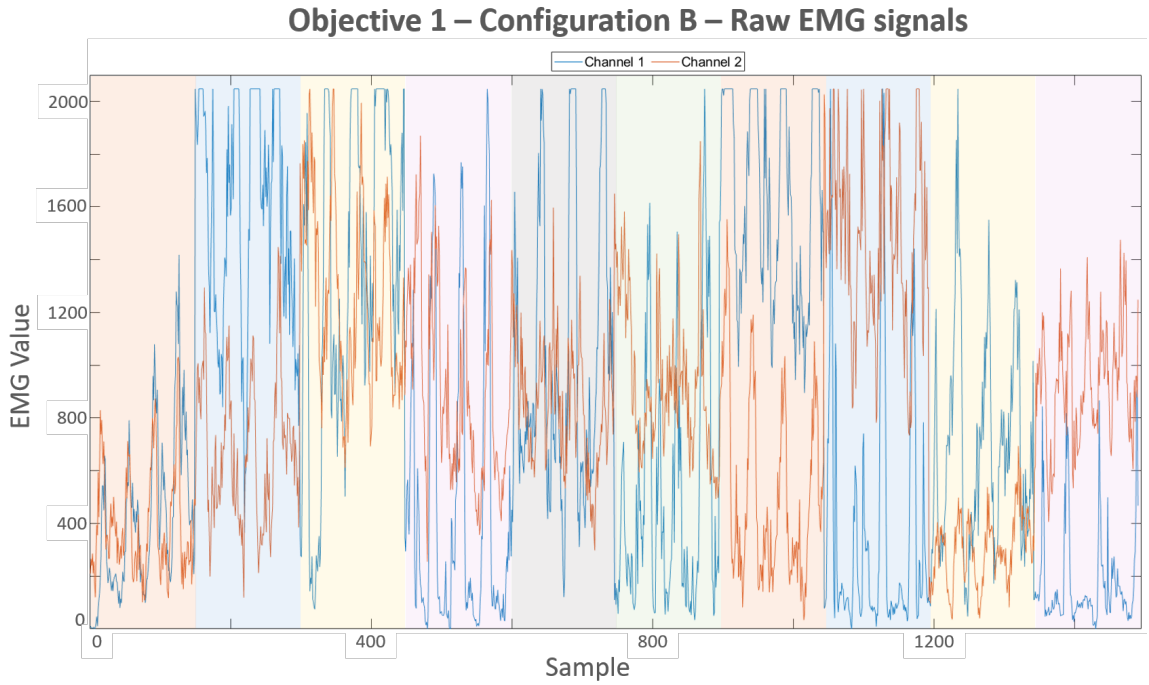

Figure A.3: Visualization of samples of electromyography (EMG) signals obtained in Objective 1 - Configuration B

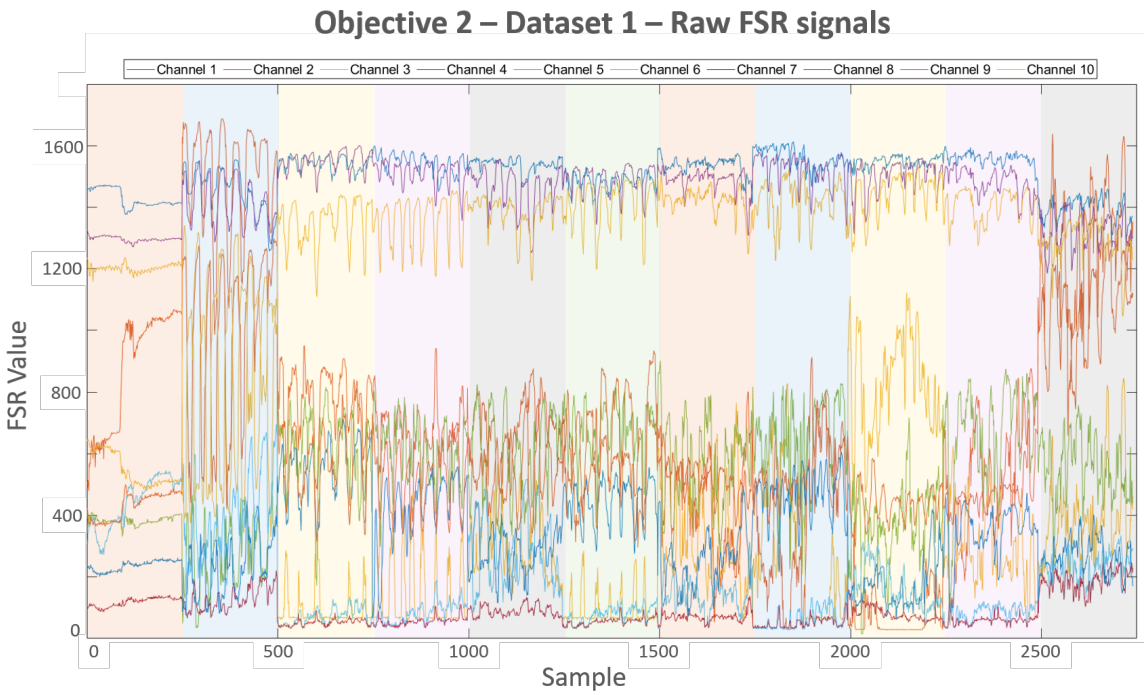

Figure A.4: Visualization of samples of force sensitive resistor (FSR) signals obtained in Objective 2 - Dataset1

Appendix B

Feature Selection for Extended Grips

In the three datasets used for the second objective of this thesis, data were available for an extended set of hand and wrist movements: 11 total classes of motion in dataset1, and 11 grips in dataset2 and dataset3. All three datasets included 6 movements that are associated with primary grips for activities of daily living (relax, open, force, tripod, finger point, and key) [21], [70], [20] which were examined in the second objective of this thesis.

The classes of motion in the three datasets are shown in Table B.1. The grips of dataset1 are shown in Figure B.1. The 5 additional grips of dataset1 were chosen since they were supported by the robotic hand used in this study and the 4 additional classes of motion of dataset2 and dataset3 were chosen for consistency with other research results [20].

Dataset	Number of Classes of Motion	Classes of Motion
1	11	relax, open, force, tripod, finger point, key, mouse, precision open, pinch, column, and active index
2 & 3	10	relax, open, force, tripod, finger point, key, wrist extension/flexion, supination, and pronation

Table B.1: Classes of motion included in three datasets used for the second objective of this thesis.

Classification accuracies using the five feature selection methods explained in Chapter 4 are shown in Figures B.2, B.3, and B.4 for dataset1, dataset2, and dataset3, respectively. Numbers of features chosen by each method are shown in Table B.2 and percentage decrease in number of features using the five methods are shown in Table B.3.

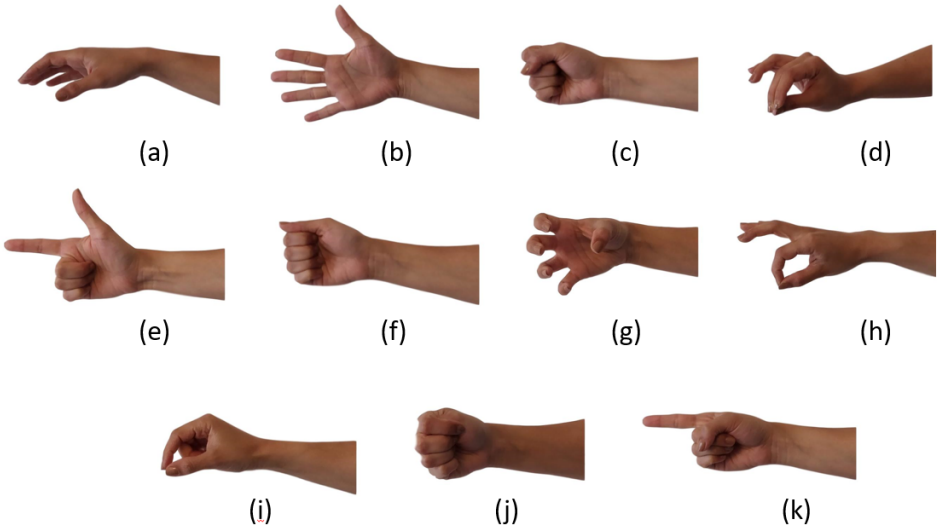

Figure B.1: Extended grips of dataset1: (a) relax, (b) Open, (c) force, (d) tripod, (e) finger point, (f) key, (g) mouse, (h) precision open, (i) pinch, (j) column, (k) active index

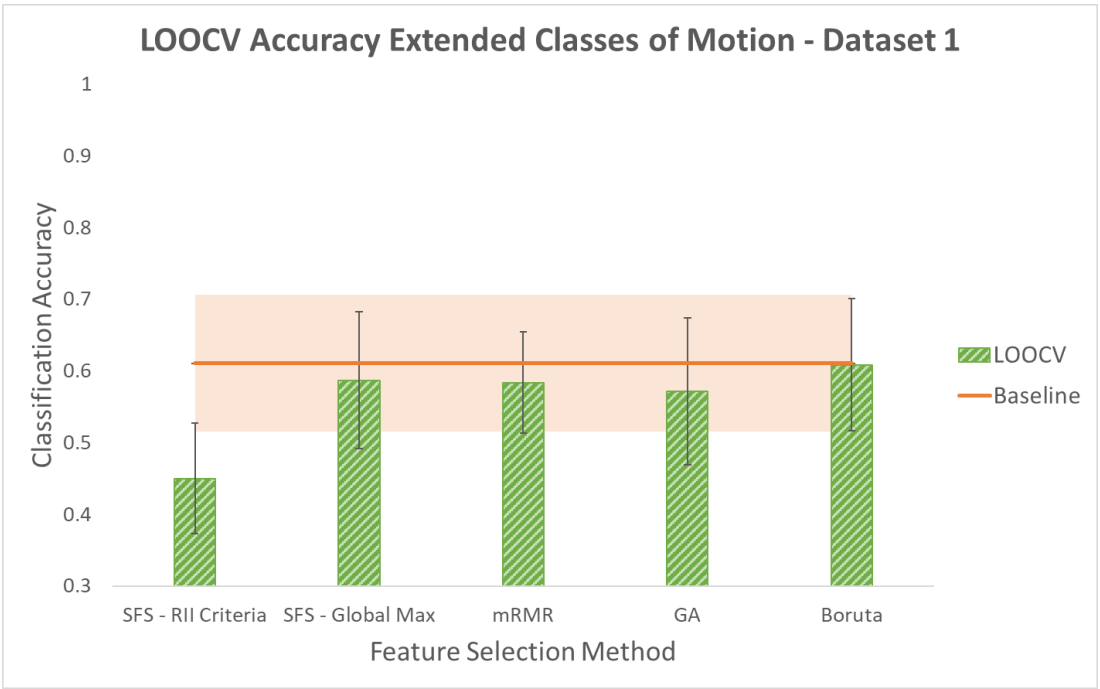

Figure B.2: Leave-One-Out Cross Validation accuracy using different feature selection methods for dataset1 with extended classes of motion. Shaded area around the baseline indicates its standard deviation.

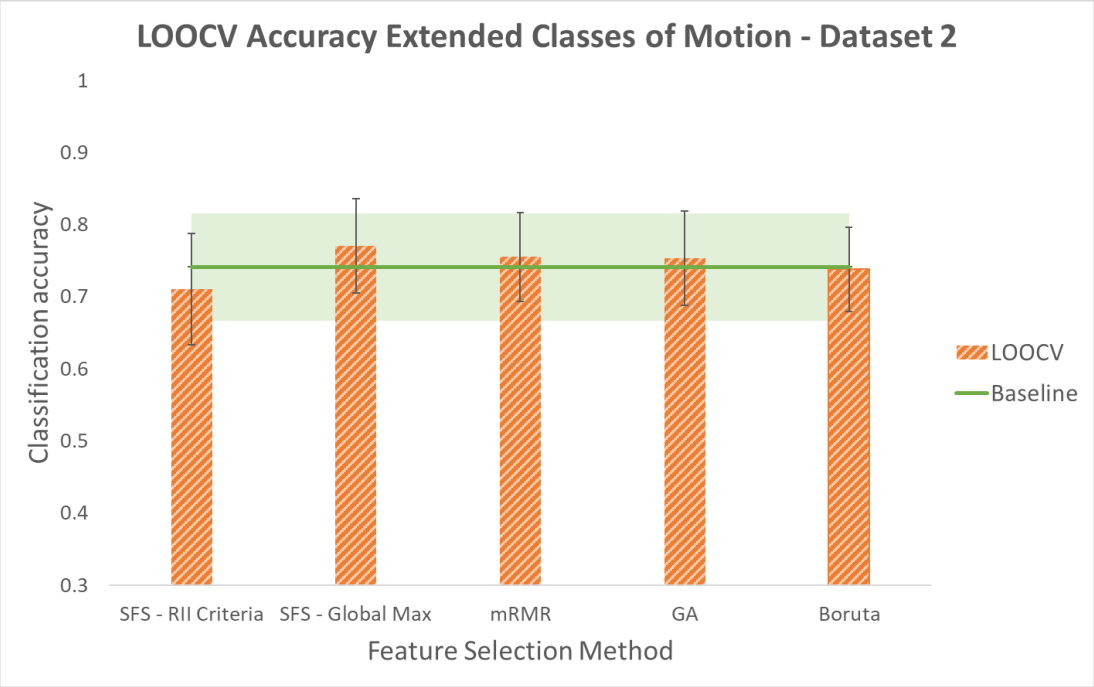

Figure B.3: Leave-One-Out Cross Validation accuracy using different feature selection methods for dataset2 with extended classes of motion. Shaded area around the baseline indicates its standard deviation.

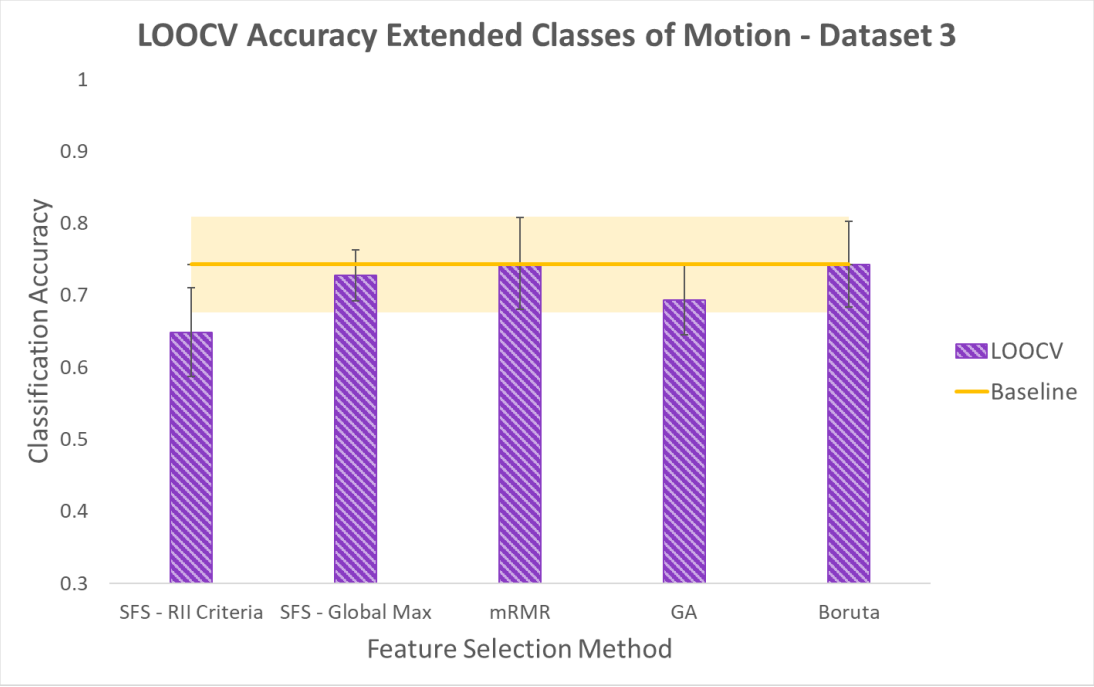

Figure B.4: Leave-One-Out Cross Validation accuracy using different feature selection methods for dataset3 with extended classes of motion. Shaded area around the baseline indicates its standard deviation.

	SFS - RII Criteria	SFS - Global Max.	mRMR	GA	Boruta
Dataset1	4	16	43	13.6	22
Dataset2	15	25	39	20.3	41
Dataset3	9	19	33	14.1	29

Table B.2: Number of features selected in LOOCV using different feature selection methods with extended classes of motion.

	SFS - RII Criteria	SFS - Global Max.	mRMR	GA	Boruta
Dataset1	93.7%	74.6%	31.7%	78.4%	65.1%
Dataset2	74.1%	56.9%	32.8%	65%	29.3%
Dataset3	75.7%	48.6%	10.8%	61.9%	21.6%

Table B.3: Percentage decrease in input features using different feature selection methods with extended classes of motion.

The Student's paired t-test with significance level of 5% was used to determine significance of change in classification accuracy obtained using the smaller feature subset and results are shown in Table B.4 where "✓" means that no significant difference was shown between the baseline accuracy and the accuracy obtained using the chosen feature subset and "X" means that the obtained accuracy was significantly different from the baseline accuracy.

	SFS - RII Criteria	SFS - Global Max.	mRMR	GA	Boruta
Dataset1	X	✓	✓	X	✓
Dataset2	✓	✓	✓	✓	✓
Dataset3	X	✓	✓	X	✓

Table B.4: Result of significant difference between accuracies obtained using the five feature selection methods and baseline accuracies.

For extended classes of motion, SFS with global max. criterion, mRMR, and Boruta were able to reduce the number of features without sacrificing performance. MRMR and Boruta were among chosen methods for both primary grips explained in Chapter 4 and the extended classes of motion.

Appendix C

Feature Selection Using an Alternate Method

Two methods can be used for feature selection toward fulfillment of the second objective of this thesis: method 1 (mutual feature selection) and method 2 (non-mutual feature selection). Method 1 is a more conservative method since it only selects features that were chosen in all five permutations of LOOCV and is explained in Chapter 4. This method has the advantage of choosing a smaller feature set.

In Method 2, each permutation of LOOCV would be treated as a separate case and average of the five resulting classification accuracies would be reported. Accuracies obtained applying this method on datasets of Chapter 4 are shown in Figures C.1, C.2, and C.3 for dataset1, dataset2, and dataset3, respectively. Number of selected features and percentage decrease in the number of features are shown in Tables C.1 and C.2.

In the real use case of the application discussed in this study, both methods are possible for feature selection based on five repetitions of collected data. Using the first method, data would be split to five sections and mutual features from LOOCV will be selected. In the second method, all available data would be used for training. This would be done to maximize data based on which feature selection decision is made since it would be assumed that more data cover more variability and thus would provide a chance for better prediction of user intention. This is resembled in method 2 that is explained in this section.

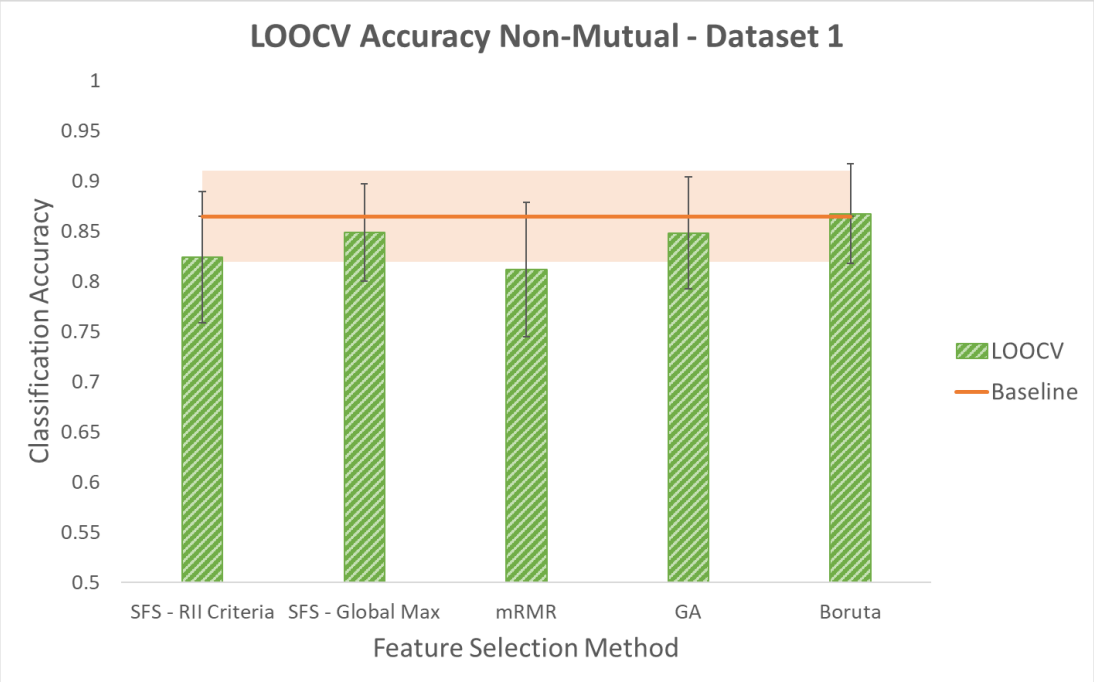

Figure C.1: Leave-One-Out Cross Validation accuracy using different feature selection methods for dataset1 using the second processing method. Shaded area around the baseline indicates its standard deviation.

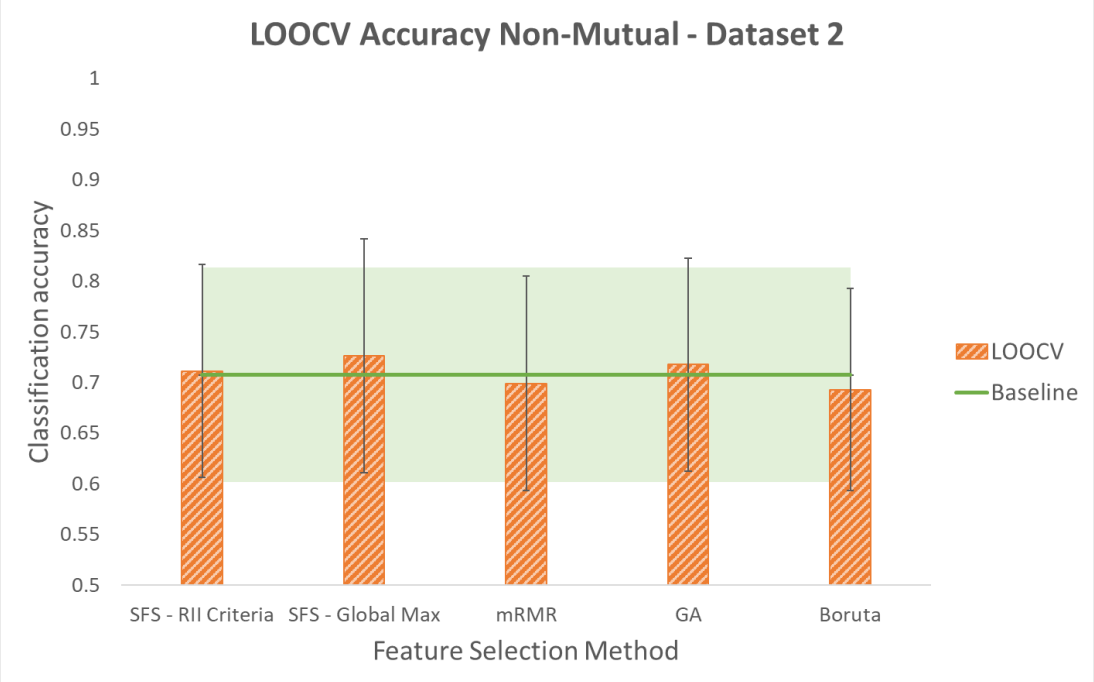

Figure C.2: Leave-One-Out Cross Validation accuracy using different feature selection methods for dataset2 using the second processing method. Shaded area around the baseline indicates its standard deviation.

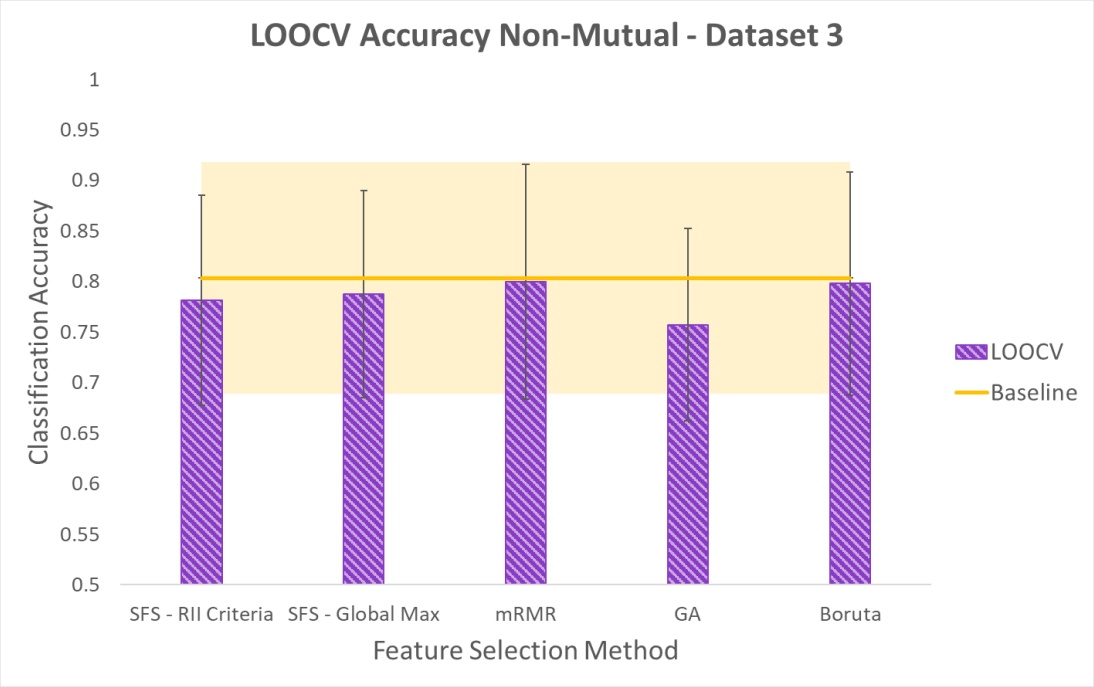

Figure C.3: Leave-One-Out Cross Validation accuracy using different feature selection methods for dataset3 using the second processing method. Shaded area around the baseline indicates its standard deviation.

	SFS - RII Criteria	SFS - Global Max.	mRMR	GA	Boruta
Dataset1	21.6	37.6	43	34.32	40
Dataset2	25.4	35.2	42.4	31.8	47.8
Dataset3	22.6	27.2	32.8	25.8	34.4

Table C.1: Number of features selected in LOOCV using different feature selection methods using the second processing method.

	SFS - RII Criteria	SFS - Global Max.	mRMR	GA	Boruta
Dataset1	65.7%	40.3%	31.7%	45.5%	36.5%
Dataset2	56.2%	39.3%	26.9%	45.1%	17.6%
Dataset3	38.9%	26.5%	11.4%	30.3%	7.0%

Table C.2: Percentage decrease in input features using different feature selection methods using the second processing method.

To determine which method is superior to the other, a more thorough study needs to be done that covers more participants, and uses more data for such decision.